

# Statistical Genetics and Direct Coupling Analysis in and out of Quasi-Linkage Equilibrium

Vito Dichio<sup>1</sup>, Hong-Li Zeng<sup>2</sup>, Erik Aurell<sup>3</sup>

<sup>1</sup> Sorbonne Université, Paris Brain Institute - ICM, CNRS, Inria, Inserm, AP-HP, Hôpital de la Pitié Salpêtrière, F-75013, Paris, France

<sup>2</sup> School of Science, Nanjing University of Posts and Telecommunications, New Energy Technology Engineering Laboratory of Jiangsu Province, Nanjing, 210023, China

<sup>3</sup> Department of Computational Science and Technology, AlbaNova University Center, SE-106 91 Stockholm, Sweden;

E-mail: [eaurell@kth.se](mailto:eaurell@kth.se)

10 March 2022

**Abstract.** This review is about statistical genetics, an interdisciplinary topic between Statistical Physics and Population Biology. The focus is on the phase of *Quasi-Linkage Equilibrium* (QLE). Our first objective is to clarify under which conditions the QLE phase can be expected to hold in population biology, and how parameters describing a QLE phase relate to underlying population dynamics. We review, supplement and extend earlier theoretical investigations in the literature, and add numerical tests. Our second objective is to clarify how the stability of the QLE phase is lost. The QLE state, which has many similarities to equilibrium statistical mechanics, was discovered by Motoo Kimura in the mid-1960ies for a two-locus two-allele model, and was extended and generalized to the global genome scale by *Neher & Shraiman (2011)*. What we will refer to as the Kimura-Neher-Shraiman (KNS) theory describes a population evolving due to the mutations, recombination, genetic drift, natural selection (pairwise epistatic fitness). The main conclusion of KNS is that QLE phase exists at sufficiently high recombination rate ( $r$ ) with respect to the variability in selection strength (fitness). Combining the results of the KNS theory with the techniques of the Direct Coupling Analysis (DCA), developed for applications in Statistical Physics and Computational Biology, we show that in QLE epistatic fitness can be inferred from the knowledge of the (dynamical) distribution of genotypes in a population. Extending upon earlier work *Zeng & Aurell (2020)* in this review we consider higher mutation and recombination rates. We further consider evolution of a population at higher selection strength with respect to recombination and mutation parameters ( $r$  and  $\mu$ ). We identify a new bi-stable phase which we call the Non-Random Coexistence (NRC) phase where variability persist in the population without either fixating or disappearing. We also identify an intermediate region in the parameter space where a finite population jumps stochastically between a QLE-like state and NRC-like behaviour. The existence of NRC-phase demonstrates that even if statistical genetics at high recombination closely mirrors equilibrium statistical physics, from a more general point of view a more apt analogy is non-equilibrium statistical physics with broken detailed balance, where self-sustained dynamical phenomena are ubiquitous.

*Keywords:* Statistical Genetics, Direct Coupling Analysis, Quasi-Linkage Equilibrium, Inference.

**Contents**

<b>1</b>	<b>Introduction</b>	<b>4</b>
<b>2</b>	<b>Statistical Genetics</b>	<b>5</b>
2.1	Subject Matter: Population Genetics in a Nutshell . . . . .	5
2.2	A brief historical overview . . . . .	8
2.3	Kimura-Neher-Shraiman Theory (KNS) . . . . .	11
<b>3</b>	<b>Direct Coupling Analysis (DCA) for Statistical Genetics</b>	<b>17</b>
3.1	Inverse Ising Problem (IIP) . . . . .	18
3.2	Maximum Likelihood for the IIP . . . . .	21
3.3	Approximate Methods for the IIP . . . . .	21
<b>4</b>	<b>Quasi-Linkage Equilibrium (QLE)</b>	<b>25</b>
4.1	QLE in the KNS theory . . . . .	25
4.2	Inference of Epistasis: $r \gg \sigma$ . . . . .	29
<b>5</b>	<b>QLE extended: a Gaussian Ansatz</b>	<b>31</b>
5.1	A Gaussian Ansatz . . . . .	32
5.2	Inference of Epistasis, improved: $\mu, r \gg \sigma$ . . . . .	38
<b>6</b>	<b>Beyond the QLE</b>	<b>40</b>
6.1	Statistical Physics of non-QLE regimes . . . . .	40
6.2	A New Phase: Non-Random Coexistence . . . . .	46
6.3	Phenomenology of the NRC . . . . .	54
6.4	A NRC-phase for E.Coli? . . . . .	56
<b>7</b>	<b>Summary and discussion</b>	<b>58</b>
	<b>Appendix A Moments vs Cumulants</b>	<b>61</b>
	<b>Appendix B Random Genetic Drift</b>	<b>63</b>
	<b>Appendix C KNS Theory for Categorical Data</b>	<b>65</b>
	<b>Appendix D Simulating Evolution with FFPopSim</b>	<b>67</b>
	<b>Appendix E Maximum Entropy and Information</b>	<b>69</b>



## 1. Introduction

This review is about Statistical Genetics. In the broad area of Theoretical Biology, this is the field concerned with the development of statistical methods to describe the distribution of genotypes in a population. The central focus of the review is the Quasi-Linkage Equilibrium (QLE) phase of Statistical Genetics, and the Kimura-Neher-Shraiman (KNS) theory of the QLE.

The review has two main objectives. The first objective is to clarify under which conditions the QLE phase can be expected to hold in population biology, and how parameters describing a QLE phase relate to underlying population dynamics. We review, supplement and extend earlier theoretical investigations in the literature, and add new numerical tests. The second objective is to clarify how the stability of the QLE phase is lost. In so doing we identify a new bistable phase which we call Non-Random Coexistence (NRC), and an intermediate region in parameter space where a finite population jumps stochastically between a QLE-like state and NRC-like behaviour.

We will explain biological concepts as we will need them throughout the review. For the reader's convenience we have also provided a Glossary (above), with concise definitions of technical terms. The following is an outline of the content of the review, without yet explaining the terms and concepts used.

The review is structured in seven sections and five technical appendices. Section 2 describes Statistical Genetics in general, followed by an introduction to the Kimura-Neher-Shraiman (KNS) theory, to be found in Section 2.3.

Section 3 is about Gibbs-Boltzmann distributions of the Ising and Potts type and how to retrieve the parameters of such distributions from samples. Techniques to achieve this task in a computationally efficient yet accurately are collectively known as "Direct Coupling Analysis" (DCA), which give the name to the section. In this section we review the most important and most widely tested DCA algorithms. Gibbs-Boltzmann distributions, which have so many applications in statistical physics and other sciences, are important in statistical genetics because the QLE phase is identical to equilibrium statistical mechanics as to its one-time properties. This means that one can use DCA to test if a simulated population is in a QLE state if one can predict the parameters of the Gibbs-Boltzmann distribution from the underlying evolutionary dynamics.

Section 4 carries out this program under the assumptions of the KNS theory which are large recombination rate, small variations in growth rate due to fitness, and some mutation rate. This leads to a forward relation between synergistic contributions to fitness and pairwise variability in the population. The forward relation can then be turned around to an inference formula where fitness parameters are determined from parameters describing variability and obtained by DCA. In this section we use this inference formula to quantitatively map out when the KNS theory holds, by comparing the true evolutionary parameters to inferred evolutionary parameters.

Section 5 continues on the previous section under alternative assumptions of high

mutation rate, low fitness variation and some recombination. We show that this also leads to a QLE state, but with another relation between evolutionary parameters and parameters describing the population. The new relation is obtained by a Gaussian closure technique, and holds for both high and low recombination rate. In the former case we can relax the assumption of high mutation rate and recover the inference formula of Section 4. We show that the new inference formula, which goes over to the formula from KNS theory in the limit of low mutation rate, holds in a much larger parameter range.

Section 6 starts by reviewing previous theoretical approaches to population genetics out of the QLE regime. We then describe a new phase which we call Non-Random Coexistence (NRC) where variability persists in the population without either fixating or disappearing. The appearance of NRC is mode for the QLE phase to disappear, and we identify an intermediate region in the parameter space where a finite population jumps stochastically between a QLE-like state and NRC-like behaviour. In Section 6.4 we discuss that NRC may be the mechanism behind the quasi-stable coexistence recently observed in the famous Long Term Evolution Experiment on *Escherichia coli* populations evolving in test tubes.

In the final Section 7 we discuss our results and give an outlook for the future.

## 2. Statistical Genetics

This section contains a brief introduction to the Biology relevant to this paper. It is primarily aimed to physicists not conversant with these matters; biophysicists and biological physicists (and biologists) may skip to the next section. As noted above, technical terms are defined in the Glossary.

### 2.1. Subject Matter: Population Genetics in a Nutshell

The crucial difference between living and non-living forms of matter is the presence Darwin's evolution, that selects the most apt individuals to the environment. In turn, the key element of evolution is heredity, *i.e.*, the possibility of inheriting information across generations. One may think at history of life on the earth as an information flow from generation to generation, in an ongoing process that has shaped the astonishing variety of complex organisms that we observe today. According to the central dogma of molecular biology, biological information is encoded in the DNA, a macro-molecule present in each cell that consists in two sugar-phosphate ribbon-like stands that coil around to form a double helix and whose horizontal rungs are pairs of complementary nucleobases: A-T, G-C, see Fig.1. The relevant information is encoded in the precise sequence of nucleobases of each strand: by means of transcription DNA is converted into the closely related molecule RNA, and by means of translation, a stretch of RNA is translated into a polypeptide chain, which upon folding and other processes will eventually result in a protein. Such proteins in turn perform the many different functions needed to sustain the life of the cells.

The word 'gene' refers to a stretch of DNA which is transcribed together, and a 'gene product' is the protein produced from the corresponding part of the RNA. In microscopic organisms (bacteria, viruses) as well as in higher organisms a number of biological mechanisms allow for the possibility that from one single gene more than

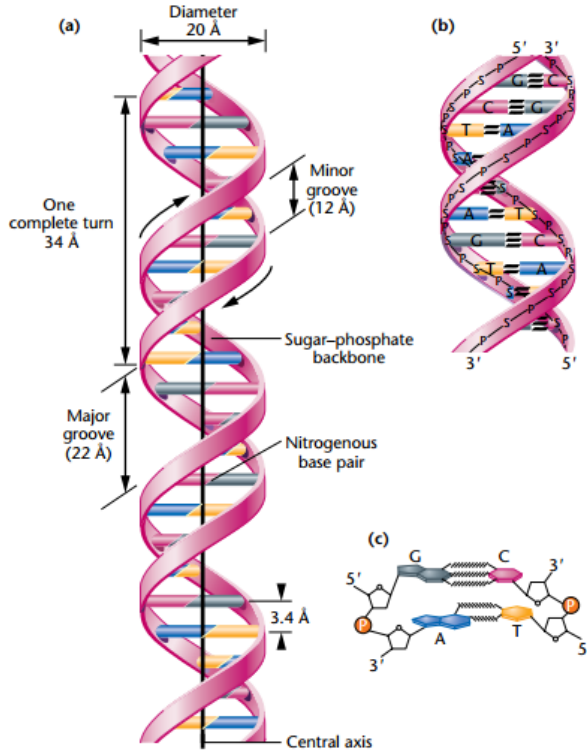


Figure 1: The DNA double helix as proposed by J. Watson and F. Crick (a). The ribbon-like strands represent the sugar-phosphate backbones, and the horizontal rungs depict the nitrogenous base pairs (b-c). From [1].

one protein are generated. In this way it is possible for *e.g.* humans to have about 20,000 genes but more than 100,000 proteins. Some types of heredity (epigenetics) exist that do not involve the sequence of nucleotides in DNA, the most well-known being chemical modifications of DNA (methylation and other) which is important in *e.g.* heritable gene silencing. Even if there are exceptions to the central dogma, it describes the overwhelming majority of biological information processing as pertaining to information stored as chemical molecules.

Complex regulatory mechanisms of the gene expression weave an intricate and largely unknown network of interactions within genes. Some such gene expression patterns can be inherited over many generations and comprise another type of epigenetics, even if often enhanced by methylation and similar processes in higher organisms. Many other gene expression patterns on the other hand change on fairly rapid time scale in response to changes in the environment. In bacteria this is in fact the main form of cellular information processing and it is vital in higher organisms as well, even if often overlaid by other and faster pathways. In eukaryotes the DNA is often condensed in the form of chromosomes: the set of chromosomes is the genetic heritage of an individual. A population in which each cell has one complete set of chromosomes is named haploid, if there are two such sets, diploid. In mammals the germ line cells (egg cell and sperm) are haploid and the soma line cells (the rest) are diploid. This form of life is hence diploid-dominated, and the organisms reproduce by going through an obligatory haploid phase where two germ line cells mix in sex. In other organisms very many different forms of reproduction and diploid/haploid division of labour are possible. Asexual reproduction has been found

to occur naturally everywhere except among mammals (among birds in domesticated turkeys and chicken), but is generally less frequent the more complex the organism. Many bacteria reproduce mostly and maybe almost only asexually, and hence live like haploid genomes copying themselves to new haploid genomes. Certain yeasts have more than two mating types (gender, so to speak) that can only mate in specific combinations.

We now broaden the perspective and consider an entire population rather than the single individual. Typically a gene can be found in one or several variants in a population. Such variants are called alleles and can also typically be found in different proportions in different sub-populations. Alleles can differ either at one genomic position (single nucleotide polymorphisms, or SNPs), or in ways that involve changes at more than one genomic position. The latter can be through multiple SNPs in a single gene or by insertions and deletions (indels). The goal of population genetics is to study the genetic composition and dynamics of biological populations. Several processes alter the genetic pool of a population. The most important of them are

- **Natural selection.** At the phenotype level, advantageous characteristics will enhance the probability for an individual to survive and reproduce (high fitness). This has consequences at the genotype level, even though the exact map between these two layers may be quite complex. Complexity here means it is not clear which characteristics of genotype elements lead to which phenotypic traits on which selection acts, especially when they act in combination.
- **Mutations.** They can arise by chance in a genomic sequence *e.g.* because of transcription errors. Mutations can have no consequences on the level of protein (*synonymous*) or cause alterations in the polypeptide chain they code for (*non-synonymous*). They represent a major source of variability for the evolutionary process.
- **Recombination.** Several mechanisms of interaction between individuals of a population can lead to the exchange of genetic material. In a general sense they can all be called forms of sex, even if acting quite differently than sex in mammals. In prokaryotes, the main forms of recombination are transduction, transformation, conjugation. In eukaryotes, recombination happens during meiosis where the mixing between two chromosomes from each of the parents is enhanced by the crossing-over mechanism. Just like mutations, recombination fuels variability in the population.
- **Chance.** Accidental events can alter the genetic pool of a population: bottlenecks, genetic drift, hybridization (...)

In the biological literature, a distinction is made between population genetics and quantitative genetics. This review is almost exclusively about the first. The second deals with the genetics of continuously varying characteristics, such as height and skin color in human. Historically this was referred to as *quantitative* (measured by a number), in opposition to characteristics that appear in only a few different types, as do *qualities* in classical philosophy. Inherited qualities are due to differences in genotypes on one or a few positions, of which one example in human is the type of ear wax, due to a single-nucleotide variation in the gene ABCC11 on chromosome 16 [2]. On the contrary, most quantitative characteristics of higher organisms are due both inheritance ("nature") and environment ("nurture"); In addition, if one could isolate the genetic component of such quantitative traits, they would be typically due

to variations in many positions. For instance, height is partly genetically determined in human, and has recently been associated to variations at about 700 positions only among individuals of European ancestry [3].

In the pre-sequencing era population genetics was the realm of theory and explanations, while quantitative genetics was the realm of what could be measured and of direct interest to biology. In modern times this relationship is partly upended: whole genome sequences of many organisms can (and have been) obtained and the predictions of population genetics can be compared to such data. This is the approach we have followed in this work. As an aside and an example of what can be done, in the ongoing COVID19 pandemic more than nine million (March 7, 2022) whole-genome sequences of the coronavirus SARS-CoV-2 have been found in different laboratories around the world, many of them likely determined to single/nucleotide accuracy [4]. Measuring quantitative traits remains however time-consuming and difficult, and the relationship between genotype and phenotype is one of the most complex and least known (though most studied) in all of science. In the spirit of Statistical Physics it is therefore natural to focus on the genotype scale (microstate), once that is measurable.

## 2.2. A brief historical overview

The similarities and differences between population genetics and statistical physics were noted quite long ago, and have been reviewed from the side of Physics multiple times, *e.g.* [5–7]. More recently, the genotype-phenotype map was reviewed in [8] and the possible predictability and control of evolution in [9].

The mathematical theory of population genetics can be said to have started in 1908 when Hardy and Weinberg showed that in a population with diploid genomes evolving only due to recombination (sex) allele frequencies reach stationary values. G. H. Hardy was one of the leading mathematicians in his time, and is supposed to have made his discovery as the answer to a question from a colleague during a cricket match [10]. Wilhelm Weinberg was a medical doctor who pioneered twin studies [11], and although the publication date of Hardy’s paper [12] is some months earlier than Weinberg’s [13], the latter was based on a public lecture Weinberg had given at the beginning of the year. In the English-language literature, the attribution of the result to both Hardy and Weinberg was first made in [14]. The problem of Hardy and Weinberg was that of the frequencies of the combinations of a dominant allele  $A$  and a recessive allele  $a$  in a population. The possible genotypes are  $AA$ ,  $Aa$  and  $aa$ , and by assumption the phenotypes of  $AA$  and  $Aa$  are the same, different from  $aa$ , without this having an effect on fitness. The solution is that the frequencies are  $f^2$ ,  $2f(1-f)$  and  $(1-f)^2$  where  $f$  is a free parameter given by the initial distribution. The Hardy-Weinberg theory thus disproved an earlier assumption that the frequencies of dominant vs. recessive phenotypes are in proportional 3 : 1 in a natural population. The *Hardy-Weinberg equilibrium* is a limit case of *Linkage Equilibrium* to be introduced below where there are no effects of fitness or mutations. There is hence not one stable Hardy-Weinberg equilibrium, but a family of marginally stable equilibria parametrized by  $f$ ; selection and mutation generally break this degeneracy.

Another important class of evolutionary models are those that describe the evolution of populations under the influence of only mutations and random genetic drift, potentially extended to mechanisms of selection and migration (island models). Such models are called Wright-Fisher models or Moran models, depending on whether generations are non-overlapping or overlapping. Mathematically both are discrete-



time processes where in the first the elementary time step is one generation, and in the second one reproduction event. From the viewpoint of statistical physics, the latter is also a "sequential update" algorithm for a continuous time process which proceeds with certain rates. For a single bi-allelic locus, evolution of one population can hence in both cases be pictured as a jump process in a lattice of sites labeled by  $n$  which can take values  $0, 1, \dots, N$ ,  $N$  being the total number of individuals.

Over multiple loci the process is more complex. As a mathematical simplification, it is interesting to first consider genetic drift acting independently on each locus. We will return to a discussion of its biological relevance, but for the moment note that evolution of one genome can then be assimilated to the dynamics of classical spin systems with independent source of randomness acting on each spin. The evolution of a population is then similar to a jump process in a multi-dimensional lattice with sites labeled  $n_1, n_2, \dots, n_L$ ,  $L$  being the number of loci, with an independent source of randomness in each direction. Such evolution laws are non-degenerate stochastic processes, and the evolution of an ensemble of genomes is described by the associated Fokker-Planck equation (forward Kolmogorov equation). The physical flavour of this change of perspective from a distribution over genomes to a distribution over allele frequencies was succinctly stated by R Fisher in the 1953 Croonian Lecture to the Royal Society

"the frequencies with which the different genotypes occur define the gene ratios characteristic of the population, so that it is often convenient to consider a natural population not so much as an aggregate of living individuals as an aggregate of gene ratios. Such a change of viewpoint is similar to that familiar in the theory of gases, where the specification of the population of velocities is often more useful than that of a population of particles"

Ronald A. Fisher [15]

Again similarly to physics, in the proper limit the evolution laws of the distribution are parabolic partial differential equations. The first model of such a law was proposed by Fisher in 1922 in the form of a standard diffusion [16, 17]. This model was not fully correct, as it overestimated the amount of genetic drift when one allele is close to fixation. In a standard diffusion the random drift in time  $\Delta t$  is order  $\sqrt{\Delta t}$ , hence if the frequency of one allele is  $1 - \epsilon$  and  $\epsilon$  is sufficiently small, the model would predict a non-zero chance of reaching frequencies larger than one, which is impossible. At the time the mathematical theory of state-dependent diffusions was not extensively developed, and it was Kolmogorov who first in 1935 wrote down the correct expression, where the strength of the random drift vanishes as one allele tends towards fixation [18]. This expression was independently re-derived by Wright [19] and Kimura [20, 21], and is usually referred to as the *diffusion approximation* or *Kimura's diffusion approximation*. The rigorous mathematical aspects of this diffusion limit have been addressed by many authors from different communities *cf.* [22–24]. The resulting diffusion process (as well as the underlying discrete process) can be or not be in detailed balance. The condition for detailed balance is that mutations satisfy an integrability condition relative to a measure induced by the random drift on genotype space, known as the Shahshahani-Svirezhev condition [25, 26]. If this condition holds one can include both additive and epistatic fitness to the model and still deduce a simple form for the stationary state (analogous to thermal equilibrium in a potential)

[27]. Properties of reversible evolutionary dynamics were considered in [28], and papers cited therein.

The log-ratio between the probability of a forward and a time-reversed stochastic process is the entropy production in the environment. This fact first established for certain models in [29] has become a corner-stone of modern stochastic thermodynamics [30–32], in particular, see [33, 34]. In evolutionary models the corresponding quantity has been called fitness flux [35, 36], and has been hypothesized to be related to directionality in biological evolution [37]. When the diffusion process describing the evolving population is in detailed balance and in a stationary state there is on average no entropy production in the environment, and similarly no expected directionality in the biological evolution.

Genetic drift in Wright-Fisher and Moran models is in fact implemented on top of mutations and selection by imagining that each individual in a population is replaced by another randomly picked individual, to which one has applied random changes (mutations), with different probabilities (selection). In this perspective genetic drift does not act independently at each locus. While it would look that way in a mathematical model when mutation rate would be so large that all memory of the randomly picked individual are erased, this would not be biologically realistic. Stable inheritance is central to life, especially complex life forms.

In a more realistic scenario of more moderate mutation rates, the replacement individual will mostly inherit the genetic type of the picked individual. If there are correlations between variations over alleles at two loci, then those correlations will at least partially remain after a wave of replacements has swept through the population. If in addition there is enhanced fitness for certain allele combinations, then such correlations will tend to grow. Eventually Fisher's proposition (above) will no longer hold since a probability distribution having non-zero correlations is not only described by the frequencies of single variables.

The way biology nevertheless approaches Fisher's proposition is by the process of recombination (or sex) which mixes up the genotypes at different loci. This leads to the *Quasi-Linkage Equilibrium* (QLE) phase discovered by Motoo Kimura in a model of two biallelic loci (two states per locus) [38]. The QLE phase is the major focus of this review. Recombination plays in population genetics the role of collisions in gas theory, and the assumption of genetic drift acting independently at each locus is formally similar to Boltzmann's molecular chaos.

Central to gas theory is the dual picture of on the one hand the dynamics of one particle, and on the other the dynamics of the probability distribution over that particle's characteristics. Typically those are position and momentum, perhaps also orientation. On the level of stochastic processes the dual picture is represented by the Langevin equation (for one particle) and the Fokker-Planck equation (for the distribution). For many particles we have similarly on the one hand the dynamics of  $N$  particles, and on the other hand the dynamics of the probability distribution over the characteristics of  $N$  particles. Interactions create correlations between the particles so that it cannot be assumed that the distribution over two or more particles is the product of one-particle distributions. Yet this assumption or molecular chaos (or Stosszahlansatz) is fundamental, since a distribution over the characteristics of many particles is an unmanageable quantity.

In statistical genetics, the probability distribution over the properties (genomes) of  $N$  individuals can similarly be represented by the one-genome distribution. Recombination then lead to a nonlinear evolution equation for the one-genome

distribution. Such a Boltzmann equation-like dynamics is at the core of the Kimura-Neher-Shraiman theory of the QLE phase which will be described in Sect. 2.3.

### 2.3. Kimura-Neher-Shraiman Theory (KNS)

We now turn to a more quantitative discussion of the Quasi-Linkage Equilibrium (QLE) of Kimura and the theoretical framework pioneered by Kimura [38] and developed further by R. Neher and B. Shraiman in [39]. We will call this the Kimura-Neher-Shraiman (KNS) theory. Before delving into the details, let us state the following qualitative analogy. As is known, thermodynamics is a description of observable physical properties of a large ensemble of particles. According to statistical mechanics, such properties are computed by taking macroscopic averages over the random motion of individual particles at thermal equilibrium. Despite the complex and chaotic single-particle motion, deterministic laws of thermodynamic emerge thanks to the statistical properties of the ensemble of particles considered. Quantitative genetics is similarly a phenomenological description of observable phenotypic traits of a population of individuals (genomes). The role of statistical genetics is akin to that of statistical mechanics *i.e.* to "bridge" the microscopical degrees of freedom (states of each locus in the genome) to the macroscopic observables of quantitative genetics, the latter to be computed by taking averages over the whole set of observed genotypes (population). The perspective (or hope) of statistical genetics is that despite the largely unknown genotype-phenotype map and uncontrolled environmental effects, laws of quantitative genetics will emerge due to the statistical properties of the ensemble of genomes.

**2.3.1. KNS Hypotheses** Let us set the stage of the KNS theory, in the form of a list of hypotheses. We start with a major simplification: by a genotype we will in the sections of the review which will follow always mean one genome out of all possible genomes of the same length. Although processes that change the length of genomes are important in Biology, the restriction to genomes of the same length brings out clearly the analogies to equilibrium and non-equilibrium spin systems, which is one of themes of this review.

- (i) **Genomic structure.** An haploid genome is a vector  $g = (s_1, \dots, s_L)$  of  $L$  loci  $s_i$  where  $i = 1, \dots, L$ . The number  $L$  of loci is fixed and equal for all the individual genomes. A population is a collection  $\{g^\alpha\}_{\alpha \in A}$ , where  $A$  is a set of indices. Each genome  $g$  appears in the population with probability  $P(g)$ .
- (ii) **Ising genes.** Loci are bi-allelic *i.e.*  $s_i = \pm 1 \forall i$ ; the genotype space is then represented by the  $2^L$  vertices of the hypercube  $\{-1, 1\}^L$ .
- (iii) **Constant population.** The total number of individuals is fixed  $|A| = \text{const.}$  With this hypothesis one models *e.g.* the struggle for survival in an environment with limited resources. Except when explicitly stated, an infinite population  $|A| = \infty$  will be assumed, which allows to neglect stochastic effects.
- (iv) **Evolution.** The genome distribution  $P(g, t)$  evolves in time. The dynamics is driven by the three operators representing natural selection Sec.(2.3.2), mutations Sec.(2.3.3) and recombination Sec.(2.3.4). Their action is encoded in a master equation *i.e.* a phenomenological first-order differential equation

$$\frac{d}{dt}P(g, t) = \frac{d}{dt}\Big|_{fit} P(g, t) + \frac{d}{dt}\Big|_{mut} P(g, t) + \frac{d}{dt}\Big|_{rec} P(g, t) . \quad (1)$$

In order to provide an explicit expression for eq.(1), single terms in the RHS must be analyzed one by one.

*2.3.2. Fitness* The approach followed is based on the definition of the *fitness function*  $F$ : in particular,  $F(g)$  is proportional to the average number of offspring of an individual whose genotype is  $g$ . In other words,  $F(g)$  expresses the propensity of a genotype to transfer its genomic material to the next generations. The explicit form of  $F(g)$  defines the *fitness landscape* of the population. Albeit broad, this definition only partially represents what (Darwinian) fitness in Biology stands for. Let us emphasize what the definition does *not* cover:

- ★ It assumes that fitness only depends on the genotype (with a proviso, to be discussed below). This is not true in general as the reproductive rate of a given genome (or genomic trait) may depend on its frequency in the population *e.g.* because of some feedback regulation system. Effects of cooperation and strategic behaviour (games) are not included in this model.
- ★ It also sets aside issues related to a possible fluctuating environment (*fitness seascapes*) and the related time-dependence of selection.

Whenever these limitations can be accepted, the first term in eq.(1) can be written as

$$\left. \frac{d}{dt} \right|_{fit} P(g, t) = [F(g) - \langle F \rangle] P(g, t) ; \quad (2)$$

$\langle F \rangle(t) = \sum_g F(g) P(g, t)$  is the average fitness that ensures the normalisation of  $P(g, t)$ . Fit individuals (high fitness) will grow in proportion, and the unfit ones will decrease; therefore, whether an individual is fit or not depends on the other individuals that are present in the population.

An explicit expression is needed for  $F(g)$ ; previous researchers have explored different possibilities [5]. For instance, one can consider the class of fitness functions with linear and pairwise interactions:

$$F(g) = \bar{F} + \sum_i f_i s_i + \sum_{i < j} f_{ij} s_i s_j . \quad (3)$$

$\bar{F}$  is a constant, irrelevant for eq.(2). The first order contribution  $f_i$  represent the *additive fitness* at locus  $i$ , which influences fitness independently of all other loci in the genome. Higher terms such as  $f_{ij}$  (and  $f_{ijk}, f_{ijkl}, \dots$  if they were present) represent genetic interactions between loci, also called epistasis. The total fitness can be characterized as a functional of the *a priori* fitness function as

$$\sigma(f) = \sqrt{\sum_i f_i^2 + \sum_{i < j} f_{ij}^2} , \quad (4)$$

Analogously, epistatic fitness by  $\sigma_e$  has the same definition as eq.(4) except that only the epistatic contribution appears and the additive fitness by  $\sigma_a$  analogously. As it is clear from eq.(2),  $F(g)$  has dimension  $[t^{-1}]$ , by consequence the same is true for all the coefficients  $f_i, f_{ij}, \dots$  and for  $\sigma, \sigma_e, \sigma_a$ .

It is worth noting that fitness in statistical genetics plays a similar role as energy (modulo a minus sign) in statistical mechanics. The terminology of *fitness landscape* underlines the analogy with an energy landscape:  $F(g)$  would be an Hamiltonian  $-\mathcal{H}$

in statistical physics. One can thus depict the evolutionary process of a population as an erratic motion of a point *on* the fitness landscape: contrary to what happens in an energy landscape, where the systems slides toward the valleys (min. energy), a point particle here climbs the fitness hill as much as possible (to where the expected number of offspring is highest).

*2.3.3. Mutations* The definition of mutation includes a multitude of different biological mechanism whose effect is to modify the genomic sequence. The model here considered includes single-locus swaps  $s_i \rightarrow -s_i$ . In mathematical terms one introduces an operator  $M_i$  the action of which on a genomic sequence is to swap the  $i$ -th bi-allelic gene *i.e.*

$$M_i(s_1, \dots, s_i, \dots, s_L) = (s_1, \dots, -s_i, \dots, s_L) .$$

Let also  $\mu$  be the tunable *mutation parameter* needed to weight the mutation mechanism in the model. It will be assumed to be constant in time and the same for all loci; analogously to  $\sigma$  it has dimensions  $[t^{-1}]$ , it is a rate. The mutation term in the master equation will simply take the form

$$\left. \frac{d}{dt} \right|_{mut} P(g, t) = \mu \sum_{i=1}^L [P(M_i g, t) - P(g, t)] . \quad (5)$$

*2.3.4. Recombination* Through mating and recombination, two parents  $g^{(1)}, g^{(2)}$  mix their genomic sequences giving birth to two new individuals  $g, g'$ . The mechanism we here have in mind is the crossing-over of homologous gametes during meiosis where haploid individuals produce an haploid offspring. Albeit relatively simple, this is sufficient to model some forms of bacterial recombination (transformation, transduction where material goes in both ways) as well as recombination in several RNA viruses including HIV and coronaviruses. In contrast, it cannot model some other biological mechanisms of genes-mixing, for instance bacterial conjugation. Following [39] it is convenient to introduce a set of random variables  $\{\xi_i\}$  to describe recombination by defining a crossover pattern. Consider the gene at locus  $i$  of the new individual  $g$ , if it has been inherited from  $g^{(1)}$  then  $\xi_i = 1$  while if it comes from  $g^{(2)}$  then  $\xi_i = 0$ . The sequence  $g'$  is simply complementary to  $g$ . In symbols  $g, g'$  can be written as

$$\begin{aligned} \mathbf{g} : s_i &= \xi_i s_i^{(1)} + (1 - \xi_i) s_i^{(2)} , \\ \mathbf{g}' : s'_i &= (1 - \xi_i) s_i^{(1)} + \xi_i s_i^{(2)} . \end{aligned} \quad (6)$$

Each different crossover pattern  $\{\xi_i\}$  comes with a probability  $C(\xi)$ . Similarly to the mutation case, let  $r$  be the tunable overall recombination parameter (dimensions  $[t^{-1}]$ ) which in this case can be accompanied by a relative parents-dependent rate  $Q(g^{(1)}, g^{(2)})$  (dimensionless). Collecting everything so far, it is possible to express the time variation of the genomic sequence due to recombination as

$$\left. \frac{d}{dt} \right|_{rec} P(g, t) = r \sum_{\xi, g'} C(\xi) \left[ Q(g^{(1)}, g^{(2)}) P_2(g^{(1)}, g^{(2)}, t) - Q(g, g') P_2(g, g', t) \right] , \quad (7)$$

where the sum runs over all possible recombination patterns and all possible sequences  $g'$  and  $P_2$  is the two-genome distribution (read two-particle distribution). Two more steps:

- (i) Until further notice, we set  $Q(g_\alpha, g_\beta) = 1 \forall g_\alpha, g_\beta$  which means that any genome pair has the same recombination rate  $r$ : this entails assuming of a *panmictic* population, where any individual is equally likely to interact with anyone else.
- (ii) It is hard to handle eq.(7) without a *closure*, so it will be assumed that

$$P_2(g_\alpha, g_\beta) = P(g_\alpha)P(g_\beta) , \quad (8)$$

which is valid if genomic sequences undergoing recombination are uncorrelated. The recombination process is therefore akin to a collision process in the kinetic theory of gases where eq.(8) is Boltzmann's *molecular chaos hypothesis* (or *Stoßzahlansatz*): the velocities of colliding particles are uncorrelated, and independent of position. As in Physics so in Biology (8) is *never* exactly true. In a realistic biological environment, several phenomena introduce correlations between different individuals *e.g.* competition for limited resources, geographical separation, existence of classes of individuals, or phylogenetic effects. Such correlations will be assumed to be weak enough for eq.(8) to hold approximately.

Inserting these assumptions in eq.(7),

$$\left. \frac{d}{dt} \right|_{rec} P(g, t) = r \sum_{\xi, g'} C(\xi) \left[ P(g^{(1)}, t) P(g^{(2)}, t) - P(g, t) P(g', t) \right] . \quad (9)$$

**2.3.5. Dynamics of Genotype Distribution** It is now possible to parameterize the distribution  $P(g, t) \forall g$  by its cumulants. The cumulants of first and second order are  $\chi_i = \langle s_i \rangle$  and  $\chi_{ij} = \langle s_i s_j \rangle - \langle s_i \rangle \langle s_j \rangle$ . According to this definition the one-locus second-order cumulant is  $\chi_{ii} = 1 - \chi_i^2$ . One can also define the frequency  $\nu_i(\alpha)$  of the allele  $\alpha$  at locus  $i$  and the element of the covariance matrix  $M_{ij}(\alpha, \beta)$  relative to the alleles  $\alpha, \beta$  at loci  $i, j$  as

$$\begin{aligned} \nu_i(\alpha) &= \langle \delta_{\alpha, s_i} \rangle , \\ M_{ij}(\alpha, \beta) &= \langle \delta_{\alpha, s_i} \delta_{\beta, s_j} \rangle - \langle \delta_{\alpha, s_i} \rangle \langle \delta_{\beta, s_j} \rangle , \end{aligned} \quad (10)$$

it is easy to find relations with the  $\{\chi_i, \chi_{ij}\}$  :  $\nu_i(1) = \frac{1}{2}(1 + \chi_i)$ ,  $\nu_i(-1) = \frac{1}{2}(1 - \chi_i)$  and  $M_{ij}(1, 1) = -M_{ij}(1, -1) = -M_{ij}(-1, 1) = M_{ij}(-1, -1) = \frac{1}{4}\chi_{ij}$ .

The starting point is now the full master equation for the evolution of  $P(g)$  obtained by plugging in (2), (5) and (9) into eq.(1):

$$\begin{aligned} \frac{d}{dt} P(g, t) &= [F(g) - \langle F \rangle] P(g, t) + \mu \sum_{i=1}^L [P(M_i g, t) - P(g, t)] + \\ &+ r \sum_{\xi, g'} C(\xi) \left[ P(g^{(1)}, t) P(g^{(2)}, t) - P(g, t) P(g', t) \right] , \end{aligned} \quad (11)$$

valid in the limit  $N \rightarrow \infty$ . In what follows, the  $t$  will be dropped in order to lighten the notation as much as possible. It is straightforward to obtain dynamical equations for  $\chi_i$  and  $\chi_{ij}$ , as shown below.

$\dot{\chi}_i$  . Recombination term has no effect on the dynamics of  $\chi_i$  since it does not create nor destroy alleles, but simply reshuffles them. Neglecting the last term in eq.(11) one has

$$\begin{aligned}
 \dot{\chi}_i &= \frac{d}{dt} \left( \sum_g s_i P(g) \right) \\
 &= \sum_g s_i \frac{d}{dt} P(g) \\
 &= \sum_g \left( s_i [F(g) - \langle F \rangle] P(g) + \mu s_i \sum_{j=1}^L [P(M_j g) - P(g)] \right) \\
 &= \langle s_i [F(g) - \langle F \rangle] \rangle - 2\mu \langle s_i \rangle ,
 \end{aligned} \tag{12}$$

where the last line follows from  $\sum_g s_i P(M_j g) = (-1)^{\delta_{ij}} \langle s_i \rangle$  .

$\dot{\chi}_{ij}$  . The dynamic of the second order cumulant (and in general all higher order cumulants) involves the recombination term. As a preliminary result, let us evaluate the time derivative of  $\langle s_i s_j \rangle$  under the recombination term alone †:

$$\begin{aligned}
 \left. \frac{d}{dt} \right|_{rec} \langle s_i s_j \rangle &= \sum_{\xi, g, g'} C(\xi) s_i s_j \left[ P(g^{(1)}) P(g^{(2)}) - P(g) P(g') \right] \\
 &\stackrel{(a)}{=} \sum_{\xi, g^{(1)}, g^{(2)}} \left[ C(\xi) (\xi_i s_i^{(1)} + (1 - \xi_i) s_i^{(2)}) \times \right. \\
 &\quad \left. \times (\xi_j s_j^{(1)} + (1 - \xi_j) s_j^{(2)}) P(g^{(1)}) P(g^{(2)}) \right] + \\
 &\quad - \sum_{\xi, g, g'} C(\xi) s_i s_j P(g) P(g') \\
 &= \sum_{\xi} C(\xi) \left[ \xi_i \xi_j \langle s_i s_j \rangle + \xi_i (1 - \xi_j) \langle s_i \rangle \langle s_j \rangle + \right. \\
 &\quad \left. + (1 - \xi_i) \xi_j \langle s_i \rangle \langle s_j \rangle + (1 - \xi_i) (1 - \xi_j) \langle s_i s_j \rangle - \langle s_i s_j \rangle \right] \\
 &= \langle s_i s_j \rangle \sum_{\xi} C(\xi) (1 - \xi_i - \xi_j + \xi_i \xi_j - 1) + \\
 &\quad + \langle s_i \rangle \langle s_j \rangle \sum_{\xi} C(\xi) (\xi_i (1 - \xi_j) - (1 - \xi_i) \xi_j) \\
 &\stackrel{(b)}{=} -c_{ij} \chi_{ij} .
 \end{aligned} \tag{13}$$

In (a) we have used eq.(6) and changed the first sum over  $g, g'$  in a sum over  $g^{(1)}, g^{(2)}$ ; in (b) we have exploited the definition of  $\chi_{ij}$  and a new characteristic quantity has been introduced

$$c_{ij} = \sum_{\xi} C(\xi) (\xi_i (1 - \xi_j) + (1 - \xi_i) \xi_j) . \tag{14}$$

† The reader will easily notice how, following the same steps of this derivation but in the easier case of a single  $\langle s_i \rangle$ , one gets  $\left. \frac{d}{dt} \right|_{rec} \langle s_i \rangle = 0$ .

Now, for  $i \neq j$ ,

$$\begin{aligned}
\dot{\chi}_{ij} &= \frac{d}{dt}(\langle s_i s_j \rangle - \chi_i \chi_j) \\
&= \frac{d}{dt} \langle s_i s_j \rangle - \dot{\chi}_i \chi_j - \chi_i \dot{\chi}_j \\
&\stackrel{(a)}{=} \langle s_i s_j [F(g) - \langle F \rangle] \rangle + \mu \sum_g s_i s_j \sum_{k=1}^L [P(M_k g) - P(g)] + r \frac{d}{dt} \Big|_{rec} \langle s_i s_j \rangle \\
&\quad + 4\mu \chi_i \chi_j - \langle s_i [F(g) - \langle F \rangle] \rangle \chi_j - \chi_i \langle s_j [F(g) - \langle F \rangle] \rangle \\
&\stackrel{(b)}{=} \langle (s_i - \chi_i)(s_j - \chi_j)[F(g) - \langle F \rangle] \rangle - 4\mu \langle s_i s_j \rangle + r \frac{d}{dt} \Big|_{rec} \langle s_i s_j \rangle + 4\mu \chi_i \chi_j \\
&\stackrel{(c)}{=} \langle (s_i - \chi_i)(s_j - \chi_j)[F(g) - \langle F \rangle] \rangle - 4\mu \chi_{ij} - r c_{ij} \chi_{ij} . \tag{15}
\end{aligned}$$

In (a) we have used eq.(11-12); in (b) we exploited  $\sum_g s_i s_j P(M_k g) = (-1)^{\delta_{ik} + \delta_{jk}} \langle s_i s_j \rangle$  and added  $\chi_i \chi_j \langle F(g) - \langle F \rangle \rangle = 0$ ; (c) comes again from the definition of  $\chi_{ij}$  and from eq.(13).

It is important to underline that so far no specific choice has been made for  $P(g)$ . Let us add a few comments on the results above.

- $c_{ij}$  . Given the definition eq.(14),  $c_{ij}$  can be easily interpreted as the probability that, in the offspring, the alleles at the two loci  $i, j$  come from different parents. When recombinations are completely random, we clearly expect  $c_{ij} = 1/2 \forall i, j$ . One can try to model  $c_{ij}$  as follows.
  - **Crossover rate.** One easy scheme for  $c_{ij}$  is to assume that, if there is recombination between two genomes, then each locus undergoes a crossover with probability  $\omega$ , called *crossover rate*; one gets  $c_{ij} = 2\omega(1 - \omega)$ . In this first model the coefficient  $c_{ij}$  ignores any spatial effect, it is the same for all pairs  $i, j$ , regardless of their position in the genome (could they be neighbours or very far apart); this is certainly not biologically realistic in most settings.
  - **Neighbouring variability.** If two loci are very far apart then they can be expected to be mostly uncorrelated, hence one may introduce a penalization for genomic distance [40]. Here we assume a fixed probability  $\rho$  that a recombination causes a crossover between any pair of neighbouring loci. The simplification with respect to Biology is that loci of variability can be spaced unevenly along a genome, and that recombination may happen at a higher rate at certain genomic positions ("recombination hot-spots"). After the recombination event, each two neighbouring loci will come from the same parent with probability  $P(SP) = 1 - \rho$ , from different parents with probability  $P(DP) = \rho$ . As a first approximation, the number of such *SP/DP* events for neighbors along the genomic chain can be assumed to be binomial distributed: the probability that we find a number  $k$  of *DP* events is  $P(k; n, \rho) = \binom{n}{k} \rho^k (1 - \rho)^{n-k}$ . To get the total probability that alleles at  $i, j$  are different after a recombination, it is sufficient to sum  $P(k; n, \rho)$  over



all odd  $k$ :

$$\begin{aligned}
 c_{ij} &= \sum_{k \text{ odd}}^n \binom{n}{k} \rho^k (1-\rho)^{n-k} \\
 &= \frac{1}{2} \left[ \sum_{k=0}^n \binom{n}{k} \rho^k (1-\rho)^{n-k} - \sum_{k=0}^n \binom{n}{k} (-\rho)^k (1-\rho)^{n-k} \right] \\
 &= \frac{1}{2} [(\rho + (1-\rho))^n - (-\rho + (1-\rho))^n] \\
 &= \frac{1}{2} [1 - (1-2\rho)^n] \\
 &\simeq \frac{1}{2} [1 - e^{-2\rho|i-j|}], \tag{16}
 \end{aligned}$$

where the last line holds if  $\rho|i-j| \sim 1$  and  $|i-j| \gg 1$ . In the limit  $|i-j| \rightarrow \infty$  one finds (consistently)  $c_{ij} \sim 1/2$ .

- **Linkage (dis)equilibrium.** The words *linkage disequilibrium* (LD) stand for a non-random association of alleles at two or more loci [41]. Contrary to what the name may suggest, LD does not ensure either linkage or a lack of equilibrium. Focusing on LD for a pair of loci, several definitions have been proposed - for instance as  $M_{ij}(\alpha, \beta)$  defined in eq.(10) - but all of them are obviously related to the quantity  $\chi_{ij} = \langle s_i s_j \rangle - \chi_i \chi_j$ . The absence of correlation  $\chi_{ij} = 0 \forall i \neq j$  is termed *linkage equilibrium* (LE) and implies no correlations between loci. If the population only evolves under mutation and recombination then  $\chi_{ij}$  tends to zero. The KNS model provides us with a law for the evolution of this last quantity, namely eq.(15), from which we see how selection drives  $\chi_{ij}$  away from zero, while mutations and recombination act in the opposite way. The tendency of natural selection is indeed to fix the most fit alleles in a population. If this process is run to completion all individuals are identical and variability is lost. In that limit of extreme LD the population may be said to be in a (trivial) state of linkage equilibrium, as all quantities  $\chi_{ij}$  vanish. Between LE and LD there is an intermediate phase of weak and steady correlations between loci called *quasi-linkage equilibrium* (QLE), which we discuss in Sec.(4).

### 3. Direct Coupling Analysis (DCA) for Statistical Genetics

In the context of Statistical Inference statistics the task of Direct Coupling Analysis (DCA) is to find the parameters in a family of generating functions like the exponential family of the Gibbs-Boltzmann distributions in equilibrium statistical mechanics [42, 43]. While maximum likelihood and analogous Bayesian point estimate methods are feasible for small enough instances, for larger instances these become computationally demanding. A number of alternative inference methods have therefore been proposed, of which the most widely used are mean-field or variational methods [42, 44], and pseudo-likelihood maximization [45, 46].

From the view of computational biology DCA was proposed as a general data analysis tool motivated by maximum-entropy arguments *e.g.* in [47]. A major breakthrough was made in relating the parameters in a model inferred from protein sequences in the same family to physical proximity of residues in the common protein structure. The first result in this direction was obtained already in 2002 [48], but the

paper was never accepted for publication in a major journal, and was therefore for a long time not widely known. The second result [49], independently obtained, relied on a computationally demanding version of DCA built on Belief Propagation [50] and was therefore first not widely appreciated for that reason. At about the same time residue-residue contacts were derived from tables of sequences by another method not explicitly in the DCA family, and also fairly computationally expensive [51].

The first result of DCA to predict residue-residue contacts and which had wide resonance used mean-field inference [52], which has remained one of the most popular approaches, and which will be reviewed below. DCA built on mean-field inference using other regulation schemes were introduced in [53–55]. The second main type of DCA is built on pseudo-likelihood maximization [56–58] which will also be reviewed below. More recent algorithms of the same general type as pseudo-likelihood were introduced in [59–61] and are known to exhibit better performance on some model problems.

Later versions of DCA on the protein structure prediction problem were typically meta-algorithms incorporating also other information sources [62–66]; although exhibiting higher performance they (and other DCA methods) have more recently been overtaken by AI/deep learning methods in this application [67, 68]. For other biological inference tasks with less abundant number of training examples and/or where the goal is uncover new biology DCA, usually either mean-field of psuedolikelihood, remains an important tool *cf.* [69–75]. The applications of DCA and DCA-like techniques to biology has been reviewed multiple times *e.g.* [7, 76–78].

### 3.1. Inverse Ising Problem (IIP)

Let us consider an Ising model with  $L$  binary spin variables<sup>‡</sup>  $s_i = \pm 1$ , with  $i = 1, \dots, L$ . The Hamiltonian for an Ising system reads

$$\mathcal{H}_{\mathbf{J}, \mathbf{h}}(\mathbf{s}) = - \sum_i h_i s_i - \sum_{i < j} J_{ij} s_i s_j, \quad (17)$$

where the  $\mathbf{J}$  are the pairwise couplings between the spin variables ( $J_{ii} = 0 \forall i$ ) and the  $\mathbf{h}$  are the local magnetic fields; they are collectively referred as the *parameters* of the Ising problem. Under equilibrium conditions, the probability of a configuration  $\mathbf{s}$  is the Boltzmann distribution

$$p(\mathbf{s}) = \frac{1}{\mathcal{Z}} e^{-\mathcal{H}_{\mathbf{J}, \mathbf{h}}(\mathbf{s})} . \quad (18)$$

The inverse temperature  $\beta$  has been set to 1, this implies no loss of generality since in eq.(18) only the products  $\beta h_i$  and  $\beta J_{ij}$  appear. The normalization  $\mathcal{Z}$  is the standard partition function

$$\mathcal{Z}(\mathbf{J}, \mathbf{h}) = \sum_{\mathbf{s}} e^{-\mathcal{H}_{\mathbf{J}, \mathbf{h}}(\mathbf{s})} . \quad (19)$$

The general expression for the expected value of a function  $Q(\boldsymbol{\sigma})$  of the spin variables is

$$\langle Q(\boldsymbol{\sigma}) \rangle = \sum_{\mathbf{s}} p(\mathbf{s}) Q(\mathbf{s}) ; \quad (20)$$

<sup>‡</sup>We use the notation  $s_i$  for a realization of the spin variable and  $\sigma_i$  indicates the spin random variable. When it is not confusing, the bold notation will indicate the whole set of spin variables  $\mathbf{s} = \{s_i\}$ . Analogously meaning for the bold notation for other quantities, *e.g.*  $\mathbf{J}, \mathbf{h}$ .

In Sec. 2.3.5 we have already assigned the notations  $\chi_i = \langle \sigma_i \rangle$  for the first order cumulant and  $\chi_{ij} = \langle \sigma_i \sigma_j \rangle - \chi_i \chi_j$  for the second order cumulant. In this chapter it will be more convenient to use the moments instead, the first ones being the same  $\chi_i$  as the first cumulants, the second ones defined as  $\phi_{ij} = \langle \sigma_i \sigma_j \rangle = \chi_{ij} + \chi_i \chi_j$ , see Appendix A. In the present context,  $\{\chi_i\}$  are the equilibrium magnetizations while  $\{\phi_{ij}\}$  are the *pair correlations*. In the Forward Ising Problem the parameters  $\mathbf{J}, \mathbf{h}$  of the Boltzmann distribution eq.(18) are known and the job is to compute statistical observables *e.g.*  $\chi_i, \phi_{ij}$ . In an *Inverse Ising Problem* (IIP) the paradigm is reversed:

**Statement of the Inverse Ising Problem (IIP):** *Let  $D = \{\mathbf{s}^m\}$ ,  $m = 1, \dots, M$  be a set of independent samples of spin configurations of an Ising system the parameters of which are unknown. The goal of the IIP is to infer the parameters from  $D$ .*

The IIP defined this way is also referred to as equilibrium Inverse Ising Problem. The problem of inferring the parameters of a kinetic Ising model, which may or may not satisfy detailed balance, is then analogously referred to a non-equilibrium Inverse Ising Problem. Depending on the kind of data available (a time series or not a time series) the non-equilibrium problem can be substantially easier or much harder than the equilibrium version, for more details, see [7, 43]. In this work we only deal with the equilibrium reconstruction, therefore from now on this specification will be implied.

*3.1.1. Thermodynamics of the IIP* The purpose of this subsection is to make the connection to the terminology of statistical mechanics. As noted above, temperature is not a pertinent concept for the inverse problem, as it cannot be separated from an overall scale of the model parameters. The starting point is thus Helmholtz free energy at a temperature which can conventionally be taken to be:

$$\mathcal{F}(\mathbf{J}, \mathbf{h}) = -\log \mathcal{Z}(\mathbf{J}, \mathbf{h}) , \quad (21)$$

In the forward problem, the first and second order moments can be evaluated by means of simple derivatives of eq.(21):

$$\chi_i = -\frac{\partial \mathcal{F}}{\partial h_i}(\mathbf{J}, \mathbf{h}) ; \quad \phi_{ij} = -\frac{\partial \mathcal{F}}{\partial J_{ij}}(\mathbf{J}, \mathbf{h}) = \frac{\partial \mathcal{F}}{\partial h_i}(\mathbf{J}, \mathbf{h}) \frac{\partial \mathcal{F}}{\partial h_j}(\mathbf{J}, \mathbf{h}) - \frac{\partial^2 \mathcal{F}}{\partial h_i \partial h_j}(\mathbf{J}, \mathbf{h}) \quad (22)$$

In the thermodynamical version of IIP the roles of the parameters  $\mathbf{J}, \mathbf{h}$  and the observables  $\phi, \chi$  are reversed: the latter are now fixed, the former to be determined. We seek accordingly a thermodynamic potential which is function of the observables and from which we can compute the parameters by means of simple derivatives, similarly to what is done in eq.(22) for the forward problem. As first noted in [79], such potential can be obtained by operating a Legendre transform of the Helmholtz free energy with respect to both couplings and fields:

$$\mathcal{S}(\phi, \chi) = \min_{\mathbf{J}, \mathbf{h}} \left[ -\sum_i h_i \chi_i - \sum_{i < j} J_{ij} \phi_{ij} - \mathcal{F}(\mathbf{J}, \mathbf{h}) \right] , \quad (23)$$

which can be seen to be the Shannon entropy function for the distribution eq.(18), see Appendix E. To see how the parameters of the Ising model follow from the latter, we perform the inverse transformation (*i.e.* again a Legendre transform, which is its own inverse) to write

$$\mathcal{F}(\mathbf{J}, \mathbf{h}) = \min_{\phi, \chi} \left[ -\sum_i h_i \chi_i - \sum_{i < j} J_{ij} \phi_{ij} - \mathcal{S}(\phi, \chi) \right] ; \quad (24)$$

setting the derivatives of the term in the square brackets to zero one gets

$$J_{ij} = -\frac{\partial \mathcal{S}}{\partial \phi_{ij}}(\boldsymbol{\phi}, \boldsymbol{\chi}), \quad h_i = -\frac{\partial \mathcal{S}}{\partial \chi_i}(\boldsymbol{\phi}, \boldsymbol{\chi}). \quad (25)$$

However, from eq.(22) we see that the derivatives of the Helmholtz free energy with respect to  $\mathbf{J}$  can be expressed in terms of those with respect to  $\mathbf{h}$ , therefore it is sufficient to operate a Legendre transform of the latter set. The Gibbs free energy can be defined accordingly as

$$\mathcal{G}(\mathbf{J}, \boldsymbol{\chi}) = \max_{\mathbf{h}} \left[ \sum_i h_i \chi_i + \mathcal{F}(\mathbf{J}, \mathbf{h}) \right] \quad (26)$$

*i.e.*  $\mathcal{G}(\mathbf{J}, \boldsymbol{\chi})$  is defined to be minus the Legendre transform of  $\mathcal{F}(\mathbf{J}, \mathbf{h})$  with respect to  $\mathbf{h}$ , in view of the relation  $\min f = -\max(-f)$ . The magnetic fields can readily be computed with

$$h_i = \frac{\partial \mathcal{G}}{\partial \chi_i}(\mathbf{J}, \boldsymbol{\chi}). \quad (27)$$

A great interest is in the second derivative of  $G$  with respect to the magnetizations

$$\frac{\partial^2 \mathcal{G}}{\partial \chi_i \partial \chi_j}(\mathbf{J}, \boldsymbol{\chi}) = \frac{\partial h_i}{\partial \chi_j}(\mathbf{J}, \boldsymbol{\chi}) \stackrel{(a)}{=} (\chi^{-1})_{ij}, \quad (28)$$

where in (a) we have used the inverse function theorem  $\left[ \frac{\partial \mathbf{h}}{\partial \boldsymbol{\chi}} \right]_{ij} = \left[ (\frac{\partial \boldsymbol{\chi}}{\partial \mathbf{h}})^{-1} \right]_{ij}$  and the linear response theory to relate the second order cumulant  $(\chi)_{ij} = \chi_{ij} = \partial \chi_j / \partial h_i(\mathbf{J}, \mathbf{h})$  to the susceptibility of the magnetization to a variation in the magnetic field [44]. Eq.(28) is at the basis of *naive mean-field inference*: the RHS can be computed from data and, if  $\mathcal{G}$  is known, the corresponding system of equations can be solved yielding the couplings  $\mathbf{J}$ .

Many of these methods are based on a *variational principle*; for the case of the Gibbs free energy it reads

$$\mathcal{G}(\mathbf{J}, \boldsymbol{\chi}) = \max_{\mathbf{h}} \left\{ \sum_i h_i \chi_i + \min_q \{U[q] - \mathcal{S}[q]\} \right\}, \quad (29)$$

which comes from eq.(26) and from the variational principle for the Helmholtz free energy

$$\mathcal{F}(\mathbf{J}, \mathbf{h}) = \min_q \{U[q] - \mathcal{S}[q]\} = \min_q \mathcal{F}[q] : \quad (30)$$

here  $q$  is a probability distribution for the spin configurations,  $U[q] = \langle \mathcal{H} \rangle_q$  and  $\mathcal{S}[q] = -\langle \log q \rangle_q$ . Eq.(30) in turn stems from asking the Kullback-Leibler distance  $D_{KL}(q||p)$  between the trial distribution  $q$  and the Boltzmann distribution  $p$  to be minimal, Appendix E. The usefulness of this approach lies in the fact that one may want to put constraints on  $q$  *i.e.* to focus on a particular family of trial distributions  $q$ , hence obtaining an upper bound for  $\mathcal{F}(\mathbf{J}, \mathbf{h})$ . As a final remark, we observe that when  $q$  is taken from the set  $\mathcal{G}$  of distributions for which  $\langle \sigma_i \rangle_q = \chi_i$ , the double extremum problem eq.(29) is equivalent to the single conditional minimization

$$\mathcal{G}(\mathbf{J}, \boldsymbol{\chi}) = \min_{q \in \mathcal{G}} \left\{ -\sum_{i < j} J_{ij} \langle \sigma_i \sigma_j \rangle_q - \mathcal{S}[q] \right\}. \quad (31)$$

### 3.2. Maximum Likelihood for the IIP

We here by describe the maximum likelihood for IIP. According to this criterion the best estimate  $\theta^{ML}$  based on the available data is given by

$$\theta^{ML} = \arg \max_{\theta} p(x_1, \dots, x_M | \theta) . \quad (32)$$

In a Bayesian context eq.(32) is a point estimate (one predicted parameter value) assuming a flat (information-free) *prior* information  $p(\theta)$  on the parameter. To avoid dealing with small numbers, it is common practice to maximize the logarithm of the likelihood, which has no consequences on the result: since the logarithm is a strictly monotonic function, the arg max is preserved. The log-likelihood per sample

$$\mathcal{L}_D(\mathbf{J}, \mathbf{h}) = \frac{1}{M} \log p(D | \mathbf{J}, \mathbf{h}) \quad (33)$$

is for the Ising parameters  $\mathbf{J}, \mathbf{h}$  upon measurement of  $M$  independent samples  $D = \{\mathbf{s}^m\}$  of the Boltzmann distribution eq.(18):

$$\begin{aligned} \mathcal{L}_D(\mathbf{J}, \mathbf{h}) &= \sum_i h_i \frac{1}{M} \sum_m s_i^m + \sum_{i < j} J_{ij} \frac{1}{M} \sum_m s_i^m s_j^m - \log \mathcal{Z}(\mathbf{J}, \mathbf{h}) \\ &= \sum_i h_i \langle \sigma_i \rangle^D + \sum_{i < j} J_{ij} \langle \sigma_i \sigma_j \rangle^D - \log \mathcal{Z}(\mathbf{J}, \mathbf{h}) , \end{aligned} \quad (34)$$

where  $\langle Q \rangle^D = \frac{1}{M} \sum_m Q(\mathbf{s}^m)$  is the *sample average* of the function  $Q(\mathbf{s}^m)$  of the spin variables  $\mathbf{s}^m$ . Nothing but the sample averages  $\langle \sigma_i \rangle^D, \langle \sigma_i \sigma_j \rangle^D$  is needed from data to determine eq.(34) *i.e.* they are *sufficient statistics* for this problem. Maximum likelihood solution of the inverse Ising Problem can schematically be written

$$\{\mathbf{J}^{ML}, \mathbf{h}^{ML}\} = \arg \max_{\mathbf{J}, \mathbf{h}} \mathcal{L}_D(\mathbf{J}, \mathbf{h}) . \quad (35)$$

where the superscript indicates the criterion/method. *Boltzmann machine learning* is a gradient-descent algorithm with an adjustable learning rate  $\eta$  so that at equilibrium (converged values) one has

$$0 = \frac{\partial \mathcal{L}_D}{\partial h_i}(\mathbf{J}^n, \mathbf{h}^n) = \langle \sigma_i \rangle^D - \langle \sigma_i \rangle , \quad (36)$$

$$0 = \frac{\partial \mathcal{L}_D}{\partial J_{ij}}(\mathbf{J}^n, \mathbf{h}^n) = \langle \sigma_i \sigma_j \rangle^D - \langle \sigma_i \sigma_j \rangle . \quad (37)$$

The disadvantage of Boltzmann machine learning is that one has to estimate ensemble averages which is computationally costly, and that convergence may be slow.

### 3.3. Approximate Methods for the IIP

**3.3.1. Mean Field inference for the Inverse Ising Problem** Mean-field inference is based on an assumption that the distribution is in the simpler class of factorizable distributions. The first step is thus to assume a trial distribution of the form

$$p^{MF}(\mathbf{s}) = \prod_i \frac{1 + \tilde{\chi}_i s_i}{2} , \quad (38)$$

where different spins are independent variables and the *effective* magnetization  $\tilde{\chi}_i$  results from both the local field  $h_i$  and from the couplings  $J_{ij}$  with all other spins. We recall that the set  $\mathcal{G}$  of distributions  $q$  over which the minimization operated is the one for which  $\langle \sigma_i \rangle_q = \chi_i$ ; in the MF case,  $\tilde{\chi}_i = \chi_i$ . The minimization is trivial, since there is only one mean-field distribution eq.(38) in  $\mathcal{G}$ , therefore

$$\mathcal{G}^{MF}(\mathbf{J}, \boldsymbol{\chi}) = - \sum_{i < j} J_{ij} \chi_i \chi_j + \sum_i \left[ \frac{1 + \chi_i}{2} \log \frac{1 + \chi_i}{2} + \frac{1 - \chi_i}{2} \log \frac{1 - \chi_i}{2} \right]. \quad (39)$$

By the variational equation eq.(27) one has for the fields  $h_i$

$$h_i^{MF} = - \sum_{j \neq i} J_{ij} \chi_j + \frac{1}{2} \frac{1 + \chi_i}{1 - \chi_i} = - \sum_{j \neq i} J_{ij} \chi_j + \text{arc tanh } \chi_i. \quad (40)$$

Since  $p^{MF}$  does not depend on interactions between spins, one more ingredient is needed to infer the couplings  $J_{ij}$  and the above is not yet defined. This is done by using correlation-response which for the Ising model is

$$(\chi)_{ij} = \frac{\partial \chi_i}{\partial h_j} \quad (41)$$

Combining the exact result (41) and the approximation (40) we find for  $i \neq j$ ,

$$J_{ij}^{MF} = -(\chi^{-1})_{ij}; \quad (42)$$

One can then insert backwards this inferred value  $J_{ij}^{MF}$  into (40) to get  $h_i^{MF}$ . This mean field inference scheme can be improved in two different directions. On the one hand one can modify the thermodynamic potential, either by adding a Onsager reaction term as in *Thouless-Anderson-Palmer* [80] or by a systematic expansion (Plevka expansion) in interaction strength [81]. On the other hand a more detailed model than (38) can be used, see for instance [82]. For a unified treatment, see [43].

*3.3.2. Pseudolikelihood Maximization for the Inverse Ising Problem* The second method discussed here is the Pseudo-Likelihood Maximization (PLM). The starting point this time is not a thermodynamic potential, instead we directly exploit the structure of the Ising Hamiltonian  $\mathcal{H}$  eq.(17) as follows. Consider a particular spin variable  $\sigma_i$  and distinguish the part  $\mathcal{H}_i$  of the Hamiltonian that depends on  $\sigma_i$  from the rest, that we collectively indicate with  $\mathcal{H}_{\setminus i}$ :

$$\begin{aligned} \mathcal{H}(\mathbf{s}) &= \mathcal{H}_i + \mathcal{H}_{\setminus i} \\ &= -h_i s_i - \sum_{j \neq i} J_{ij} s_i s_j + \mathcal{H}_{\setminus i}(\mathbf{s}_{\setminus i}). \end{aligned} \quad (43)$$

Summing up explicitly the terms related to  $\sigma_i$  in the partition function eq.(19),

$$\mathcal{Z}(\mathbf{J}, \mathbf{h}) = \sum_{\mathbf{s}_{\setminus i}} 2 \cosh \left( h_i + \sum_j J_{ij} s_j \right) e^{-\mathcal{H}_{\setminus i}(\mathbf{s}_{\setminus i})}, \quad (44)$$

and from eq.(22) one gets the first and second moments (one and two spin expectations) involving  $\sigma_i$ , by simple derivatives with respect to the parameters:

$$\langle \sigma_i \rangle = \left\langle \tanh \left( h_i + \sum_{j \neq i} J_{ij} \sigma_j \right) \right\rangle, \quad (45)$$

$$\langle \sigma_i \sigma_j \rangle = \left\langle \sigma_j \tanh \left( h_i + \sum_{k \neq i} J_{ik} \sigma_k \right) \right\rangle. \quad (46)$$

The average in the RHS of the last equations is over the entire Boltzmann distribution eq.(18) and these are still exact equations. The approximation is implemented in the next step, substituting the (computationally prohibitive) averages in eq.(45 - 46) with sample averages, labelled with the superscript  $D$ :

$$\langle \sigma_i \rangle^D = \left\langle \tanh \left( h_i^{PL} + \sum_{j \neq i} J_{ij}^{PL} \sigma_j \right) \right\rangle^D, \quad (47)$$

$$\langle \sigma_i \sigma_j \rangle^D = \left\langle \sigma_j \tanh \left( h_i^{PL} + \sum_{k \neq i} J_{ik}^{PL} \sigma_k \right) \right\rangle^D. \quad (48)$$

The simplification is self-evident: eq.(47 - 48) are a system of non-linear equations in the  $L$  variables  $h_i^{PL}, \{J_{ij}^{PL}\}_{j \neq i}$  that can be solved with standard methods. The net effect of the approximation hence is to split the problem of estimating  $L^2$  parameters (fields and couplings) in  $L$  separate problems, each of them involving only  $L$  parameters.

A different but equivalent interpretation of this approximation scheme is the following: let  $\sigma_i$  be a spin variable, consider the conditional probability of  $s_i$  under the observation of the other variables  $\mathbf{s}_{\setminus i}$

$$p(s_i | \mathbf{s}_{\setminus i}) = \frac{1}{1 + e^{-2s_i(h_i + \sum_{j \neq i} J_{ij} s_j)}} = \frac{1}{2} \left[ 1 + s_i \tanh \left( h_i + \sum_{j \neq i} J_{ij} s_j \right) \right] \quad (49)$$

which depends only on the field  $h_i$  and on the couplings  $\{J_{ij}\}_{j \neq i}$ . The last quantities also appear in the log-likelihood per sample  $\mathcal{L}_D^i$  for the last distribution of probability, which reads

$$\mathcal{L}_D^i(J_{i*}, h_i) = \frac{1}{M} \sum_m \log \frac{1}{2} \left[ 1 + s_i^m \tanh \left( h_i + \sum_{j \neq i} J_{ij} s_j^m \right) \right], \quad (50)$$

cf eq.(33), we used the notation  $J_{i*} = \{J_{ij}\}_{j \neq i}$ . eq.(47 - 48) simply follow from setting the derivatives of  $\mathcal{L}_D^i$  with respect to  $h_i$  and  $\{J_{ij}\}_{j \neq i}$  to zero, hence they are found to maximize the log-likelihood. Altogether, one might define the so-called *pseudolikelihood* as

$$\mathcal{L}^{PL}(\mathbf{J}, \mathbf{h}) = \sum_i \mathcal{L}_D^i(J_{i*}, h_i) \quad (51)$$

whose maximization yields the whole set of Ising parameters. Note that in general for the inferred couplings  $J_{ij} \neq J_{ji}$ , even if the underlying model has symmetric couplings, due to sampling noise; in the latter case, a practical solution is to use the average  $\frac{1}{2}(J_{ij} + J_{ji})$ .

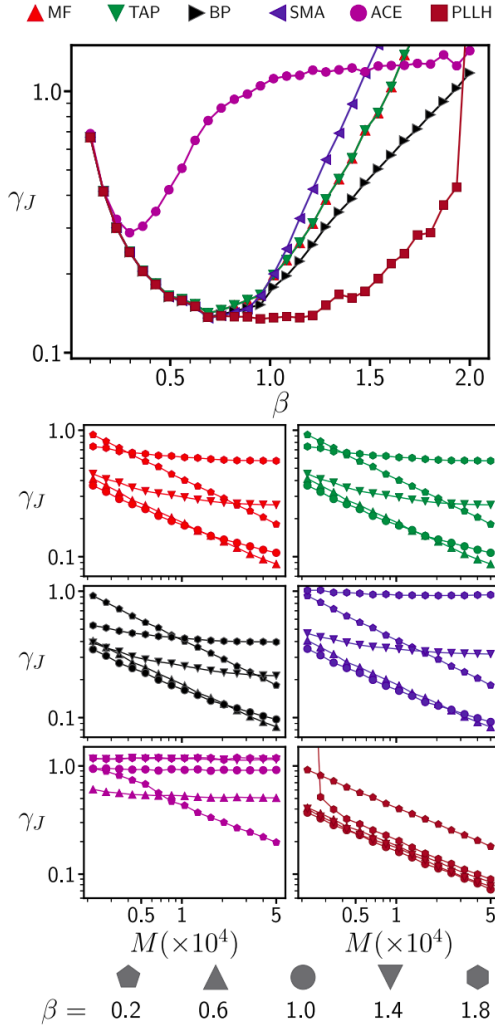


Figure 2: Reconstruction of a fully connected Ising model. Both panels show the reconstruction error as in eq.(52), in the upper one  $\gamma_J(\beta)$  for  $M = 15000$ , in the lower one  $\gamma_J(M)$  for different values of  $\beta$ .  $L = 64$ . Results are shown for the following approximations: **Mean Field (MF)**, TAP reconstruction (TAP), Bethe-Peierls method (BP), Sessak-Monasson method (SMA), Adaptive Cluster Expansion (ACE), **Pseudolikelihood Maximization (PLLH)**. Figure taken from [43], reproduced here with permission from J. Berg and Taylor & Francis Ltd ([www.tandfonline.com](http://www.tandfonline.com)).

**3.3.3. MF vs PLM** A standard procedure to test an approximate solution of the IIP (especially for uncontrolled ones) is to simulate data from an Ising model with known fields and couplings, then compare the results of the inference with the input values of the parameters. As mentioned above, the reconstruction errors depend on many factors (network topology of the couplings, ergodicity of the system...), we here focus on the dependence on the size  $M$  of the dataset  $D$  and on the coupling strength, by re-establishing and tuning the inverse temperature  $\beta$  in eq.(18). The high temperature limit  $\beta \rightarrow 0$  hence corresponds to that of low couplings/fields and vice versa. In Fig.2 the performance of several inverse techniques are shown. The underlying data are generated from a Sherrington-Kirkpatrick model where  $J_{ij} \sim \mathcal{N}(0, \beta/\sqrt{L})$  and a fully connected graph of interactions is assumed. For each couple  $(\beta, M)$ ,  $10^4 L$  Monte Carlo steps with Metropolis transition rule are used to reach an equilibrium state and collect the samples. Let  $J_{ij}^0$  be the input parameters of the simulation, the reconstruction



error  $\gamma_J$  can be quantified as follows:

$$\gamma_J = \sqrt{\frac{\sum_{i<j} (J_{ij} - J_{ij}^0)^2}{\sum_{i<j} (J_{ij}^0)^2}}. \quad (52)$$

Overall, it is possible to see that the PLM approximation yields a more accurate reconstruction of the model parameters with respect to the MF theory; the latter is indeed known to overestimate large couplings. In the top panel, all methods equally fail for  $\beta \rightarrow 0$ , since for too low coupling strengths the reconstruction is democratically hampered by sampling noise. On the other hand, for sufficiently high  $\beta$  the approximations on which our methods are based break down and the errors blow up, a possible cause being the ergodicity breaking for strong coupling. As for the dependence on  $M$ , differently from the MF, in a PLM algorithm the reconstruction error can always be compensated by a larger dataset, which leads to the polynomial behaviour shown in the lower panel for all the tested values of  $\beta$ . If the true couplings are not known a priori - this is usually the case with real data -, one possibility might be to try different methods and compare the likelihood of the resulting parameters, the better techniques resulting in higher likelihoods; alternatively, one can compare the statistics resulting from data generated from reconstructed parameters with those observed.

#### 4. Quasi-Linkage Equilibrium (QLE)

The goal of this section is to leverage the DCA inference methods described above to learn about the fitness landscape of an (observed) evolving population. In contrast to a maximum-entropy approach, it will be assumed that distributions over genotypes in a population are actually of the Gibbs-Boltzmann type, an assumption justified for an evolving population in the so-called Quasi Linkage Equilibrium (QLE) state. Technically it is still needed to infer parameters of a Gibbs-Boltzmann distribution from samples, which is the same task solved by DCA.

##### 4.1. QLE in the KNS theory

The last ingredient needed in master eq.(11) is a precise mathematical form for the distribution  $P(g)$ . The fundamental insight came from the pioneering work of Motoo Kimura in 1965 [38], who showed that in a population genetics model which includes recombination, if selection is weak on the time scale of recombination  $\sigma \ll r$  then the allele frequencies change slowly and the selection-induced correlations are weak, steady and can be treated as perturbations. Such a state for a population Kimura termed *quasi-linkage equilibrium* (QLE). In [39], the authors consider instead the problem on the genome scale and not only for one pair of loci. In particular, the following *ansatz* is introduced for the parameterization of the one-genome probability distribution:

$$P(g, t) = \frac{1}{\mathcal{Z}(t)} \exp \left( \sum_i h_i(t) s_i + \sum_{i<j} J_{ij}(t) s_i s_j \right) \quad (53)$$

Eq. (53) is the Gibbs-Boltzmann distribution of an Ising model with time dependent parameters. The factor  $\mathcal{Z}(t) = \sum_g \exp(\sum_i h_i(t) s_i + \sum_{i<j} J_{ij}(t) s_i s_j)$  is a normalization (partition function) while  $h_i(t)$  and  $J_{ij}(t)$  are time dependent single-site

and pairwise coefficients (external magnetic fields and interactions), respectively; the  $t$  will be dropped in the following.

The QLE hypothesis is implemented here: the second order terms  $\{J_{ij}\}$  capture to the leading order the correlations induced by selection, hence they are assumed to be small. The exponential distribution in eq.(53) satisfies (like all equilibrium distributions in statistical physics) a *maximum entropy principle* [83]: it is the one that maximizes information (Shannon entropy) under the constraints of having  $\{\chi_i\}$  and  $\{\chi_{ij}\}$  as first and second order cumulants, see Sec.(3) and Appendix E. The following relations hold:

$$\chi_i = \frac{\partial \log \mathcal{Z}}{\partial h_i}, \quad \chi_{ij} = \frac{\partial^2 \log \mathcal{Z}}{\partial h_i \partial h_j}. \quad (54)$$

These quantities can be evaluated in the QLE regime. We first evaluate perturbatively the partition function,

$$\begin{aligned} \mathcal{Z} &= \sum_g e^{\sum_i h_i s_i + \sum_{i<j} J_{ij} s_i s_j} \\ &\stackrel{(a)}{\sim} \sum_g e^{\sum_i h_i s_i} \left( 1 + \sum_{k<j} J_{kj} s_k s_j \right) \\ &= \sum_g e^{\sum_i h_i s_i} + \sum_{k<j} J_{kj} \sum_g e^{\sum_i h_i s_i} s_k s_j \\ &= \prod_i 2 \cosh h_i + \sum_{k<j} J_{kj} \left( \prod_{i \neq j \neq k} 2 \cosh h_i \right) (2 \sinh h_k) (2 \sinh h_j) \\ &= 2^L \left( 1 + \sum_{k<j} J_{kj} \tanh h_k \tanh h_j \right) \prod_i \cosh h_i, \end{aligned} \quad (55)$$

where in (a) we have used  $J_{ij} \sim 0 \forall i \neq j$  and expanded to the first order in  $|J_{ij}|$ . Using eq.(54) we get

$$\begin{aligned} \chi_i &\sim \frac{1}{\mathcal{Z}} \frac{\partial}{\partial h_i} \left[ 2^L \left( 1 + \sum_{k<j} J_{kj} \tanh h_k \tanh h_j \right) \prod_i \cosh h_i \right] \\ &= \frac{2^L}{\mathcal{Z}} \left[ \left( 1 + \sum_{k<j} J_{kj} \tanh h_k \tanh h_j \right) \prod_{l \neq i} \cosh h_l \sinh h_i + \right. \\ &\quad \left. + \left( 1 + \sum_{i \neq j} J_{ij} \frac{\tanh h_j}{\cosh^2 h_i} \right) \prod_i \cosh h_i \right] \\ &\sim \tanh h_i + \frac{1}{1 + \sum_{k \neq j} J_{kj} \tanh^2 h_k \tanh h_j} \sum_{i \neq j} J_{ij} (1 - \tanh^2 h_i) \tanh h_j \\ &\sim \tanh h_i + \sum_{i \neq j} J_{ij} (1 - \tanh^2 h_i) \tanh h_j \end{aligned} \quad (56)$$

$$\chi_{ii} \stackrel{(a)}{\sim} 1 - \tanh^2 h_i \stackrel{(b)}{\sim} 1 - \chi_i^2 \quad (57)$$

$$\chi_{ij} \stackrel{(a)}{\sim} J_{ij} (1 - \tanh^2 h_i) (1 - \tanh^2 h_j) \stackrel{(b)}{\sim} J_{ij} (1 - \chi_i^2) (1 - \chi_j^2) \quad (58)$$

where in (a) we have derived eq.(56) w.r.t.  $h_i$  or  $h_j$ , while in (b) we have used again eq.(56), upon moving the sum to the LHS . All of the eq.(56 - 58) are correct to the first order in  $|J_{ij}|$ . Note also that QLE is very reminiscent of the high-temperature expansion.

*4.1.1. The Central Result of KNS theory* The goal now is to understand the dynamics of the parameters in the genotype distribution as a function of the KNS-theory parameters and the observable first and second order cumulants. Following [39], we also assume for simplicity the mutation rate is sufficiently small for the approximation  $\mu \sim 0$  to be valid. Note that it cannot be  $\mu = 0$  otherwise QLE in an infinite population would only be a long-lived transient as the population drifts towards fixation, see eq.(12). Non-zero mutations are necessary to maintain any variability, yet we assume that their rate is small enough to forget their contribution in what comes next. Rewriting eq.(11) as an equation for  $\log P(g)$  and substitute eq.(53) one gets:

$$-\frac{\dot{Z}}{Z} + \sum_i \dot{h}_i s_i + \sum_{i < j} \dot{J}_{ij} s_i s_j = F(g) - \langle F \rangle + r \sum_{\xi, g'} C(\xi) P(g') \left[ \frac{P(g^{(1)}) P(g^{(2)})}{P(g) P(g')} - 1 \right] \quad (59)$$

Let us analyze separately the last term of the RHS . Setting  $\bar{\xi}_i = 1 - \xi_i$ :

$$\begin{aligned} \sum_{\xi, g'} C(\xi) P(g') \left[ \frac{P(g^{(1)}) P(g^{(2)})}{P(g) P(g')} - 1 \right] &= \\ &\stackrel{(a)}{=} \sum_{\xi, g'} C(\xi) P(g') \left( e^{\sum_{i < j} J_{ij} [(\xi_i s_i + \bar{\xi}_i s'_i)(\xi_j s_j + \bar{\xi}_j s'_j) + (\bar{\xi}_i s_i + \xi_i s'_i)(\bar{\xi}_j s_j + \xi_j s'_j) - s_i s_j - s'_i s'_j]} - 1 \right) \\ &= \sum_{\xi, g'} C(\xi) P(g') \left( e^{\sum_{i < j} J_{ij} [(\xi_i \xi_j + \bar{\xi}_i \bar{\xi}_j - 1)(s_i s_j + s'_i s'_j) + (\xi_i \bar{\xi}_j + \bar{\xi}_i \xi_j - 1)(s_i s'_j + s'_i s_j)]} - 1 \right) \\ &\stackrel{(b)}{\sim} \sum_{\xi, g'} C(\xi) P(g') \sum_{i < j} J_{ij} [(\xi_i \xi_j + \bar{\xi}_i \bar{\xi}_j - 1)(s_i s_j + s'_i s'_j) + (\xi_i \bar{\xi}_j + \bar{\xi}_i \xi_j)(s_i s'_j + s'_i s_j)] \\ &\stackrel{(c)}{=} \sum_{\xi} C(\xi) \sum_{i < j} J_{ij} [(\xi_i \xi_j + \bar{\xi}_i \bar{\xi}_j - 1)(s_i s_j + \langle s_i s_j \rangle) + (\xi_i \bar{\xi}_j + \bar{\xi}_i \xi_j)(s_i \langle s_j \rangle + \langle s_i \rangle s_j)] \\ &\stackrel{(d)}{=} \sum_{i < j} c_{ij} J_{ij} [(s_i \langle s_j \rangle + \langle s_i \rangle s_j) - (s_i s_j + \langle s_i s_j \rangle)] \quad (60) \end{aligned}$$

In (a) we have used eq.(53), inverted the relations eq.(6) to express  $s_i^{(1)} = \xi_i s_i + \bar{\xi}_i s'_i$ ,  $s_i^{(2)} = \bar{\xi}_i s_i + \xi_i s'_i$ , clearly  $s_i^{(2)} + s_i^{(1)} - s_i + s'_i = 0$  cancel for each field  $h_i$ ; in (b) we have expanded to the first order in  $|J_{ij}|$ ; in (c) we have averaged over  $P(g')$ ; in (d), finally, we have used  $c_{ij} = \sum_{\xi} C(\xi) (\xi_i \bar{\xi}_j + \bar{\xi}_i \xi_j) = \sum_{\xi} C(\xi) (1 - \xi_i \xi_j - \bar{\xi}_i \bar{\xi}_j)$ .

Substituting eq.(60) into eq.(59) and using eq.(3):

$$\begin{aligned}
 -\frac{\dot{Z}}{Z} + \sum_i \dot{h}_i s_i + \sum_{i<j} \dot{J}_{ij} s_i s_j &= \\
 = \bar{F} - \langle F \rangle + \sum_i f_i s_i + \sum_{i<j} f_{ij} s_i s_j + r \sum_{i<j} c_{ij} J_{ij} [(s_i \langle s_j \rangle + \langle s_i \rangle s_j) - (s_i s_j + \langle s_i s_j \rangle)] &
 \end{aligned} \tag{61}$$

Dynamical equations for  $\{h_i, J_{ij}\}$  emerge when collecting together terms with the same monomials in  $s_i$ :

$$\dot{h}_i = f_i + r \sum_{j \neq i} c_{ij} J_{ij} \chi_j \tag{62}$$

$$\dot{J}_{ij} = f_{ij} - r c_{ij} J_{ij} \tag{63}$$

In the case where the recombination rate is very high  $\sigma/r \ll 1$ , the  $\{J_{ij}\}$  rapidly reach the steady state:

$$f_{ij} = J_{ij} \cdot r c_{ij} \tag{64}$$

This is a crucial result for the KNS theory because it paves the way for the inference of the epistatic fitness landscape encoded in the  $\{f_{ij}\}$  from the couplings  $\{J_{ij}\}$  that, even if not observable, can be inferred from data, as shown in Sec.(3). Substituting the steady-state eq.(64) in eq.(62), one finds

$$\dot{h}_i = f_i + \sum_{j \neq i} f_{ij} \chi_j = \hat{f}_i, \tag{65}$$

where  $\hat{f}_i$  is the effective strength of selection on locus  $i$  and it collects the contribution of every  $\chi_i$  by means of the epistatic interaction. From eq.(57 - 58) it is possible to note that while the  $\chi_{ii}$  depends exclusively on the frequency  $\chi_i$ , the off-diagonal correlations are determined by the trade-off between epistasis and recombination *i.e.*  $\sigma_e/r$ .

As for the dynamics of the first and second order cumulants, they can be understood as follows. In view of eq.(64) and considering eq.(15) with  $\mu \sim 0$ , the correlations will rapidly approach the expression:

$$\bar{\chi}_{ij} = \frac{f_{ij}}{r c_{ij}} (1 - \chi_i^2)(1 - \chi_j^2), \quad i \neq j. \tag{66}$$

Neglecting all terms but the one due to recombination in eq.(15), the dynamics of the second order cumulants  $\chi_{ij}$  can be written as an exponential decay to the asymptotic value  $\bar{\chi}_{ij}$  *i.e.*

$$\chi_{ij} = \bar{\chi}_{ij} (1 - e^{-r c_{ij} t}); \tag{67}$$

as it can be verified by

$$\dot{\chi}_{ij} = r c_{ij} \bar{\chi}_{ij} e^{-r c_{ij} t} \stackrel{(a)}{=} r c_{ij} (\bar{\chi}_{ij} - \chi_{ij}) \stackrel{(b)}{=} f_{ij} (1 - \chi_i^2)(1 - \chi_j^2) - r c_{ij} \chi_{ij}, \tag{68}$$

where in (a) we have used eq.(67) and in (b) eq.(66).

The first order cumulants instead evolve according to the following dynamical equations:

$$\dot{\chi}_i \stackrel{(a)}{=} \langle s_i F \rangle - \chi_i \langle F \rangle = \partial_{h_i} \langle F \rangle \stackrel{(b)}{\sim} \sum_j \partial_{\phi_i} \chi_j \partial_{\chi_j} \langle F \rangle \stackrel{(c)}{=} \sum_j \chi_{ij} \partial_{\chi_j} \langle F \rangle, \tag{69}$$

where in (a) we have used eq.(12) with  $\mu = 0$ ; in (b) the chain rule of differentiation; in (c) the fact that  $\chi_{ij} = \partial\chi_i/\partial h_j$ , see eq.(54). We see from the RHS of eq.(69) that the allele means evolve so to maximize  $\langle F \rangle$ , there are  $L$  such equations and they are all coupled by the correlations  $\{\chi_{ij}\}$ .

This is nevertheless an enormous simplification with respect to the  $2^L$  ordinary differential equations for each possible  $g$  that one would have in general: in the QLE regime where  $\sigma/r \ll 1$  and the correlations rapidly approach their steady state, the  $L$  eq.(69) are the only relevant dynamical equations and they define the  $L$ -dimensional QLE manifold. As long as the QLE holds, the genotype distribution (hence the population average of any trait) is confined on such manifold *i.e.* it can be parametrized by the set of time-dependent first cumulants  $\{\chi_i(t)\}$ .

For variations of the theory presented here to finite-size populations or to genomes with multi-allelic loci, we refer to Appendix B and Appendix C, respectively.

#### 4.2. Inference of Epistasis: $r \gg \sigma$

Eq.(64) as developed in the KNS theory can be tested, as done in [40]. The testing strategy is very similar to the one employed in Sec.(3.3.3) and it is based on the following three steps: simulating evolutionary data by means of **FFPopSim**, inferring couplings by means of **MF/PLM**, finally comparing the epistatic parameters as they result from eq.(64) with the input ones.

- (i) **Simulating data.** The simulation tool **FFPopSim** is employed to generate evolutionary data, as discussed in Appendix D. Since the goal is testing the QLE regime, the initial parameters accordingly. A crucial choice is that of the fitness landscape, here encoded in a Sherrington-Kirkpatrick fitness function, setting  $f_i = 0 \forall i$  and  $f_{ij} \sim \mathcal{N}(0, \sigma_e)$ . A comprehensive summary of the initial parameters for the simulations is shown in Tab.(1), we will refer to this set as the Neher-Shraiman Test (NST).

	FFPopSim	NST	Description
Drivers Structure	$N$	200	carrying capacity
	$L$	25	n. of loci
	$T$	2.500	n. of generations
	$\omega$	0.5	crossover rate
	$r$	[0.0, 1.0]	outcrossing rate
	$\mu$	[0.005, 0.1]	mutation rate
	$\sigma_e$	[0.001, 0.02]	$f_{ij} \sim \mathcal{N}(0, \sigma_e)$

Table 1: Parameters on the NST. In light gray the parameters that are varied, the range indicated in the square brackets. SK fitness function. Random initial conditions.

- (ii) **Inferring couplings.** Raw data from the previous point are a sequence of states of the population at each time  $t$ . From such data, empirical population averages can be computed and feeded to one or more of the inverse techniques discussed in this section, in particular **MF** (sometimes also referred as *naive* mean field **nMF**) and **PLM**. Due to random drift, the empirical quantities (averages over the population) fluctuate in time; in order to smooth fluctuations out, the averages are computed not only on the final state of the population but on the whole time series: if a

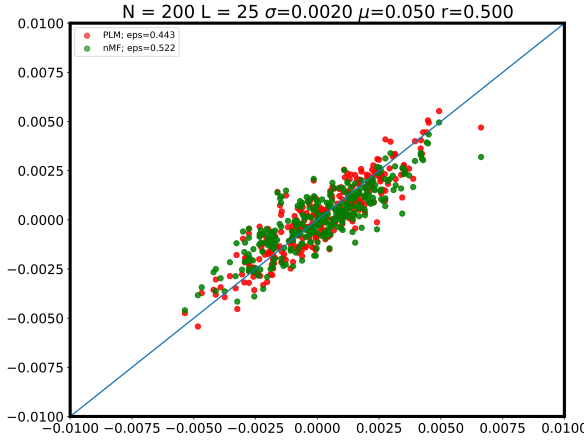


Figure 3: Example of a scatter plot for the *reconstructed* epistatic fitness components  $f_{ij}^*$  (y-axis) versus the *true* parameters  $f_{ij}$  (x-axis). Simulation NST, Tab.(1). Here  $r = 0.5, \mu = 0.05, \sigma_e = 0.002$ . The RMSE (Root Mean Square Error) is the reconstruction error as in eq.(70). Both MF (green) and PLM (red) are used for the inference procedure, their performances are similar in this regime.

single state is a matrix  $N \times L$ , the whole time series is a matrix  $(N \cdot T) \times L$ ; as an example,  $\langle \sigma_i \rangle = \frac{1}{NT} \sum_{j=1}^{NT} s_i(j)$ , where  $j$  is the row index. The MF and PLM inference on data obtained from the whole time series are referred as *alltime*-MF and *alltime*-PLM, this specification will be always implied hereinafter.

- (iii) **Testing epistasis.** The couplings resulting from the inverse methods allow to reconstruct the epistasis by means of eq.(64):  $r$  is the known (input) recombination rate,  $c_{ij}$  in [40] is computed as in eq.(16) with  $\rho = \omega = 0.5$ . Let  $f_{ij}^*$  be the inferred value of the epistatic fitness component between the loci  $i, j$ , similarly to eq.(52), the reconstruction error  $\varepsilon$  is quantified by

$$\varepsilon = \sqrt{\frac{\sum_{i < j} (f_{ij}^* - f_{ij})^2}{\sum_{i < j} f_{ij}^2}}. \quad (70)$$

Obviously,  $\varepsilon$  should be as small as possible, a wrong functional dependence of  $f_{ij}^*$  on the model parameters will yield  $\varepsilon \gg 0$ .

In Fig.3 we see a typical outcome of the procedure described just now, for the case when the inference procedure is reasonably accurate. The input and reconstructed epistatic fitness components are compared by means of a scatter plot; in the optimal case we would see the points along the diagonal line indicated, this is usually the case for the ML reconstruction, in the few cases when it is feasible. We also observe no relevant difference between MF and PLM in the final result of the inference procedure. One can repeat the same steps for different values of the parameters and see if/how the performance of the NS inference of epistasis changes. This is done in Fig.4, where the parameter space is explored in the directions  $r - \mu, r - \sigma_e$ . We observe that:

- ★  $\mu$ . The NS fitness reconstruction fails for low mutation rates. In fact, when mutation is insufficient, the structure of the population is essentially frozen and even if a defined fitness structure is present, for finite  $N, T$  it is not reflected in data. On the other hand, eq.(64) is not expected to work for high  $\mu$ , too, since in deriving it has been assumed  $\mu \sim 0$ . We will discuss this case in Sec.(5).
- ★ *High*  $\sigma_e/r$ . The reconstruction error  $\varepsilon$  blows up for sufficiently low values of  $r$ , which can be easily understood in view of eq.(64) *i.e.*  $f_{ij}^* = J_{ij}^* \cdot rc_{ij} \sim 0$  which implies  $\varepsilon \sim 1$  regardless of the inference method employed. The case of high values of  $\sigma_e$  will be discussed in Sec.(6).

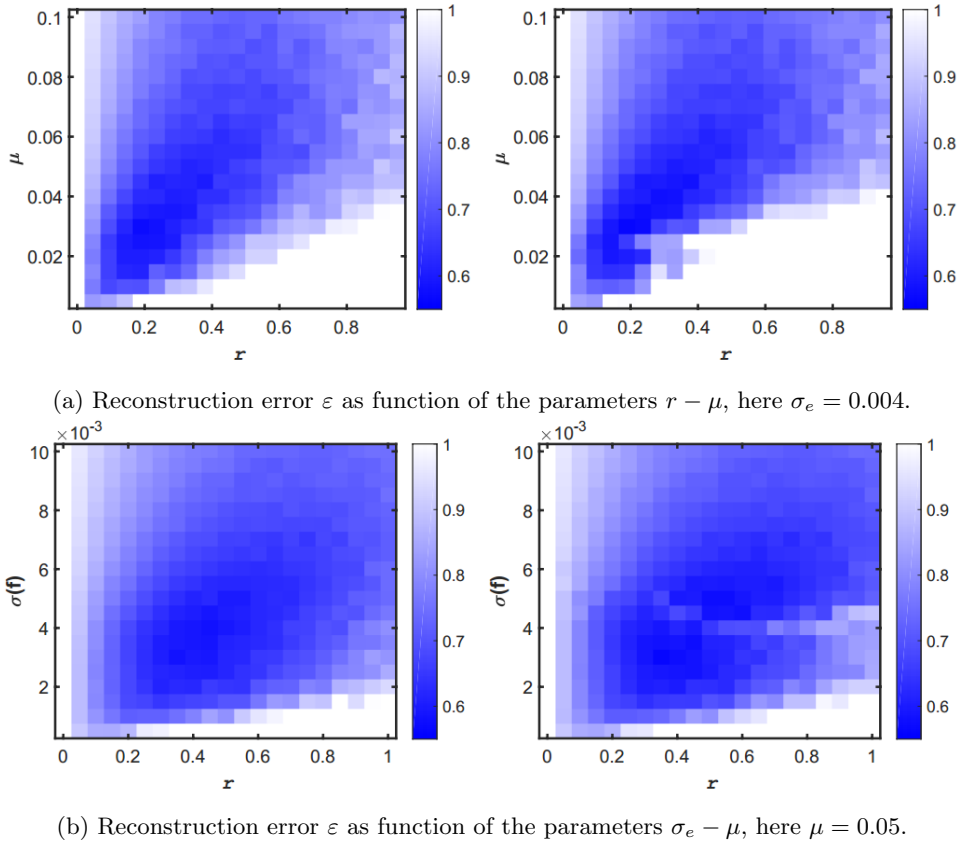


Figure 4: Phase diagrams for the reconstruction of the epistatic fitness components, from eq.(64). NST simulations, as in Tab.(1). In the left column, *alltime*-MF is used to infer the couplings  $J_{ij}$  from data, in the right column *alltime*-PLM. The magnitude of the reconstruction error eq.(70) is encoded in the colours of the heat-map. From [40]

- ★ *Low  $\sigma_e/r$ .* Results also are worse for sufficiently high recombination rates  $r$  : this is due to the fact that the higher the reshuffling the smaller the couplings  $J_{ij}$  inferred from data, which become subject more and more to small-sample noise. For the same reason, worse results are observed for sufficiently small  $\sigma_e$ .

## 5. QLE extended: a Gaussian Ansatz

Let us go back to the NS theory as encoded in Eqs (12) and (15). Those equations are not closed, *i.e.* the right hand sides of both equations depend on moments higher than the first and the second. They can be closed by assuming a specific expression for  $P(g)$ . The Gibbs-Boltzmann distribution (53) with the factorization ansatz (8), derived above in the high-recombination limit, provides one such closure. Since means and correlations are sufficient statistics for the Ising (and Potts) models, all higher moments are in fact implicit functions of those first and second order moments. It is therefore quite generally possible to close Eqs (12) and (15) within the class of

distributions (53). The method to do it in Sec. (4.1) was by a perturbation expansion in the small parameter  $1/r$  where  $r$  is the recombination rate, eventually leading to the inference formula Eq. (64). Formally mutations were assumed negligible ( $\mu \sim 0$ ), although, as discussed in Sec. (4.1), actually mutation rate cannot be taken to be exactly zero, especially not when checking Eq. (64) in numerical simulations. In principle it is possible to close Eqs. (12) and (15) within the class (53) in more general parameter ranges. However, without additional assumptions, such a closure requires for each time step both solving for the Ising/Potts parameters by DCA, and estimating all the higher moments from those parameters, and would therefore be very cumbersome.

Our goal in this section is to relax the hypothesis of  $\mu \sim 0$ , and generalizing Eq. (64) to the case where the mutation rate is arbitrarily high with respect to the fitness variation. The approach is a Gaussian closure of Eqs (12) and (15). This means that when estimating higher moments, Eq. (53) is interpreted as for real variables, which greatly simplifies the estimation of these higher moments, and allows to close Eqs (12) and (15) without solving for the Ising/Potts parameters in the intermediate step. We will thus arrive at a new inference formula Eq. (88), which certainly rests on other assumptions to be discussed below, but where mutations can be the fastest process, and  $\mu$  can be larger than all other parameters describing the evolutionary process.

The discussion in this Section is based on two recent papers [84, 85] where the second also contains an alternative derivation of the new inference formula similar to the derivation of the inference formula in the high-recombination limit presented above in Sec. (4.1). The Gaussian Ansatz is presented in Sec. (5.1) where Sec. (5.1.1) contains the logic of the method and the details of the closure, and Sec. (5.1.2) the new inference formula in different variants. In Sec. (5.2) we finally assess the performance of the new formula, parallel to the tests discussed above in Sec. (4).

### 5.1. A Gaussian Ansatz

*5.1.1. The Logic Of The Gaussian Ansatz* Let us start by substituting in the dynamical equations for first and second order cumulants eq.(12, 15) the explicit form of the fitness landscape eq.(3), up to pairwise terms:

$$F(g) = \sum_i f_i s_i + \sum_{i < j} f_{ij} s_i s_j , \quad (71)$$

where we set  $f_{ii} = 0 \forall i$  and  $f_{ij} = f_{ji} \forall i, j$ . The resulting expressions are

$$\begin{aligned} \dot{\chi}_i &= \langle s_i [F(g) - \langle F \rangle] \rangle - 2\mu \chi_i \\ &= \sum_j f_j \langle s_i s_j \rangle + \sum_{j < k} f_{jk} \langle s_i s_j s_k \rangle - \sum_j f_j \chi_i \chi_j - \sum_{j < k} f_{jk} \chi_i \langle s_j s_k \rangle - 2\mu \chi_i \end{aligned} \quad (72)$$

$$\begin{aligned} \dot{\chi}_{ij} &= \langle (s_i - \chi_i)(s_j - \chi_j) [F(g) - \langle F \rangle] \rangle - (4\mu + rc_{ij}) \chi_{ij} ; \\ &= \langle s_i s_j [F(g) - \langle F \rangle] \rangle - \chi_i (\dot{\chi}_j + 2\chi_j \mu) - \chi_j (\dot{\chi}_i + 2\chi_i \mu) - (4\mu + rc_{ij}) \chi_{ij} \\ &= \sum_k f_k \langle s_i s_j s_k \rangle + \sum_{k < l} f_{kl} \langle s_i s_j s_k s_l \rangle - \sum_k f_k \chi_k \langle s_i s_j \rangle - \sum_{k < l} f_{kl} \langle s_i s_j \rangle \langle s_k s_l \rangle + \\ &\quad - \chi_i (\dot{\chi}_j + 2\chi_j \mu) - \chi_j (\dot{\chi}_i + 2\chi_i \mu) - (4\mu + rc_{ij}) \chi_{ij} ; \end{aligned} \quad (73)$$



for the latter we have used eq.(12) and left implicit  $\dot{\chi}_i$ . The goal is to express the expectations in the RHS of eq.(72, 73), in terms of the cumulants of the distribution  $P(g)$  (of all orders, in principle). By definition, for the 2–points expectation  $\langle s_i s_j \rangle$  one has  $\chi_{ij} = \langle s_i s_j \rangle - \chi_i \chi_j$ . Evidently, the crucial step is evaluating  $\langle s_i s_j s_k \rangle$  and  $\langle s_i s_j s_k s_l \rangle$  which are respectively the 3, 4–points expectation. Since for Ising-alleles  $s_i^2 = 1$ , it is enough to know  $\langle s_i s_j s_k \rangle_{i \neq j \neq k}$ ,  $\langle s_i s_j s_k s_l \rangle_{i \neq j \neq k \neq l}$ , no two same indices. To evaluate these higher-order moments (and only these) we introduce the Gaussian Ansatz.

Consider a population where the mutation rate is high enough with respect to the fitness strength that no two individuals are present with the same genotype (clones). In such a system, where  $\mu \gg \sigma$  or  $r \gg \sigma$  or both, correlations of order  $> 2$  are expected to be negligible, therefore, for the purpose of estimating 3, 4–points expectations, the distribution of probability can be modelled as:

$$P(g, t) = \frac{1}{\mathcal{Z}} \exp \left[ -\frac{1}{2} \sum_{i,j} (s_i - \chi_i) (\chi^{-1})_{ij} (s_j - \chi_j) \right], \quad (74)$$

where  $\mathcal{Z}$  is a normalization and  $\chi$  is the covariance matrix *i.e.*  $\chi_{ij} = \langle s_i s_j \rangle - \langle s_i \rangle \langle s_j \rangle$ . In words,  $P(g)$  is taken to be a *multivariate Gaussian distribution*, whose cumulants (connected correlation functions) of order  $> 2$  are *exactly* zero, see Appendix A. For eq.(74) to be valid, we are formally forced to allow  $s_i \in \mathbb{R}$ . Metaphorically, we are describing a population as a cloud of similar sequences distributed around the value  $\{\chi_1, \dots, \chi_L\}$ , where  $L$  as usual is the number of loci [84]. A first advantage of the Gaussian ansatz is that it allows to write only  $L(L+1)/2$  dynamical equations for  $\{\chi_i\}_i$  and  $\{\chi_{ij}\}_{i \neq j}$  instead of  $2^L$  for each possible  $g$ . Using eq.(74), one is able to express the 3, 4–points correlations in terms of the first and second order cumulants, a proof is provided in Appendix A.

$$\langle s_i s_j s_k \rangle_{i \neq j \neq k} = \chi_i \chi_j \chi_k + \chi_i \chi_{jk} + \chi_j \chi_{ik} + \chi_k \chi_{ij} \quad (75)$$

$$\begin{aligned} \langle s_i s_j s_k s_l \rangle_{i \neq j \neq k \neq l} = & \chi_i \chi_j \chi_k \chi_l + \chi_i \chi_j \chi_{kl} + \chi_i \chi_k \chi_{jl} + \chi_i \chi_l \chi_{jk} + \chi_j \chi_k \chi_{il} + \\ & + \chi_j \chi_l \chi_{ik} + \chi_k \chi_l \chi_{ij} + \chi_{ij} \chi_{kl} + \chi_{ik} \chi_{jl} + \chi_{il} \chi_{jk} \end{aligned} \quad (76)$$

In the RHS of eq.(72, 73), apart from parameters of the model, only  $\{\chi_i\}$ ,  $\{\chi_{ij}\}$  will be found; this is the reason why the Gaussian assumption above is termed *closure* (GC). We can now carry out the calculation of the dynamical equations.

$\dot{\chi}_i$  Dynamics of the first cumulants, from eq.(72).  $\forall i \in 1, \dots, L$

$$\begin{aligned}
\dot{\chi}_i &= \sum_j f_j \langle s_i s_j \rangle + \sum_{j < k} f_{jk} \langle s_i s_j s_k \rangle - \sum_j f_j \chi_i \chi_j - \sum_{j < k} f_{jk} \chi_i \langle s_j s_k \rangle - 2\mu \chi_i \\
&\stackrel{(a)}{=} \sum_j f_j \chi_{ij} + \sum_{j \neq i} f_{ij} \chi_j + \sum_{\substack{j < k \\ j, k \neq i}} f_{jk} (\chi_i (\chi_j \chi_k + \chi_{jk}) + \chi_j \chi_{ik} + \chi_k \chi_{ij}) + \\
&\quad - \sum_{j < k} f_{jk} \chi_i (\chi_{jk} + \chi_j \chi_k) - 2\mu \chi_i \\
&= \sum_j f_j \chi_{ij} + \sum_{j \neq i} f_{ij} \chi_j - \sum_{j \neq i} f_{ij} \chi_i (\chi_{ij} + \chi_i \chi_j) + \sum_{\substack{j < k \\ j, k \neq i}} f_{jk} (\chi_j \chi_{ik} + \chi_k \chi_{ij}) - 2\mu \chi_i \\
&= \sum_j f_j \chi_{ij} - \sum_{j \neq i} f_{ij} \chi_i \chi_{ij} + \sum_{j \neq i} f_{ij} \chi_j (1 - \chi_i^2) + \sum_{\substack{j \neq k \\ j, k \neq i}} f_{jk} \chi_j \chi_{ik} - 2\mu \chi_i \\
&\stackrel{(b)}{=} \sum_j f_j \chi_{ij} - \sum_{j \neq i} f_{ij} \chi_i \chi_{ij} + \sum_{j \neq i} f_{ij} \chi_j \chi_{ii} + \sum_{\substack{j \neq i \\ k \neq j}} \sum_{k \neq j} f_{jk} \chi_j \chi_{ik} - 2\mu \chi_i \\
&\stackrel{(c)}{=} \sum_j f_j \chi_{ij} - \sum_{j \neq i} f_{ij} \chi_i \chi_{ij} + \sum_{j \neq i} \sum_{k \neq j} f_{jk} \chi_j \chi_{ik} \pm \sum_{k \neq i} f_{ik} \chi_i \chi_{ik} - 2\mu \chi_i \\
&= \sum_j f_j \chi_{ij} - 2 \sum_{j \neq i} f_{ij} \chi_i \chi_{ij} + \sum_j \sum_{k \neq j} f_{jk} \chi_k \chi_{ij} - 2\mu \chi_i \\
&\stackrel{(d)}{=} \sum_j \chi_{ij} (f_j + \sum_k f_{jk} \chi_k - 2f_{ij} \chi_i) - 2\mu \chi_i \tag{77}
\end{aligned}$$

In (a) we expanded  $\langle s_j s_k \rangle$  and, after distinguishing the case where  $i \neq j \neq k$ , we exploited eq.(75); in (b) we used  $\chi_{ii} = \langle s_i^2 \rangle - \langle s_i \rangle^2 = 1 - \chi_i^2$ ; in (c) we added and subtracted a sum; in (d) we used  $f_{ii} = 0 \forall i$ . This first result deserves to be emphasized,  $\forall i$

$$\boxed{\dot{\chi}_i = \sum_j \chi_{ij} \left( f_j + \sum_k f_{jk} \chi_k - 2f_{ij} \chi_i \right) - 2\mu \chi_i .} \tag{78}$$

$\dot{\chi}_{ij}$  Dynamics of the second cumulants, from eq.(73).  $\forall i, j \in 1, \dots, L \wedge i \neq j$

$$\begin{aligned}
\dot{\chi}_{ij} &= \sum_k f_k \langle s_i s_j s_k \rangle + \sum_{k < l} f_{kl} \langle s_i s_j s_k s_l \rangle - \langle s_i s_j \rangle \left( \sum_k f_k \chi_k + \sum_{k < l} f_{kl} \langle s_k s_l \rangle \right) + \\
&\quad - \chi_i \sum_k \chi_{jk} (\hat{f}_k - 2f_{jk} \chi_j) - \chi_j \sum_k \chi_{ik} (\hat{f}_k - 2f_{ik} \chi_i) - (4\mu + r c_{ij}) \chi_{ij} \tag{79}
\end{aligned}$$

where we have substituted the result eq.(78) and the definition  $\hat{f}_k = f_k + \sum_j f_{jk} \chi_j$ . For the sake of clarity, let us analyze separately the terms highlighted in blue (B), red (R) and violet (V) and cyan (C). In order to substitute eq.(75, 76) we again have to deconstruct the sums distinguishing cases where some of the indices are

equal.

$$\begin{aligned}
V &= (\chi_{ij} + \chi_i \chi_j) \left( \sum_k f_k \chi_k + \sum_{k < l} f_{kl} (\chi_{kl} - \chi_k \chi_l) \right) \\
&= (\chi_{ij} + \chi_i \chi_j) \left( \sum_{k \neq i, j} f_k \chi_k + f_i \chi_i + f_j \chi_j + \sum_{\substack{k < l \\ k, l \neq i, j}} f_{kl} (\chi_{kl} + \chi_k \chi_l) \right) \\
&\quad + \sum_{k \neq i, j} [f_{ik} (\chi_{ik} + \chi_i \chi_k) + f_{jk} (\chi_{jk} + \chi_j \chi_k)] + f_{ij} (\chi_{ij} + \chi_i \chi_j) \\
B &= \sum_{k \neq i, j} f_k \langle s_i s_j s_k \rangle + f_i \chi_j + f_j \chi_i \\
&= \sum_{k \neq i, j} f_k (\chi_i \chi_j \chi_k + \chi_i \chi_{jk} + \chi_j \chi_{ik} + \chi_k \chi_{ij}) + f_i \chi_j + f_j \chi_i \\
R &= \sum_{\substack{k < l \\ k, l \neq i, j}} f_{kl} \langle s_i s_j s_k s_l \rangle + \sum_{k \neq i, j} [f_{ik} \langle s_j s_k \rangle + f_{jk} \langle s_i s_k \rangle] + f_{ij} \\
&= \sum_{\substack{k < l \\ k, l \neq i, j}} f_{kl} (\chi_i \chi_j \chi_k \chi_l + \chi_i \chi_j \chi_{kl} + \chi_i \chi_k \chi_{jl} + \chi_i \chi_l \chi_{jk} + \chi_j \chi_k \chi_{il} + \chi_j \chi_l \chi_{ik} + \\
&\quad + \chi_k \chi_l \chi_{ij} + \chi_{ij} \chi_{kl} + \chi_{ik} \chi_{jl} + \chi_{il} \chi_{jk}) + \sum_{k \neq i, j} [f_{ik} (\chi_{jk} + \chi_j \chi_k) + \\
&\quad + f_{jk} (\chi_{ik} - \chi_i \chi_k)] + f_{ij} \\
C &= \chi_i \sum_k \chi_{jk} (f_k + \sum_l f_{kl} \chi_l - 2f_{jk} \chi_j) \\
&= \chi_i \sum_{k \neq i, j} \chi_{jk} (f_k + \sum_l f_{kl} \chi_l - 2f_{jk} \chi_j) + \chi_i \chi_{ij} (f_i + \sum_l \chi_{il} \chi_l - 2f_{ij} \chi_j) + \\
&\quad + \chi_i (1 - \chi_j^2) (f_j + \sum_l f_{jl} \chi_l)
\end{aligned}$$

In the last line we have used  $\chi_{ii} = 1 - \chi_i^2$ ,  $f_{ii} = 0 \forall i$  and the definition of  $\hat{f}_i$ . In addition, note that there is a term in eq.(79) which is nothing but (C) after exchanging  $i \leftrightarrow j$ .

Summing the all the terms in eq.(79) and simplifying everything possible:

$$\begin{aligned}
\dot{\chi}_{ij} = & -(4\mu + rc_{ij}) - 2f_i\chi_i\chi_{ij} - 2f_j\chi_j\chi_{ij} + f_{ij}(1 - \chi_{ij}^2 - \chi_i^2\chi_j^2 + 2\chi_i\chi_j\chi_{ij}) + \\
& + \sum_{k \neq i,j} f_{ik}(\chi_{jk} + \chi_j\chi_k - \chi_{ij}\chi_{ik} + \chi_{ik}\chi_i\chi_j - \chi_{ij}\chi_i\chi_k - \chi_i^2\chi_j\chi_k) + \\
& + \sum_{k \neq i,j} f_{jk}(\chi_{ik} + \chi_i\chi_k - \chi_{ij}\chi_{jk} + \chi_{jk}\chi_i\chi_j - \chi_{ij}\chi_j\chi_k - \chi_i\chi_j^2\chi_k) + \\
& + (\chi_i^2\chi_j - \chi_j - \chi_i\chi_{ij}) \sum_l f_{il}\chi_l + (\chi_i\chi_j^2 - \chi_i - \chi_j\chi_{ij}) \sum_l f_{jl}\chi_l + \\
& + \sum_{\substack{k < l \\ k,l \neq i,j}} f_{kl}(\chi_{ik}\chi_j\chi_l + \chi_{jk}\chi_i\chi_l + \chi_{il}\chi_j\chi_k + \chi_{jl}\chi_i\chi_k + \chi_{ik}\chi_{jl} + \chi_{il}\chi_{jk}) + \\
& - \sum_{k \neq i,j} \chi_i\chi_{jk} \sum_l \chi_l f_{kl} - \sum_{k \neq i,j} \chi_j\chi_{ik} \sum_l \chi_l f_{kl}. \tag{80}
\end{aligned}$$

For the sake of elegance, it is possible to rewind the sums (*i.e.* reversing the “decomposition” where cases in which some indices are equal are treated separately). The outcome is, for  $i \neq j$ ,

$$\begin{aligned}
\dot{\chi}_{ij} = & -(4\mu + rc_{ij})\chi_{ij} - 2\chi_{ij}(f_i\chi_i + f_j\chi_j) + 2f_{ij}\chi_{ij}(\chi_{ij} + 2\chi_i\chi_j) + \\
& - 2\chi_{ij} \sum_k \left[ f_{ik}(\chi_{ik} + \chi_i\chi_k) + f_{jk}(\chi_{jk} + \chi_j\chi_k) \right] + \sum_{k,l} f_{kl}\chi_{ik}\chi_{jl}. \tag{81}
\end{aligned}$$

*5.1.2. A Broader Inference Formula* A primary interest with eq.(78, 80) is to understand their stationary solutions, which entails solving simultaneously  $\mathcal{O}(L^2)$  equations. The task is much simpler in the regime with high mutation and/or recombination rate *i.e.*  $(4\mu + rc_{ij}) \rightarrow \infty$ . As a first step, the authors of [85] investigate the further subcase where there is a purely epistatic fitness landscape and  $\chi_i = 0 \forall i$ , therefore the results will not hold when  $f_i \neq 0$  or when something else causes the first order cumulants to substantially deviate from zero. Since the first cumulants all vanish, it is sufficient to examine eq.(80), starting by rewriting it in the simpler form of current interest:

$$\begin{aligned}
\dot{\chi}_{ij} = & -(4\mu + rc_{ij})\chi_{ij} + f_{ij}(1 - \chi_{ij}^2) + \sum_{k \neq i,j} \left[ f_{ik}(\chi_{jk} - \chi_{ij}\chi_{jk}) + f_{jk}(\chi_{ik} - \chi_{ij}\chi_{jk}) \right] + \\
& + \sum_{\substack{k < l \\ k,l \neq i,j}} f_{kl}(\chi_{ik}\chi_{jl} + \chi_{jk}\chi_{il}). \tag{82}
\end{aligned}$$

Let us define  $\epsilon = 1/(4\mu + rc_{ij}) \rightarrow 0^+$ , to be used as small parameter for the expansion.§ The trick is now to assume:

$$\chi_{ij} = \chi_{ij}^{(0)} + \epsilon\chi_{ij}^{(1)} + \epsilon^2\chi_{ij}^{(2)} + \epsilon^3\chi_{ij}^{(3)} + \mathcal{O}(\epsilon^4) \tag{83}$$

§In principle, we should write  $\epsilon_{ij}$  but since in this work we typically have a crossover rate  $\sim \mathcal{O}(1)$ , see Sec.(2.3.5), we can safely assume it is indeed constant and forget about this unimportant complication.

and impose the stationary condition  $\dot{\chi}_{ij} = 0$  from eq.(82), order by order in  $\epsilon$ :

$$\begin{aligned}
\mathcal{O}(\epsilon^{-1}) : \chi_{ij}^{(0)} &= 0 \\
\mathcal{O}(1) : \chi_{ij}^{(1)} &= f_{ij} \\
\mathcal{O}(\epsilon) : \chi_{ij}^{(2)} &= 2 \sum_{k \neq i,j} f_{ik} f_{jk} \\
\mathcal{O}(\epsilon^2) : \chi_{ij}^{(3)} &= \sum_{\substack{k < l \\ k,l \neq i,j}} f_{kl} (f_{ik} f_{jl} + f_{jk} f_{il}) + \sum_{k \neq i,j} f_{ik} \left( 2 \sum_l f_{jl} f_{kl} - f_{ij} f_{ik} \right) + \\
&\quad + \sum_{k \neq i,j} f_{jk} \left( 2 \sum_l f_{il} f_{kl} - f_{ij} f_{jk} \right) - f_{ij}^3
\end{aligned}$$

Therefore, up to the first order in  $\epsilon$ ,

$$\chi_{ij} = \frac{f_{ij}}{4\mu + rc_{ij}} \quad (84)$$

to be compared with eq.(64). Note that the  $n$ -th order term is of relative size  $L\sigma(f)$  compared to the  $(n-1)$ -th; therefore, the first order is expected to be accurate as far as  $L\sigma(f) < 1$ .

The hypothesis of  $\chi_i = 0 \forall i$  can be dropped so to consider the full eq.(80) with the assumption eq.(83); following the same steps as above the result is

$$\begin{aligned}
\mathcal{O}(\epsilon^{-1}) : \chi_{ij}^{(0)} &= 0 \\
\mathcal{O}(1) : \chi_{ij}^{(1)} &= f_{ij} (1 - \chi_i^2) (1 - \chi_j^2) \\
\mathcal{O}(\epsilon) : \chi_{ij}^{(2)} &= \sum_k f_{ik} (\chi_{jk}^{(1)} + \chi_{ik}^{(1)} \chi_i \chi_j - \chi_i \chi_k \chi_{ij}^{(1)}) + \\
&\quad - \sum_{k,l} f_{kl} \chi_i \chi_l \chi_{jk}^{(1)} - \sum_l f_{il} \chi_l \chi_i \chi_{ij}^{(1)} + \\
&\quad + \sum_{k < l} f_{kl} (\chi_{ik}^{(1)} \chi_j \chi_l + \chi_{il}^{(1)} \chi_j \chi_k - 2f_{ij} \chi_i \chi_{ij}^{(1)}) + \\
&\quad + f_{ij} \chi_i \chi_j \chi_{ij}^{(1)} + \{i \leftrightarrow j\}
\end{aligned} \quad (85)$$

where, for the sake of clarity, in the last equation the terms like  $\chi_{ij}^{(1)}$  as specified in eq. (85) are left implicit.

Up to the first order in  $\epsilon$ ,

$$\chi_{ij} = \frac{f_{ij}}{4\mu + rc_{ij}} (1 - \chi_i^2) (1 - \chi_j^2). \quad (87)$$

As it should be, eq.(84) is recovered by setting  $\chi_i = 0 \forall i$ . Turning around this into an inference formula:

$$f_{ij}^* = \chi_{ij} \cdot \frac{4\mu + rc_{ij}}{(1 - \chi_i^2)(1 - \chi_j^2)}, \quad (88)$$

where the star in  $f_{ij}^*$  means that these are regarded as *inferred* fitness parameters. eq.(88) has a major advantage with respect to eq.(64): there is *no more need for*

any DCA inference, since epistasis is reconstructed directly from the population averages  $\{\chi_i\}, \{\chi_{ij}\}$ . This result is important for practical reasons, since the inference procedure, even in its most streamlined versions (*e.g.* MF), can be very expensive in terms of computational time. In the following section we will test Eq. (88), and verify that it also allows to accurately infer epistatic fitness from samples of a population in wider parameter ranges.

### 5.2. Inference of Epistasis, improved: $\mu, r \gg \sigma$

In [85], the authors test eq.(88) versus eq.(64). The approach follows the one presented in Sec.(4) based on [40]; it is briefly summarized here together with the description of the setup.

- **Simulation Settings** The simulation tool FFPopSim is exploited to simulate evolving population of genotypes under mutations, recombination and selection, see Appendix D. The fitness function chosen is  $F(g) = \sum_i f_i s_i + \sum_{i < j} f_{ij} s_i s_j$ . Since the Gaussian Closure is expected to work also for non-zero  $\{\chi_i\}$ , differently from [40], non-zero additive components  $\{f_i\}$  of  $F(g)$  is assumed. Specifically, both additive and epistatic fitness parameters will be Gaussian distributed with zero means and standard deviations  $\sigma_a, \sigma_e$ , respectively:  $f_i \sim \mathcal{N}(0, \sigma_a)$ ,  $f_{ij} \sim \mathcal{N}(0, \sigma_e)$ . In the range of parameters tested in [85], there is no evidence of a dependence of the fitness effects on the specific realizations of the Gaussian distributed parameters, therefore  $\sigma_a, \sigma_e$  will be considered as effective coarse-grained descriptors of additive and epistatic fitness. Simulations are run for different parameters  $\mu, r, \sigma_e$ , fixing all the others. The simulation ranges/values for each parameter are shown in Tab.(2).  $c_{ij}$  as in eq.(16).

	FFPopSim	Values	Description
Structure	$N$	200	carrying capacity
	$L$	25	n. of loci
	$T$	10,000	n. of generations
	$\rho$	0.5	crossover rate
Drivers	$\sigma_a$	0.05	$f_i \sim \mathcal{N}(0, \sigma_a)$
	$r$	[0.0, 1.0]	outcrossing rate
	$\mu$	[0.05, 0.5]	mutation rate
	$\sigma_e$	[0.004, 0.04]	$f_{ij} \sim \mathcal{N}(0, \sigma_e)$

Table 2: Simulation settings for FFPopSim as employed in [85]. Light Gray for parameters that are varied in order to test the reconstructions routes GC vs KNS.

- **Probing Gaussian Closure: Algorithm.** *All-time* data are used to smooth out fluctuations due to the finite size of the population. From them, it is possible to get population-averaged quantities  $\{\chi_i\}, \{\chi_{ij}\}$  and enforce the two approaches under examination: either inferring epistatic fitness components directly from correlations and means exploiting eq.(88) or implementing DCA to reconstruct  $\{J_{ij}\}$ , then finally using eq.(64) with a Mean Field inference MF, results for PLM are found to be similar (data not shown). The latter is used as a benchmark to compare the relative improvement of the new formula with respect to the one obtained ignoring the contribution of mutations. Finally, the results of the

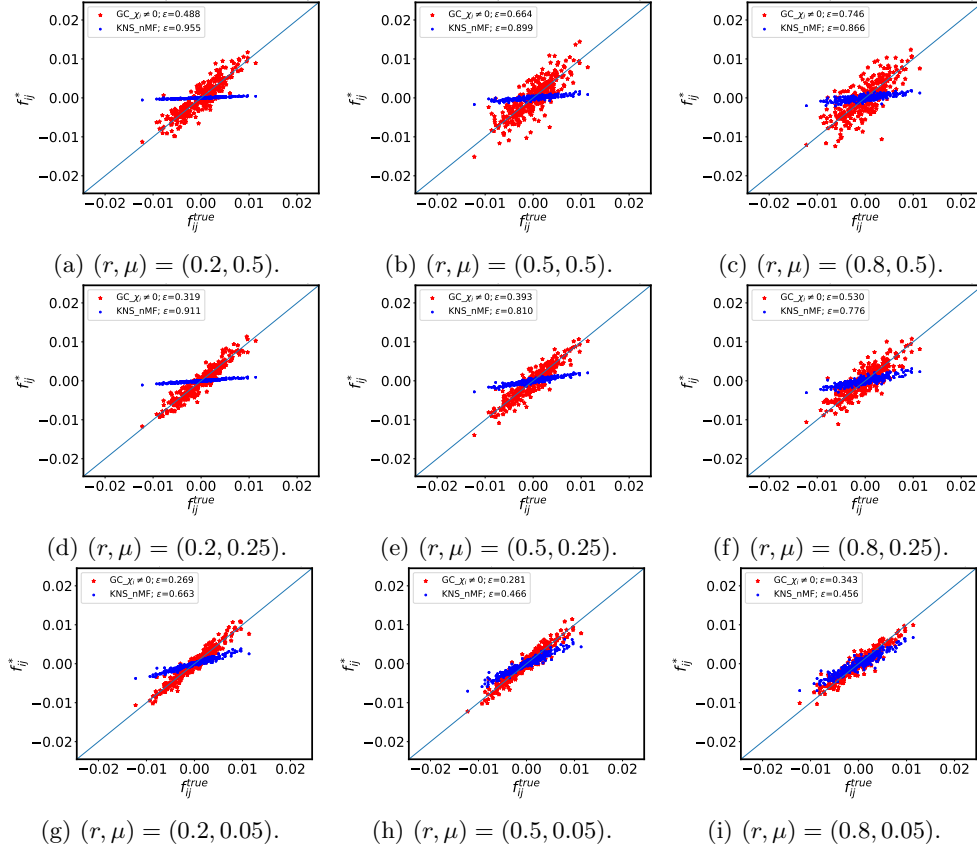


Figure 5: Scatter Plots for MR. The red stars result from the inference based on the Gaussian Ansatz, eq.(88); blue dots for KNS reconstruction eq.(64) with MF inferred couplings. Epistatic fitness strength  $\sigma_e = 0.004$ , other parameters as shown in Tab.(2). From [85].

reconstructed  $\{f_{ij}^*\}$  (by GC and KNS) are compared with the true values  $\{f_{ij}\}$  in input. The error in the reconstruction can be quantified by the root mean square error introduced in eq.(70).

- Scanning the parameter space.** The simulations are divided in two sets. The first one, named MR, aims to explore the parameter space in the  $\mu, r$  directions for a fixed epistatic strength  $\sigma_e = 0.004$ . In Fig.5 some scatter plots are shown as resulting from the algorithm aforementioned; each column has the same  $r$ , increasing from left to right, and each row has the same mutation rate, increasing from bottom to top. For each inference technique, the core information of each scatter plot can be captured by  $\epsilon \in \mathbb{R}^+$ , eq.(70). In Fig.6 there is an heat map for  $\epsilon$ , as evaluated while scanning the parameter space in the directions  $\mu \in [0.05, 0.5]$  and  $r \in [0.0, 1.0]$ . The second set of simulations, called ER, is intended to ascertain the performances of the two reconstructions as a function of  $\sigma_e, r$ , for a fixed  $\mu = 0.2$ . In Fig.7 each column has the same  $r$ , increasing from left to right, and each row has the same epistatic strength, increasing from

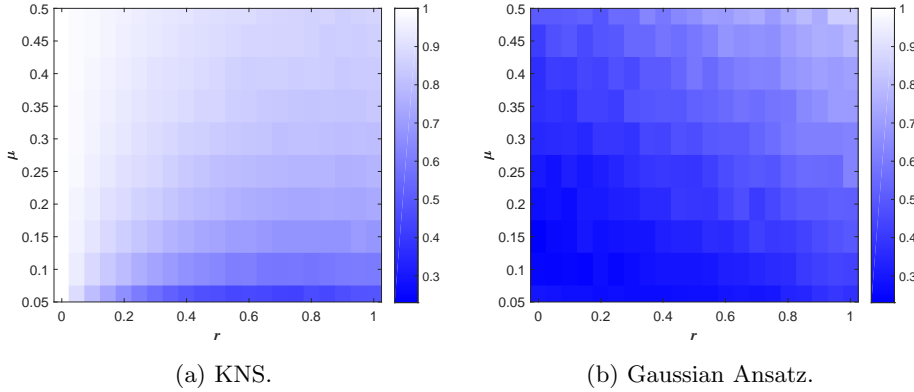


Figure 6: Heat Maps for the MR set. The colour represents the reconstruction error  $\varepsilon$  given in eq.(70). Left: KNS reconstruction eq.(64) with MF inferred couplings. Right: inference based on the Gaussian Ansatz, eq.(88). Epistatic strength  $\sigma_e = 0.004$ , other parameters as in Tab.(2). From [85].

bottom to top. In Fig.8, finally, the heat map for  $\varepsilon$  by tuning  $\sigma_e \in [0.005, 0.04]$  and  $r \in [0.0, 1.0]$ .

MR, Fig.5, 6. Reconstruction based on eq.(88) has a better performance everywhere throughout the MR set, in particular for high mutation rates. For extremely high recombination and mutation rates (top-right) the noise due to the strength of the reshuffling of the population is likely to worsen the accuracy of the allele statistics (means and correlations) for a finite-time simulation, which ultimately results in a sparser scatter plot and a slightly higher reconstruction error  $\varepsilon$ .

ER, Fig.7, 8. Since an high value of the mutation rate  $\mu = 0.2$  is fixed, the KNS is expected not to work anywhere: indeed, it does not. Inference based on the Gaussian Ansatz on the other hand has excellent performances except in a region of high epistasis and high recombination. We noted in Sec.(5.1.2) that the perturbative expansion is meant to be accurate whenever  $L\sigma_e < 1$ ; accordingly in Fig.8b the error increases for increasing  $\sigma_e$ . However, this is not sufficient to explain the behaviour in the top right corner of Fig.7, which shows a clear pattern: (*i.e.* the two *symmetric clouds* of reconstructed points) are inexplicable in terms of a simple increased amount of noise.

Finally, for the Gaussian Ansatz to hold, the  $\{f_i\}$  also have to be small. Increasing the overall magnitude of additive fitness, the evolutionary process has a stronger tendency to drive some alleles to fixation. The minor allele as such loci will then be present in only a few copies in a finite population, and often not be present at all. The actual distribution then differs from the one assumed by the Gaussian ansatz, making this inaccurate.

## 6. Beyond the QLE

### 6.1. Statistical Physics of non-QLE regimes

So in Statistical Physics as in its applications to Population Genetics, when stepping beyond the equilibrium regime a rich variety of new behaviours emerges, whose



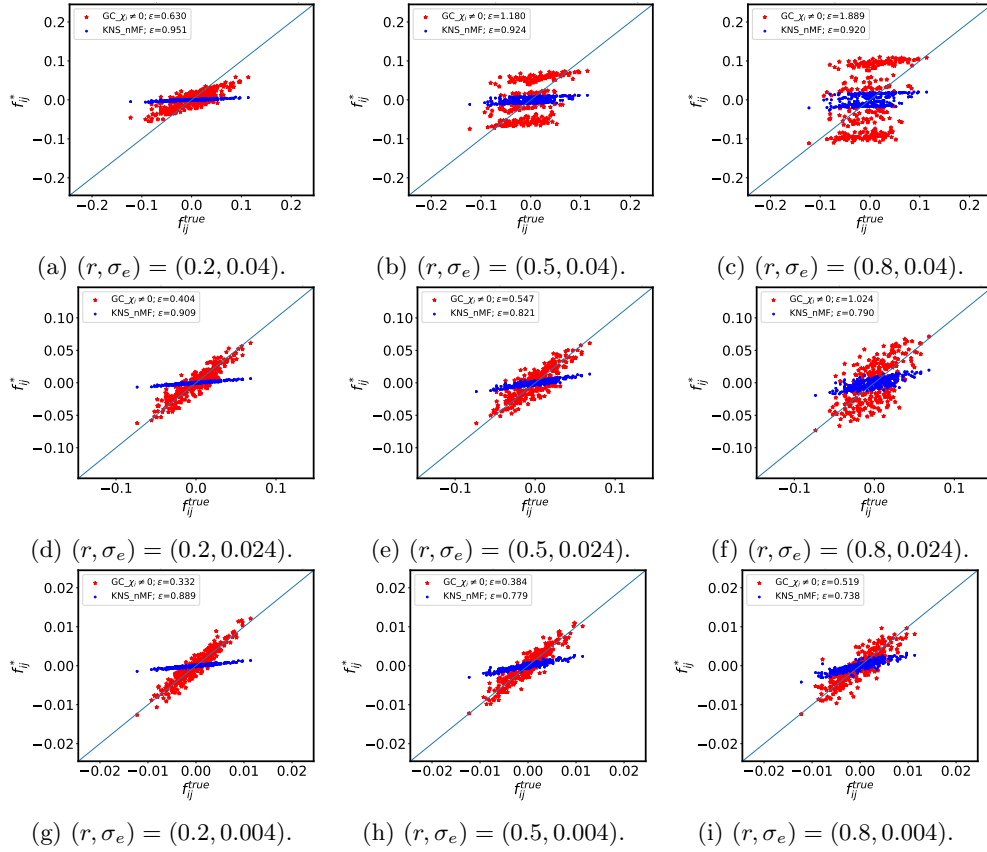


Figure 7: Scatter Plots for set ER. The red stars result from the inference based on the Gaussian Ansatz, eq.(88); blue dots for KNS reconstruction eq.(64) with nMF inferred couplings. Mutation rate  $\mu = 0.2$ , other parameters as in Tab.(2). From [85].

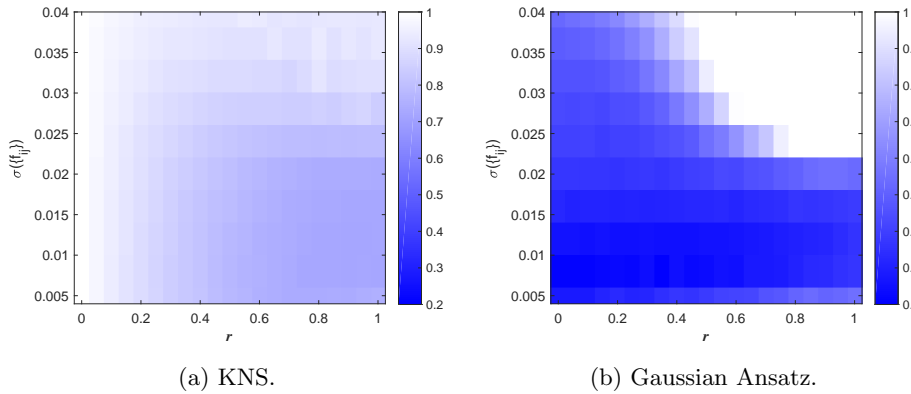


Figure 8: Heat Maps for the ER set. The colour represents the reconstruction error  $\varepsilon$  given in eq.(70). Left: KNS reconstruction eq.(64) with nMF inferred couplings. Right: inference based on the Gaussian Ansatz, eq.(88). Mutation rate  $\mu = 0.2$ , other parameters as in Tab.(2). From [85].

theoretical understanding is, however, more challenging. In a larger perspective, a number of mathematical models have been proposed to tackle different non-equilibrium problems of population genetics. In models without recombination there is no interchange of genetic material between individuals. The evolution of the distribution of genotypes in a population is then a stochastic process, and a rich set of tools can be brought to bear. Time reversal of stochastic processes is the basis of Kingman's coalescent which allows to estimate properties of genealogies [86, 87]; a theory with many later developments, see *e.g.* [88–90]. In the forward dynamics, in a phase quite far from QLE, the competition between clones and competitions between mutations in different clones have been studied extensively [91, 92], as have effects of fast adaptation [93] and time-changing fitness [35]. A comprehensive review of them is beyond the scope of this review, where instead we focus on when and how a QLE phase breaks down, how to characterize transient phases, and which other dynamical states can be reached. The reader interested in different approaches can find further useful entries in [8, 9, 94, 95] and references therein.

*6.1.1. Mutation-selection balance* When considering a population with its fitness distribution, a particular interest is in the tail of fittest individuals, whose fate can dramatically change the one of the whole population; indeed, rare events can cause fluctuations in the size of the fittest classes that in turn propagate towards the "core" of the distribution.

One notable example is the so called Muller's Ratchet [96–98]: a *click* of Muller's ratchet is the loss of the most fit class of individuals; the rate of the ratchet is given by the inverse of the mean time between successive clicks of the ratchet. A quantitative understanding of this phenomenon has been reached in [99]: the simple model proposed considers  $N$  individual of an asexual population ( $r = 0$ ), grouped into discrete classes, each characterized by the number  $k$  of deleterious mutations. Only deleterious mutations are allowed and they happen at rate  $u$ , causing a fixed fitness loss  $s \ll 1$ . A master equation

$$\frac{d}{dt}n_k = s(\bar{k} - k)n_k - un_k + un_{k-1} + \sqrt{n_k}\eta_k \quad (89)$$

drives the stochastic evolution of  $n_k$  = number of individuals in the  $k$ -th class,  $\eta_k$  is the noise term. When  $\lambda = u/s \gg 1$  the top fit class of individuals contains only a few individuals and is susceptible to an accidental extinction. In general, the magnitude of the fluctuations in the number of individuals of the most-fit class is governed by the combination  $Ns$ . The latter in turn induce those (delayed) of the mean fitness and accounting for both it is possible to estimate the mean time between clicks by exploiting a stochastic path integral approach, the result being given by:

$$T_{\text{click}} = \frac{2.5\zeta(\lambda)}{\alpha(\lambda)s\sqrt{Nse^{-\lambda}}} e^{Ns\alpha(\lambda)e^{-\lambda}}, \quad (90)$$

where  $\alpha(\lambda) \sim \mathcal{O}(1)$  and  $\zeta(\lambda) \sim \log \lambda$ . Repeated clicks of the Muller's ratchet lead to the accumulation of deleterious mutations; if the selection is too weak, this inevitably leads to the degradation of each genotype - sometimes referred as decay paradox [100]. In the absence of recombination or epistasis [101, 102], the only way to escape the mutational meltdown of a population is the appearance of beneficial mutations [103, 104], which becomes more and more common as the population falls back in

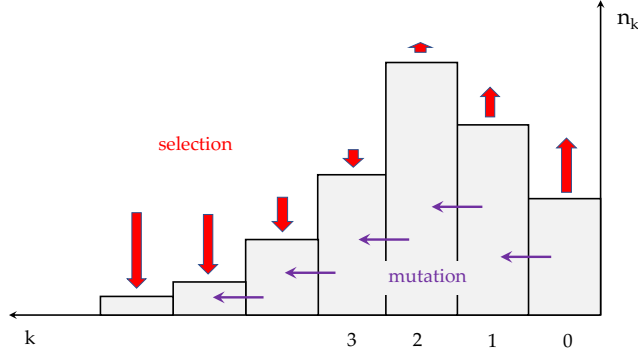


Figure 9: Deleterious mutation–selection balance. The population is distributed among classes of individuals carrying  $k$  deleterious mutations. Classes with few mutations grow due to selection (red arrows), but lose individuals through mutations (green arrows), while classes with many mutations are selected against but replenished by mutations.

fitness [105]. Deleterious and beneficial mutations thus are opposing forces: adaptation - led by the former - will drive the population up in the fitness hills, the Muller’s ratchet - expressed by the latter - will make it slide down.

In order to quantitatively understand the resulting dynamic of the genomic population, one may extend the deterministic part of Eq.(89) to

$$\frac{d}{dt}n_k = s(\bar{k} - k)n_k - un_k + u_d n_{k-1} + u_b n_{k+1} \quad (91)$$

where now  $u$  is the total mutation rate,  $\lambda = u/s$ ,  $u_b = \varepsilon u$  is the fraction of beneficial mutations, and  $u_d = (1 - \varepsilon)u$  the fraction of deleterious ones. The analysis of the selection-mutation balance defined by the latter equation is carried out in [106] and shows the existence of a stable evolutionary attractor (stable fixed point) in correspondence of a critical fraction  $\varepsilon_c$ , for any population size  $N$ , mutation rate  $u$  and selection pressure  $s$ . In particular, in the slow-ratchet regime ( $sNe^{-\lambda} > 1$ ),  $\varepsilon_c \ll 1$  since it depends exponentially on the combination  $sNe^{-\lambda}$ : selection is able to promote efficiently the genotypes in the fittest tail of the distribution and a relatively small number of beneficial mutations is needed. On the contrary, in the fast-ratchet regime ( $sNe^{-\lambda} < 1$ ),  $\varepsilon_c$  has a weaker dependence on the population parameters and it has to be larger to counterbalance the fast accumulation of deleterious mutations. Despite the simplicity of the model, evidence seems to emerge from experimental data on the general prediction of this model i.e. the dependence of the dynamic of the population on the value of  $\varepsilon_c$  [107, 108], see [106] for a more detailed discussion. Alternative approaches for a quantitative understanding of the mutation-selection dynamics can

also be found in [109] - where the problem of the Muller's ratchet is tackled in a Moran framework (overlapping generations) - or in [110] - which discusses both the scenarios of the Muller's ratchet (deleterious mutations only) and adaptation (beneficial mutations only) enforcing a traveling wave approach: the bulk of the fitness distribution evolves deterministically while a stochastic treatment is given only of the highest-fitness class.

*6.1.2. Recombination-selection dynamic: CC - transition* On relatively short time scales, the mutational influx in a population can be negligible and the only mechanism capable of fueling diversification is recombination. This is particularly relevant e.g. when two diverged strains of a population are merged together, the hybridization being driven solely by recombination events by individuals from the two strains. Understanding the role of recombination with respect to selection and drift is crucial in this case: we know from Sec.(4) that for  $r \gg 1$  there is a QLE phase, yet there are interesting analytical results recently found in [111] - building on the phenomenological intuitions of [112] - for the opposite regime ( $r \ll 1$ ), where the population is composed in whole or in part by large clones i.e. the so called clonal-competition (CC) regime.

In order to quantify the genomic composition of a recombinant population, an observable originally lifted from spin glass theory is the probability  $Y = \langle \delta(\|g - g'\|) \rangle$  that two random individuals in the population have the same genotype. In the CC phase one expects  $Y \sim \mathcal{O}(1)$ , while  $Y \sim 0$  in a QLE phase. As an example, in the even simpler case where selection is the only evolutionary force in action, the number of individuals with genotype  $g_i$ , using the master equation in Eq.(2), is given by

$$\dot{n}_i = (F_i - \langle F \rangle_t) n_i(t) \Rightarrow n_i(t) = e^{F_i t - \int_0^t dt' \langle F \rangle_{t'}} ; \quad (92)$$

assuming  $F_i \sim \mathcal{N}(0, \sigma)$  and averaging over the initial realizations of the set  $\{F_i\}$ , in the limit of large populations one gets

$$\langle Y_t \rangle = \left\langle \frac{1}{N^2} \sum_i n_i^2(t) \right\rangle \sim \begin{cases} \mathcal{O}(N^{-1}) & t < t_c \\ 1 - \frac{t_c}{t} & t > t_c \end{cases} , \quad (93)$$

where  $t_c \sim \sigma^{-1} \sqrt{2 \log N}$ . As expected, in the absence of mutations and/or recombination, after waiting a critical time  $t_c$ , an increasing fraction of the population is composed by growing clones. The statistics of the clones in Eq.(92) is the one of the Random Energy Model (REM) [113] which has a spin-glass transition below a critical temperature; here the time  $t$  plays the role of the inverse temperature  $1/T$ . The quantity  $Y$  plays the same role as the Parisi order parameter  $\overline{P}(q)$  (average overlap) [114].

In order to include the effect of recombination in the latter calculation, the following model is proposed in [111, 112]. A general function parametrized in Eq.(3) is represented as  $F = A + E$ , where  $A$  is an additive part - corresponding to the 1-spin terms, inherited in a recombination event - and an epistatic part  $E$  - corresponding to 2-spin and higher order interaction, lost upon recombination. When two individuals recombine, the additive fitness of the offspring is drawn from  $\sim \mathcal{N}(\langle A \rangle, \sigma_A)$  while its epistatic fitness is drawn from  $\sim \mathcal{N}(0, \sigma_E)$ . Overall, the governing master equation reads

$$\dot{P}(A, E) = (F - \langle F \rangle - r) P(A, E) + \frac{r}{2\pi\sigma_E\sigma_A} e^{-\frac{(A - \langle A \rangle)^2}{\sigma_A^2} - \frac{E^2}{2\sigma_E^2}} . \quad (94)$$

One can set up simulations to study the equation above, the relevant parameters being: the elapsed time  $t/t_c$  - which again plays the role of the inverse temperature

–; the ratio  $r/\sigma$  - which quantifies the strength of the recombination with respect to the selection pressure  $\sigma^2 = \sigma_A^2 + \sigma_E^2$ ; the heritability  $h$ , defined by

$$h^2 = \frac{\sigma_A^2}{\sigma_A^2 + \sigma_E^2}, \quad (95)$$

which encodes the structure of the fitness function, from purely epistatic ( $h = 0$ ) to purely additive ( $h = 1$ ). See Fig.(4) in [111].

When  $r/\sigma \gg 1$  is sufficiently large, Eq.(94) admits a factorized QLE solution  $P(A, E) = \theta(A, t)\omega(E)$  where

$$\theta(A, t) = \frac{e^{-\frac{(A-\sigma_A t)^2}{2\sigma_A^2}}}{\sqrt{2\pi\sigma_A^2}}, \quad \omega(E) = \frac{r}{r + \langle E \rangle - E} \frac{e^{-\frac{E^2}{2\sigma_E^2}}}{\sqrt{2\pi\sigma_E^2}}. \quad (96)$$

In words, the solution has a steady epistatic fitness distribution while it travels towards higher additive fitness with velocity  $\sigma_A$ . We note that this kind of behaviour is also seen in a full description of QLE phase, if one considers the transient state after e.g. the birth of a single beneficial mutation. Pairwise statistics are then stationary while single-site statistics drift towards fixation. For a discussion and possible observation in very large SARS-CoV-2 genomic data sets, see [115].

Returning to the model at hand, the travelling solution breaks down when there are individuals with epistatic fitness  $E > r + \langle E \rangle$ , beyond this threshold the population has not anymore a QLE-like Gaussian distribution but is made of growing clones the sizes of which are strongly fluctuating (random), and which depend on when and where they appeared in the population. Therefore, the breakdown of the QLE solution depends on the value of  $r$ , and a CC phase sets in for sufficiently low recombination rates. The features of this transition however depend of the structure of the fitness function, as quantified by  $h$ . In the purely epistatic case  $h = 0$ , the mean fitness increases until a balance is reached between the selection of the fittest genotype  $E_{\max} - \langle E \rangle$  and the recombination rate  $r$ . Quantitatively, one finds for the probability  $Y_t(r, h)$

$$\langle Y_t(r, 0) \rangle \sim \exp \left[ -N e^{-\sqrt{2 \log N} \left(1 - \frac{r}{r_c} t \sigma\right)} \right], \quad (97)$$

valid for  $r \sim r_c$ , where  $r_c \sim \sigma \sqrt{2 \log N}$ . The CC phase, as characterized by  $Y_t(r, 0) \sim \mathcal{O}(1)$ , sets in when  $r < r_c$  and

$$t > t_c(r) = \sigma^{-1} \sqrt{\frac{1}{2} \log N} \cdot \frac{r_c}{r - r_c}$$

Since there is no heritability in the present case, the dynamic of the population in this CC regime is the one of a "record process" [116] : when a new fitter genotype appears in the population, it can grow until replacing the previous record holder; the more time goes on, the lower the chances of seeing such a record replacement.

In the opposite limit of a purely additive fitness function ( $h = 1$ ), at low recombination rates  $r$  the population consists of few clones but none of them ever fixates in the population, since new ones with higher additive fitness are constantly produced. When a fit genotype appears in the population, it grows in size as clone, but then it shrinks and disappears new fitter ones overtake it in fitness. This kind of CC dynamic sets in when  $r < \sigma/\sqrt{2 \log N}$  for which  $Y_\infty(r, 1) \sim \mathcal{O}(1)$ .

Finally, the evolutionary dynamics for values of heritability  $0 < h < 1$  has intermediate characteristics between the two described above. At low  $r$ , the population is dominated by few large clones whose fitness function is partly non-heritable. None of them overwhelms the population but rarely they are overtaken by new fit clones appeared by chance, the more frequently the higher the parameters  $h$  and  $r$ . At the same time, since the epistatic fitness is lost upon recombination, the population has a tendency to partition in a fraction of fit clones with high epistatic fitness and a cloud of other individuals with random epistatic fitness. In this case, one finds  $Y_i(r, h) \sim \mathcal{O}(1)$  when  $r < r_c = \sigma(\sqrt{2} - \sqrt{\gamma})\sqrt{2 \log N}$ , where  $\gamma = v/\sigma^2$  is the ratio between the velocity with which the population moves toward higher fitness values (in the additive case,  $v = \sigma_A^2$ , in general  $v < \sigma_A^2$ ), and the selection pressure. We refer to [111] for details and limits of validity of the calculations summarized here.

## 6.2. A New Phase: Non-Random Coexistence

If in the previous section we have discussed separately the roles of mutations and recombination with respect to fitness and drift. In this part we introduce and characterize the behaviour of a population of genomes in a regime where mutations and recombination operate at the same time, the epistatic components of the fitness landscape are not small and dominate the dynamics. We shall call it NRC-phase, since its first clear signature is for each locus the *Non-Random Coexistence* of all the alleles in the population. Qualitatively speaking, we explore a regime characterized by a high mutation rate  $\mu$  and high epistasis  $\sigma_e$ . The NRC hence appears in a different parameter range than QLE and the state captured by the Gaussian Ansatz. As a first example, we will start from describing the behaviour of genomes that are allowed to recombine  $r \neq 0$  and that try to maximise a purely epistatic fitness function

$$F(g) = \sum_{i < j} f_{ij} s_i s_j ,$$

*i.e.* an Sherrington-Kirkpatrick (SK) fitness function, where  $f = \{f_{ij}\}_{i,j}$  is an symmetric matrix of Gaussian distributed random numbers  $f_{ij} \sim \mathcal{N}(0, \sigma_e)$ ,  $f_{ii} = 0 \forall i$ ,  $f_{ij} = f_{ji} \forall i, j$ . We observe that such a fitness function is invariant under the transformation  $g \rightarrow -g$ , hence we expect an eventual stationary state to be two-fold degenerate. Let us note that out of the domain of the QLE and the Gaussian Ansatz, we do not expect either eq.(64) or eq.(88) to work: indeed, they both fail, as will be made clear. The task of inferring evolutionary parameters from data in an NRC phase and in other phases different from QLE and the Gaussian Ansatz, is an important problem for the future, not covered in this review.

**6.2.1. Hallmarks of the NRC-phase** For illustration purposes, a suitable set of parameters is summarized in Tab.(3): we shall call it **RS** (Reference Simulation) and refer to it for future comparisons.

It is not a random choice of values, instead they are tuned so that the system dynamics lies at the border-line between the QLE phase and the new NRC phase. Our line of attack will then be to describe the latter in contrast to the former, exploiting the computational and visualization tools introduced in Appendix D.

- (i)  **$\chi_i$  : First Order Cumulants.** In Fig.10a we show the dynamics of the set of magnetizations  $\chi_i = \langle s_i \rangle$  of all the "spins sites" (dominance of one allele at

	FFPopSim	RS	Description
Drivers Structure	$N$	500	carrying capacity
	$L$	25	n. of loci
	$T$	10,000	n. of generations
	$\rho$	0.5	crossover rate
	$r$	0.5	outcrossing rate
	$\mu$	0.5	mutation rate
	$\sigma_e$	0.024	$f_{ij} \sim \mathcal{N}(0, \sigma_e)$

Table 3: Parameters of the RS. High mutation and recombination regime, random crossovers. SK fitness function. Quenched  $f_{ij} \sim \mathcal{N}(0, \sigma_e)$ ,  $f_{ii} = 0$ ,  $f_{ij} = f_{ji} \forall i, j$ . Random initial configuration.

one locus), cf. Fig.D1. We observe the first cumulants intermittently hovering between the expected behaviour in a QLE phase, *i.e.*  $\chi_i \sim 0$ , and a new phase where qualitatively  $|\chi_i| \sim \alpha \neq 0$  *i.e.* where for each locus both the alleles are found in the population in a non-random fashion. The value of  $\alpha$  is observed to primarily depend on  $\mu$  and  $\sigma_e$ . When increasing the strength of epistasis  $\sigma_e$  the large fluctuations disappear, and the dynamic of the system is always of the second type which we will call NRC-like. Obviously, as the rate of mutations is large ( $\mu \gg 0$ ) no allele is able to fixate; the steady influx of mutations will always tend to destroy patters established by selection. This balance rapidly leads to an equilibrium *i.e.* to a specific value of  $\alpha$ . The existence of a *transition* in both directions QLE  $\leftrightarrow$  NRC is not trivial, and it would be incorrect to assume the same dominating mechanism in both directions (see below). Furthermore, there is an additional element of regularity in Fig.10a: the time trajectory of all the  $\chi_i$  in the latter are either of the shape shown in Fig.10b or the mirror reflected one in Fig.10c but never a mixture of these two. The symmetry of the the chosen fitness function  $g \rightarrow -g$  is here manifest.

- (ii)  **$\chi_{ij}$  : Second Order Cumulants.** In Fig.11 the dynamics of a subset of the allele correlations  $\{\chi_{ij}\}_{j=1}^L$  is displayed. The choice of subset is for visualization, analogous plots are observed  $\forall i$ , cf. Fig.D2. The same pattern of intermittency as for the first order cumulants can be noticed: while in QLE  $\chi_{ii} = 1 - \chi_i^2 \sim 1$  and  $\chi_{ij} \sim 0$ , in the NRC regime one qualitatively has  $\chi_{ii} < 1$  and  $|\chi_{ij}| \sim \beta \neq 0$ , where  $\beta$  again depends primarily on  $\mu$  and  $\sigma_e$ . In this case such behaviour is almost overshadowed by the fluctuations.
- (iii) **Clonal Structure.** We can assess if the observed behaviour of the first and second cumulants are due to the dynamical clonal structure of the population, in particular to a Clonal Competition (CC) regime. For instance, it is well known that increasing epistasis with respect to recombination (in absence of mutations) enhances the probability of the onset of a CC-phase [111, 112]. The mutation mechanism nevertheless is likely to affect this picture and to test these hypothesis we plot the clonal structure, as shown in Fig.12, cf. Fig.D4a. As a result, a CC-phase can be ruled out, since in correspondence to a NRC region, most of the population is made by single-clone genotypes (dust-like region); however at least one non-singular clone emerges from the dust: its (fluctuating) relative size depends on  $\mu, \sigma_e$  and this observation is true until the NRC-phase melts in

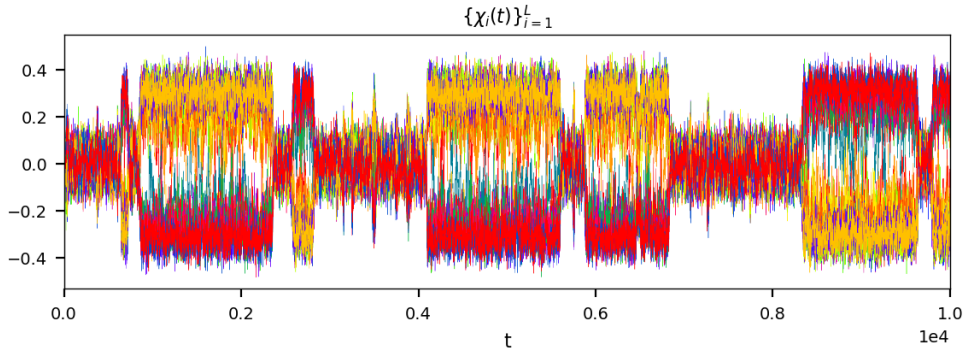
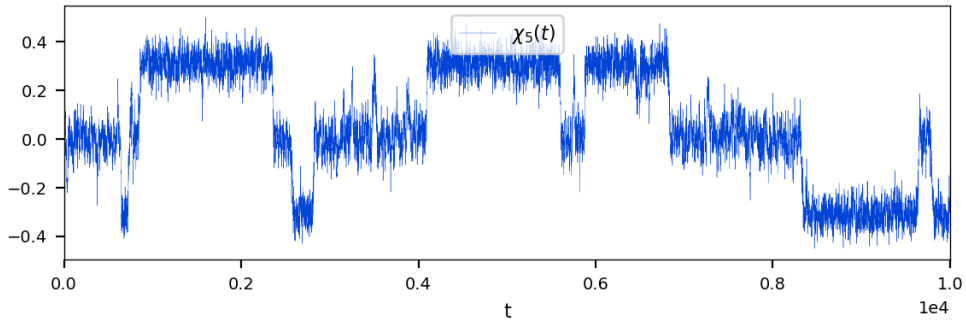
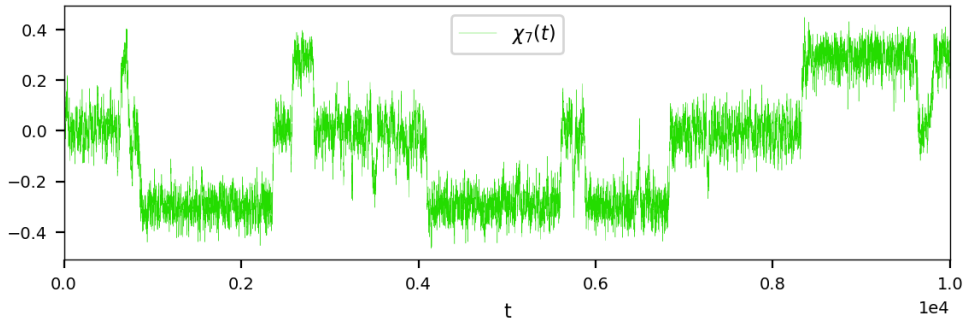

 (a) Evolution of all the  $L$  first order cumulants  $\{\chi_i\}$ .

 (b) Evolution of  $\chi_5$ , that follows the orange-like pattern in Fig.10a.

 (c) Evolution of  $\chi_7$ , that follows the red-like pattern in Fig.10a.

Figure 10: RS, Tab.(3). Evolution for the first order cumulants  $\{\chi_i\}$  at the edge of instability  $\text{QLE} \leftrightarrow \text{NRC}$ . While  $\chi_i \sim 0$  in QLE, we see  $|\chi_i| \sim \alpha \neq 0$  in a NRC phase. Two different groups of alleles emerge, following two symmetric trajectories.

the QLE randomness. Moreover, the observed fraction of individuals within the largest clone is not sufficient to explain the value  $|\chi_i| \sim \alpha$ : if a single large clone (in an otherwise random population) were responsible for  $|\chi_i| \sim 0.3$  as in Fig.10, it would need to represent a fraction  $\alpha \sim 0.3$  of the total population, which is clearly not the case of Fig.12.



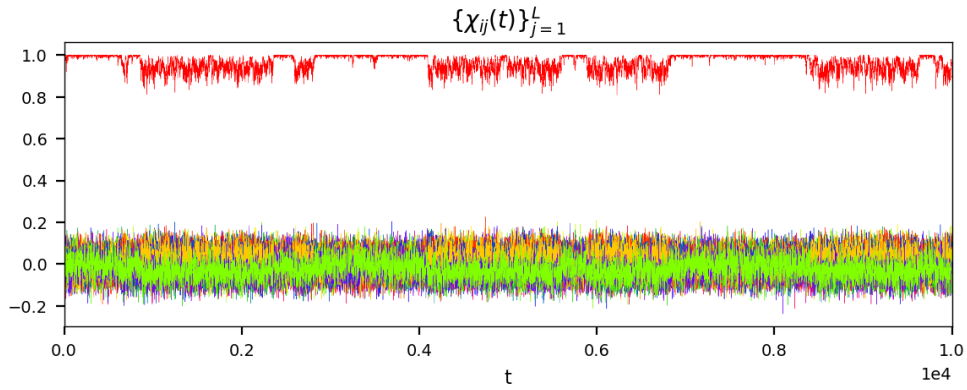


Figure 11: RS, Tab.(3). Evolution of the second order cumulants  $\{\chi_{ij}\}$  with  $i = 1$  at the edge of instability  $QLE \leftrightarrow NRC$ . While  $\chi_{ij} \sim 0$  for  $i \neq j$  and  $\chi_{ii} \sim 1$  in QLE, we see  $|\chi_{ij}| \sim \beta \neq 0$  for  $i \neq j$  and  $\chi_{ii} < 1$  in a NRC phase. The segregation in two different families of trajectories is present also for the correlations.

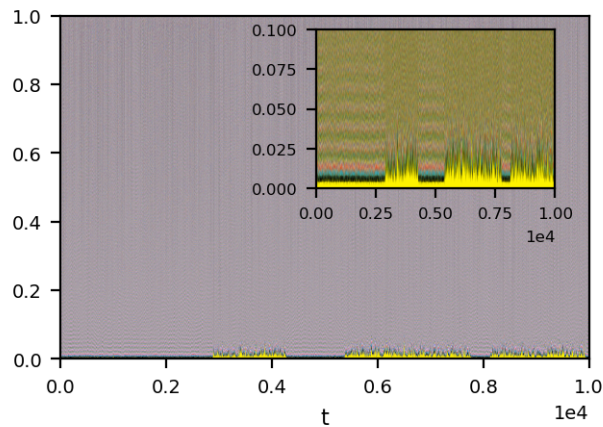


Figure 12: RS, Tab.(3). Clonal structure throughout evolution. For each  $t$ , all the clones in the population are first ordered in descending order by size, then each one is assigned a different color (six colors repeated in the order: yellow - black - cyan - red - white - blue). Their relative size for each  $t$  is displayed as a vertical line, the largest at the bottom; a zoom is provided to the first 10% of the population. The NRC phase is marked by the emergence of non-trivial clones, yet too small for the population to be regarded as in a CC-phase, this results in a mostly dust-like plot, cf. Fig.D4.

- (iv) **Fitness Statistics.** As last all-time plot we show the population-wide fitness statistics (mean, st.dev.), see Fig.13, cf. Fig.D3. The NRC phase is characterized by a higher fitness mean with respect to the QLE expectation, therefore selection will enhance the former at the expense of the latter. Mutations, on the other hand, represent a counter-force since they destroy existing genotypes: in a regime where both of them are important, their balance is crucial. Building on this observation, we may advance the hypothesis that at the edge between the two phases, the accidental appearance of very fit clones is responsible for the transition  $\text{QLE} \rightarrow \text{NRC}$ , their accidental disappearance due to mutations is responsible for the opposite ones.

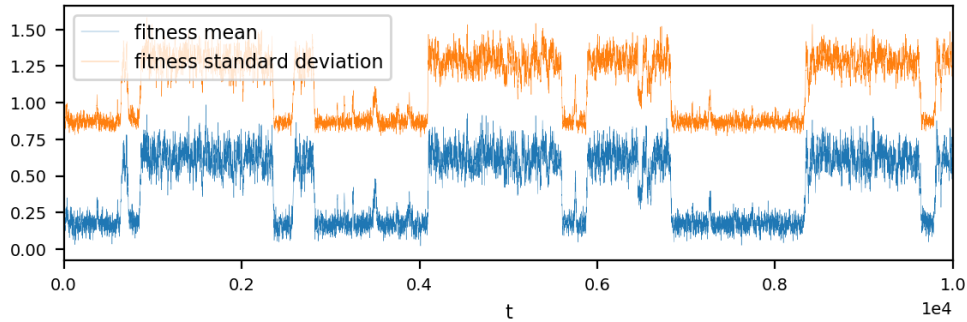


Figure 13: RS, Tab.(3). Evolution of fitness mean and st.dev. . The  $\text{QLE} \leftrightarrow \text{NRC}$  pattern is clearly visible and entails a jump in both mean and st.dev. to higher values, suggesting the emergence of very fit genotypes.

- (v) **Genotype Snapshot.** In addition to time series plots, we can observe the population instantaneously at some point during the evolution. As a first example, a snapshot of the population in a NRC phase can be plotted *e.g.* fixing  $T = 8500$ , see Fig.14, cf. Fig.D5. The difference from the QLE phase is self-evident: strong patterns of regularity emerge, consistently with the allele means fluctuating around non-zero values.

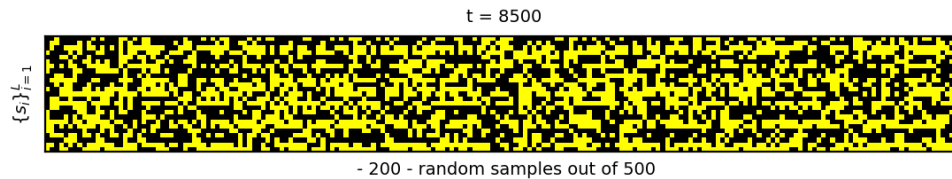


Figure 14: RS, Tab.(3). Population snapshot for 200 samples at  $t = 8500$ . Y/B for  $\chi_i = \pm 1$ . Strong patterns emerge in a NRC phase, as suggested by the dynamics of the first order cumulants.

- (vi) **Fitness Distribution.** We report in appendix (in Fig.D6) that in QLE the instantaneous fitness distribution for a population evolving in a Sherrington-Kirkpatrick fitness landscape with mutations and recombination has

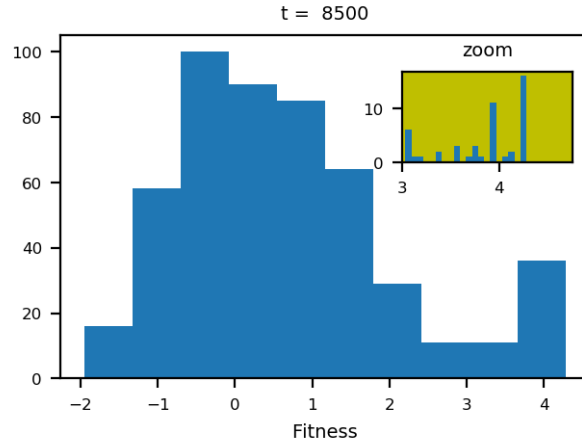


Figure 15: **RS**, Tab.(3). Fitness distribution at  $t = 8500$ , zoom on the high fitness tail. The asymmetry of the distribution is due to the mechanism of selection, that penalizes unfit individuals. The presence of spikes in the high fitness region is peculiar of the NRC phase: its (dis)appearance follows the same pattern of instability  $\text{QLE} \leftrightarrow \text{NRC}$  as in Fig.10a.

approximately the shape of a Gaussian  $\sim \mathcal{N}(0, \sqrt{L}\sigma_e)$ . The analogous plot in a NRC phase shows relevant differences, a typical result is the one in Fig.15. Two major points are to be stressed:

- *Asymmetry*. Ignoring for the moment the high fitness tail, let us focus on the main body of the distribution. This is not symmetric, but clearly biased towards positive values. This asymmetry is due to the balance between mutation and strong selection: while the first favours randomness, the second tends to encourage the emergence of individual whose fitness is higher than the average, penalizing unfit individuals.
  - *Fit Spikes*. The NRC phase is marked by the rise of a group of very fit individuals, see *zoom* in Fig.15. Their (dis)appearance is an hallmark of the transition out from / into the NRC phase. This in turn is consistent with the jump observed in the fitness statistics, since fluctuations in the number of individuals in the fittest region have strong (delayed) effects of the fitness mean [99]. Finally, as one might expect, simulations show that the size of the fit peaks grows by increasing the fitness strength.
- (vii) **Quenched disorder** As a final observation, we report the dependence of the behaviour of the simulation from the *specific realization* of the  $\{f_{ij}\}$ . In other words, at the edge of instability, the dynamics of the system strongly depends on the details of the fitness landscape. The designation of quenched disorder comes from the analogy with the spin-glasses [117]. This tells us that  $\sigma_e$  is only one hyper-parameter, and it not suitable to capture all the relevant information about the epistatic fitness landscape. This is true in particular at the edge of instability between QLE-NRC but not for weak epistasis (always QLE) or extreme epistasis (always NRC), as we shall see in Sec.(6.2.2).

6.2.2. *What If(s)* Some further observations on the behaviour at the edge between the QLE and the NRC phase are here reported. These are variations of the case illustrated above and we put them in the form of answers to questions like "What if ... ?":

- $\mathbf{f}_{\mathbf{j}} > \mathbf{0} \forall \mathbf{i} \neq \mathbf{j}$  (analogously for  $f_{ij} < 0 \forall i \neq j$ ). Recall that  $F(g) = \sum_g f_{ij} s_i s_j$ ,  $f_{ij} \sim \mathcal{N}(0, \sigma_e)$ : such system shows frustration if the epistatic components have erratic sign, while this behaviour vanishes if the  $f_{ij}$  all have the same sign. In the latter case, and for sufficiently strong epistasis with respect to other destructive forces, selection will favour either the state  $\bar{g} : \{s_i = +1 \forall i\}$  or  $-\bar{g}$ , and it is only a matter of chance whether the dynamics will lead the system toward one or the other. In practice, in Fig.10-11 all the means/correlations will behave in the same way, following the same branch, symmetry will disappear. This trivial prediction is indeed confirmed by simulations, see Fig.16

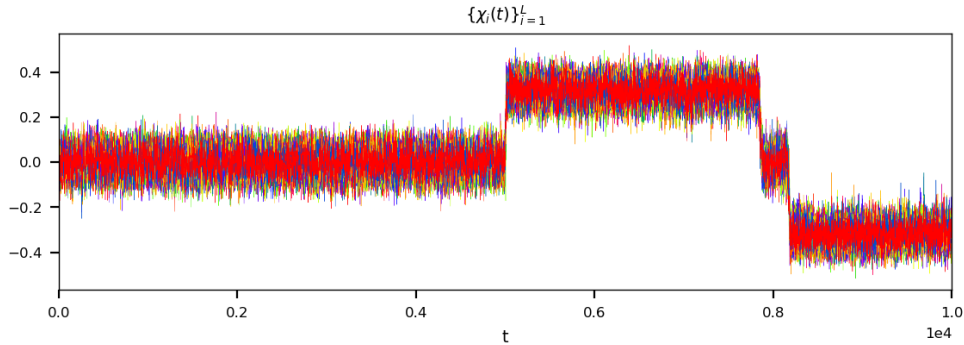


Figure 16: Evolution of first order cumulants. Parameters of the simulation as for RS, Tab.(3), except for  $\sigma_e = 0.0087$  and  $f_{ij} \geq 0 \forall i, j$ . The symmetry observed in Fig.10 is broken.

- **No recombination**  $r = 0$ . Recombination, along with mutations, contributes to reshuffle the genetic pool, hence increasing the probability of the appearance of new genotypes in the population. Recent theoretical efforts have investigated the role of recombination both at the genotype and phenotype level [111, 118, 119]. The understanding of its interaction with other evolutionary forces however remains limited to specific cases, and a general understanding is lacking. In the context of the NRC phase, we can assess the simulations in absence of recombination,  $r = 0$ . Simply using RS Tab.(3) with  $r = 0$  eliminates any signature of the NRC and a QLE behaviour is observed throughout the evolution. This supports the hypothesis that the probability of the appearance of fit individuals is crucial for the transition QLE→NRC: the less the recombination, the less the such probability. One way to compensate this effect is to increase the fitness strength  $\sigma_e$ . In fact, for a sufficiently high epistasis, we see again a behaviour of allele means similar to that observed in Fig.10, although trajectories are much more unstable, see *e.g.* Fig.17. In general, stronger fluctuations appear, which forces to choose an high value of the system expected size  $N$  in order to reduce the noise. Transition probabilities appear to be sensitive to recombination as well. Moreover, when  $r = 0$ , even for very high values of fitness strength, no

QLE-NRC oscillation is observed in the plots for the clonal structure, fitness statistics and instantaneous fitness distribution, as described in the previous section. In other words, the mechanisms that sustain the birth/death of fit individuals in the high fit tail of the fitness distribution strongly depends on the presence of recombination. In general these remarks support the hypothesis that the drivers (or consequences) of the transitions between the two phases here are fundamentally different from those in the case with recombination and one cannot regard the latter as a mere "additive" complication to the model.

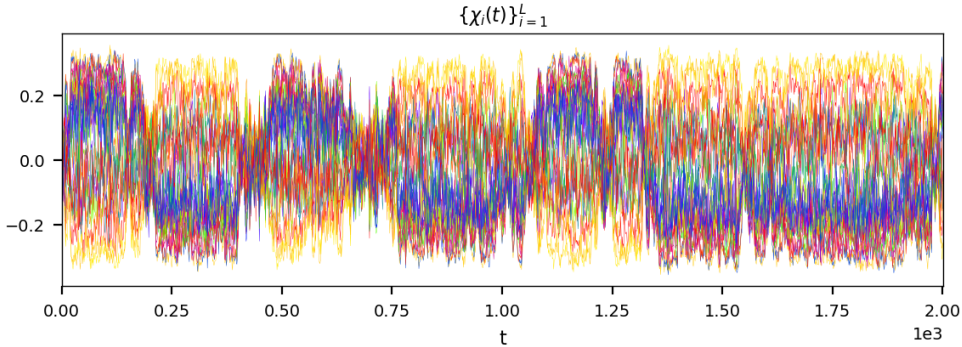


Figure 17: Evolution of first order cumulants. Parameters of the simulation as for RS, Tab.(3) except for  $N = 10.000, T = 2.000, \sigma_e = 0.09, r = 0$ . In the case with no recombination, the behaviour of the system shows substantial differences with respect to the case  $r \neq 0$ .

- **Additive fitness,  $\mathbf{f}_i \neq \mathbf{0}$ .** Additive fitness has the effect of driving each allele to fixation. The dynamics of one locus can then be summarized as  $s_i \xrightarrow{add.} \text{sgn}(f_i)$ . Differently from epistasis, additive fitness acts independently in each locus. We here focus on the narrower question: is the NRC due to the specific role of epistasis? To test it, additive components of fitness can be turned on. For instance, using RS with in addition  $f_i \sim \mathcal{N}(0, \sigma_a)$ , with  $\sigma_a = 2.0 \gg \sigma_e$ . As a result, we observe that even in the case high additive fitness, the observation of the QLE-NRC behaviour is present. Evidently as long as the overall fitness is sufficiently high, it does not matter whether it is additive or epistatic. In the case where both of them are present, a more suitable selection parameter is  $\sigma^2 = \sigma_a^2 + \sigma_e^2$ .
- **$N - \sigma_e$  tuning.** The size of fluctuations grow as  $\sqrt{N}$ . The higher the fluctuations, the higher the probability of finding the system in an atypical state. If the transition QLE  $\rightarrow$  NRC is triggered by the system hitting a small subset of the possible states, then larger fluctuations are expected to enhance the corresponding chances. Accordingly, for a fixed  $\sigma_e$ , QLE will be observed for sufficiently low  $N$  and NRC for sufficiently high  $N$ . On the other hand, for fixed  $N$ , we already know that higher epistasis will favour a NRC phase. In Fig.18 tests qualitatively these expectations for different values of  $N - \sigma_e$ . With regard to the intermediate region in  $\sigma_e$ , we see explicitly the dependence of the system fate on the specific realization of the  $\{f_{ij}\}$  (some simulations may seem to be QLE or NRC for  $T < \infty$

even if in a instability region); on the contrary, the extrema do not show such behaviour.

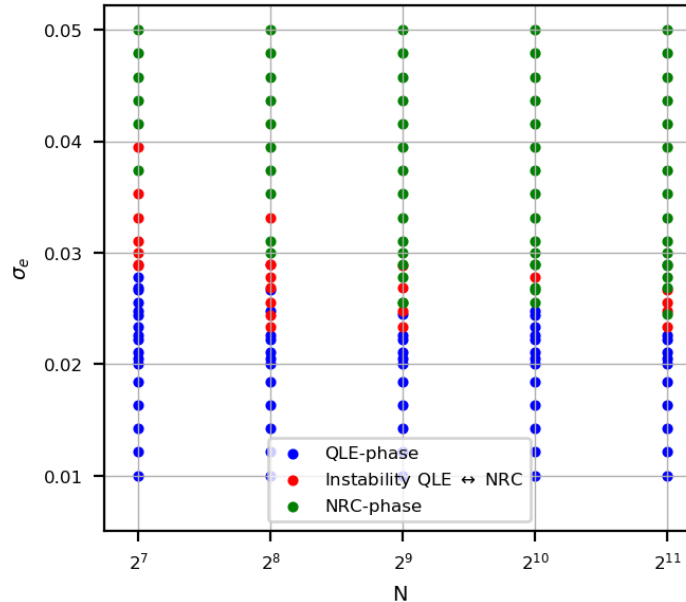


Figure 18: Qualitative scan of the parameter space in the  $N$ ,  $\sigma_e$  directions, all other settings as in RS, Tab.(3). Each point is obtained as follows: we fix a pair  $(N, \sigma_e)$  and run two simulations for  $T = 10.000$  generations. If at any point we observe a transition QLE $\leftrightarrow$ NRC, we mark the point as red, instability. If the system throughout the simulations appears to always be in a QLE/NRC phase, we colour the point in blue / green, respectively. In order to classify the two phases automatically, we choose the fitness mean, cf. Fig.13, as an observable and set a threshold. Due to the finite simulation time and to the dependence on the quenched disorder, the instability region is likely to be broader than what shown here.

### 6.3. Phenomenology of the NRC

**6.3.1. QLE to NRC: heuristics** A number of previous contributions have investigated the balance between mutations and selection, *e.g.* [104, 120]. A typical approach consists in estimating the typical timescales for the appearance, establishment (*i.e.* survival to random drift) and fixation of new mutations, depending on the parameters of the model. We can pursue a similar line of thought to develop a plausible mechanism that could drive the QLE  $\rightarrow$  NRC transition. Considering a system such as the one in RS, two processes should be relevant:

1. Appearance of a genotype with high fitness in the population. Let's call  $P_A(g|\mu, r, N, \{f_{ij}\})$  the probability for a sufficiently fit genotype  $g$  to appear. We have only  $N \ll 2^L$  individuals, there should be some  $t_A(\mu, r, N, \{f_{ij}\})$  typical waiting time. How to estimate the  $t_A$  is an open question.

2. Establishment of the clone with the genotype  $g$  *i.e.* the clone is large enough so that it manages to survive to the random drift, mutations and recombination. Let's call  $P_E(g|\mu, r, N, F(g))$  the corresponding probability. One may think to a threshold value  $F^*(\mu, r, N)$  above which a clone is likely to emerge. This could suggest an explanation for the behaviour observed Fig.18: let us define  $F_{\max} = \max_g F(g)$ , if  $\sigma_e$  is low enough,  $F_{\max} < F^*$  and no genotype is able to emerge (QLE phase). When  $\sigma_e$  is such that  $F_{\max} > F^*$  then it is possible for one or more clones to emerge (QLE/NRC instability), here the quenched disorder plays a fundamental role. Finally, for very high values of  $\sigma_e$ ,  $F_{\max} \gg F^*$ , several clones emerge and disruptive forces (or whatever) do not manage to sweep them all out (NRC phase).

**6.3.2. Escape Times** There is no *a priori* reason to believe that the two transitions QLE  $\leftrightarrow$  NRC are governed by the same mechanism: indeed, we will show in this section that they are not. In order to target this question, the escape times from one phase to the other can be studied. Let us call  $t_{\text{QLE}}, t_{\text{NRC}}$  the escape times from the QLE and NRC phases, respectively, from Sec.(6.1.1), we expect in a rough approximation  $T_{\text{click}} \sim \exp(N)$ . The numerical algorithm is the following, see [121] for the implementation.

- (i) **Simulation.** Tuning parameters so to set the system in a region of strong instability QLE  $\leftrightarrow$  NRC and running simulations for  $T$  as large as possible, the system will undergo multiple transitions in both directions. Let us call such a simulation ET, for instance we can set Tab.(4)

	FFPopSim	ET	Description
Drivers Structure	$N$	575	carrying capacity
	$L$	25	n. of loci
	$T$	$150.000 \times 10$	n. of generations
	$r$	0.5	outcrossing rate
	$\rho$	0.5	crossover rate
	$\mu$	0.5	mutation rate
	$\sigma_e$	0.029	$f_{ij} \sim \mathcal{N}(0, \sigma_e)$

Table 4: Parameters of the ET. The total number of generations simulated is 150 times higher with respect to RS.

- (ii) **Classification.** The mean fitness of the population is a suitable observable in order to set a threshold and automatically classify the two phases (above: NRC; below: QLE), hence to evaluate the number of generations spent in one phase since the last transition (escape time). As an output of this last step, a list of escape times is obtained from the QLE phase and, analogously, from the NRC phase.
- (iii) **Distribution.** Histograms are drawn out of those two lists and observe the distributions of the escape times  $t_{\text{QLE}}, t_{\text{NRC}}$ , see Fig.19. In both cases, the distribution in a first approximation can be described as exponential, so we try to fit it with

$$y(T) = \gamma_i e^{-a_i T}, \quad i = \text{QLE, NRC.} \quad (98)$$

In particular we are interested in  $a_{\text{QLE}}$ ,  $a_{\text{NRC}}$ , that set the rates of the transitions, and use  $t_{\text{QLE}} \sim 1/a_{\text{QLE}}$ ,  $t_{\text{NRC}} \sim 1/a_{\text{NRC}}$  as qualitative measures of the expected escape time from the two phases.

- (iv)  **$N$  Dependence.** Finally, in order to check the dependence of these last quantities on the population size, as suggested in the previous section, steps 1.-3. are repeated for different values of  $N$ , the behaviour of  $t_{\text{QLE}}(N)$ ,  $t_{\text{NRC}}(N)$  is plotted in Fig.20.¶

As a result, the estimate of the escape time from the QLE phase appears to be almost insensitive to the size of the system, while that from the NRC phase is compatible with an exponential behaviour  $\sim \exp(N)$ . This latter result is consistent with the previous discussion on the Muller's Ratchet and could be used as a starting point for a model of the phenomenon *e.g.* in terms of an escape time over a potential barrier, akin the Arrhenius formula  $T_{\text{esc}} \sim \gamma \exp[(U(b) - U(a))/D]$ , where  $U(b) - U(a)$  is the height of the potential barrier and  $\gamma, D$  constants [122].

#### 6.4. A NRC-phase for *E.Coli*?

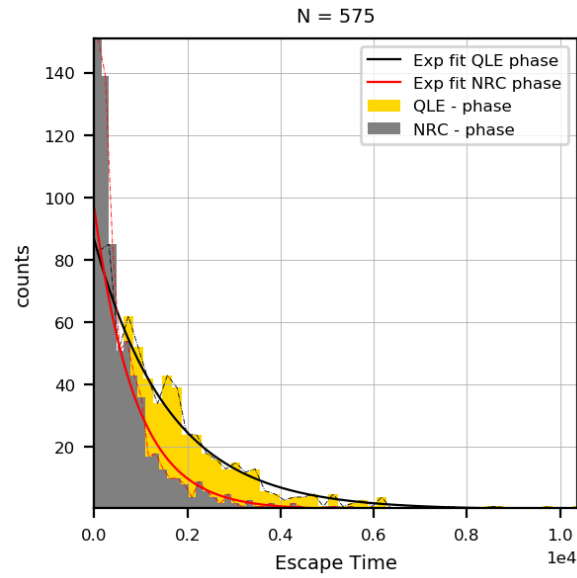
Lenski's celebrated *E.coli Long Term Evolution Experiment* (LTEE) is an ongoing study that has been tracking genetic evolution in 12 initially identical populations of asexual *Escherichia coli*, in the same media, since 24 February 1988 (currently more than 70,000 generations observed). The paramount interest in this experiment lies in the fact that it is the largest dataset available that puts evolution under the spotlight of the experiment: bacteria grow, mutate, evolve (recombination is negligible for *E.coli*). The complexity of the evolutionary process emerges clearly from the ensemble of observed behaviours across populations: clades arise and diverge, small mutations leading to genetic catastrophes, intricate interactions with the environment. In a recent contribution, the authors of [123] have worked out the latest analysis of the LTEE, enquiring the stochastic dynamical process that governs how mutations arise and spread through the populations. In particular, we focus on what the authors call *quasi-stable coexistence* therein. The result of the experiment is showed in Fig.21.

Let us focus *e.g.* on the lineage Ara-6. Current models of both "periodic selections" (where individual driver mutations fix in a sequence of discrete selective sweeps), or clonal-competition predict that, sooner or later, mutations should either fixate in the population or go extinct. But in Fig.21 we observe clearly mutations segregating into (at least) two intermediate-frequency clades that coexist for long periods, hence the name *quasi-stable coexistence*; specifically, 9/12 populations have clades that coexist for more than 10.000 generations, the relative abundance of the two clades varies from population to population.

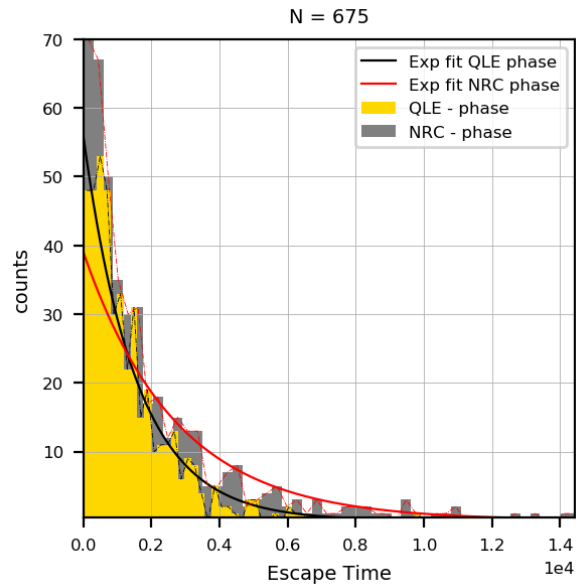
There is so far no understanding on the mechanisms that sustain this behaviour. The authors of the study suggest that a crucial role could be played by *negative frequency-dependent selection* (removal of deleterious alleles that depends on the current fraction of such alleles) or *coupling between ecologically divergent phenotypes and fitness gain* (which entails interaction at the phenotype layer between individuals and environment, projected in the genotype space through the unknown genotype-phenotype map). On the other hand, the coupling environment-selection is exactly

¶The range of  $N$  values that can be tested is both upper and lower bounded by the computational resources: whenever the transitions are rarer, it is necessary to simulate more generations in order to collect a sufficient statistics for the histograms.





(a)



(b)

Figure 19: Distribution of Escape Times from the QLE phase (yellow) and from the NRC phase (gray). Parameters of the simulations as in Tab.(4), two example system sizes  $N = 575$  and  $N = 675$ . For each phase, we perform a linear fit in the semi-log scale, in particular we get  $a_{QLE}, a_{NRC}$  in eq.(98). The exponential curves in linear scale resulting from the fitting procedures are also shown.

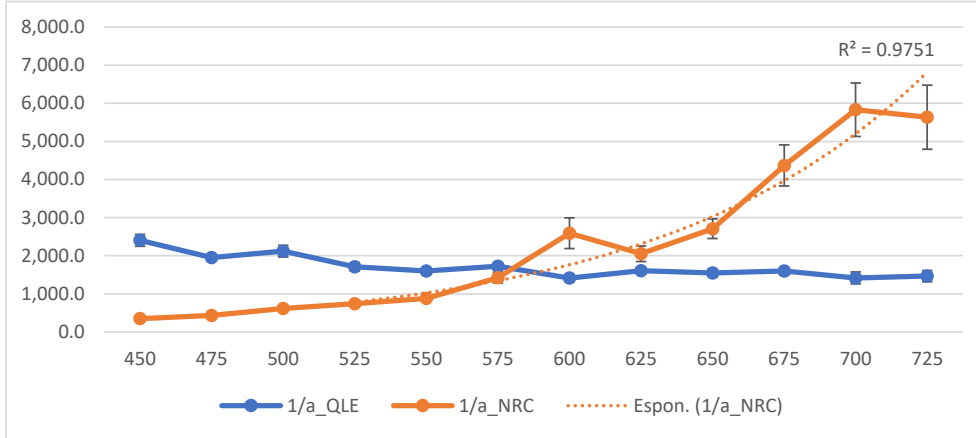


Figure 20: Behaviour of  $t_{QLE} \sim 1/a_{QLE}$ ,  $t_{NRC} \sim 1/a_{NRC}$  as a function of the carrying capacity  $N$ . The plot is a strong evidence of the fact that the transitions  $QLE \rightarrow NRC$  and  $NRC \rightarrow QLE$  are due to different mechanisms. While  $t_{QLE}$  seems to be almost insensitive to  $N$ ,  $t_{NRC}$  is compatible with a behaviour  $\sim \exp N$ , as confirmed by the coefficient of determination  $R^2 \sim 1$ .

what we encode when using a selection based on a fitness function. We hence hypothesise that such behaviour of the *E.coli* is induced and sustained by the same fundamental mechanisms that induce or sustain the NRC phase in our simulations with  $r \sim 0$ .

This hypothesis offers undoubtedly an exciting line of research for the next future. On the other hand, despite the number of observations, the NRC phase remains obscure in some respects, even at the stage of the synthetic simulation. In particular, there is not a full understanding on which are the drivers of the transitions  $QLE \leftrightarrow NRC$  and which mechanisms sustain the NRC phase. Filling this gap will, we believe, be a fundamental step towards a meaningful application of NRC predictions to biological data.

## 7. Summary and discussion

In this work we have provided a self-contained review of the dynamics of a population evolving under selection (Darwinian evolution, survival of the fitness), mutation and recombination. We have shown how high rates of mutation or recombination (or both) relative to the rate of selection naturally leads to the Quasi-Linkage Equilibrium (QLE) phase first described by Kimura [38]. The QLE phase is characterized by:

- correlations between allele distributions at different loci are weak;
- multi-genome distributions approximately factorize into products of one-genome distributions;
- the distributions of individuals in the population over genotypes are well described by the Gibbs-Boltzmann distribution;
- the parameters of the Gibbs-Boltzmann distribution are related to evolutionary parameters, including fitness.

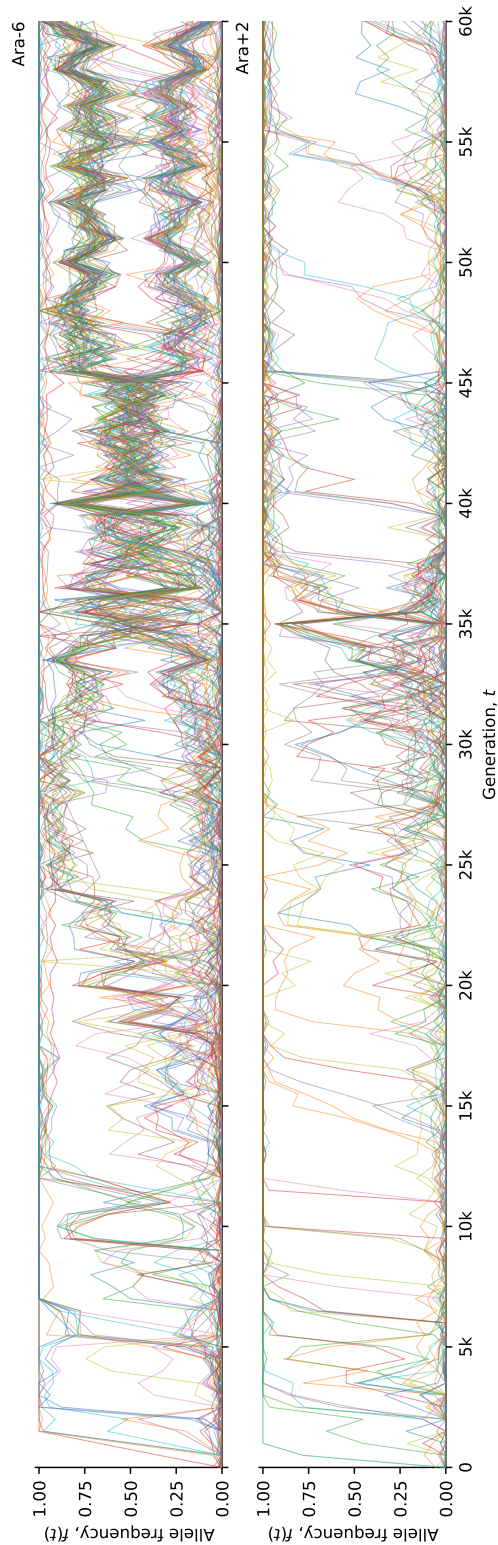


Figure 21: Allele frequency trajectories  $\nu_i = (1 - \chi_i)/2 \in [0, 1]$  of all *de novo* mutations detected in the 2 of the 12 LTEE populations reported in [123], specifically the ones labeled Ara-6 and Ara+2. While Ara-6 (top row) shows an example of quasi-stable coexistence of clades, such behaviour is not present in the population Ara+2 (bottom row), where mutations fix rapidly. The analysis in [123] reveals quasi-stable coexistence in 9 out of 12 observed populations. Figure previously unpublished, private communication from B.H. Good and M.M. Desai, reproduced here with permission. Data obtained from same set of experiments as described in [123].

The last property is a kind distributional phenotype-genotype relation (dPGR), because it is phenotype which determines fitness, and it is the distribution law over genotypes which is determined by fitness. We have shown that different albeit quite similar dPGRs hold in the limits of respectively high recombination rate (but not mutation rate), and high mutation rate (but not recombination rate). A single formula encompasses both cases. When it holds, evolutionary parameters such as additive and epistatic fitness can be inferred from Gibbs-Boltzmann model parameters which in turn can be inferred from data, using dPGR to make the translation. We have demonstrated that the above scheme works *in silico* experiments, and we have also demonstrated how to derive higher-order inference schemes than the ones alluded to above. We suggest that QLE is a fertile field for future applications of statistical physics concepts to population genetics on the whole-genome level.

On a different track we have considered the dynamics at relatively higher values of selection. We have described a new behaviour which breaks time translation symmetry. For sufficiently strong epistatic selection the state of the population switches randomly between a behavior qualitatively similar to QLE, and a phase of Non-Random Coexistence (NRC) where the population is dominated by one fit genotype and its neighbours. We have determined how the stability boundaries of the QLE phase going towards the NRC phase and vice versa change with model parameters, including population size  $N$ . We surmise that also the NRC phase constitutes an interesting application area of statistical physics, albeit to non-equilibrium processes not in detailed balance. We have further related the NRC phase to behavior observed experimentally in long-time evolution experiments.

On a general level the conclusion of this work is that the statistical physics analogy is both useful and of limited use in population genetics. It is a fact that reasonable models of evolution in certain parameter ranges settle down to stationary distributions of the same form as in equilibrium statistical mechanics, which is the basis for theories such as those developed in [124–126]. A whole collection of methods, collectively known as Direct Coupling Analysis (DCA) can then be used to infer evolutionary parameters from the distribution of sequences in a population. Naturally, if and when one has access to time series data, other inference methods can be used, and they will often be more powerful. Large-scale sequencing data on are however rarely of this type: more typically one knows the distribution of sequences (genotypes) at one or at most a few time points, and one does not have information on which sequences gave rise to which other sequences except from their similarity. In this setting the knowledge that the distribution is of the Gibbs-Boltzmann type can be leveraged to extract parameters describing the dynamics from what is essentially static information.

On the other hand, the underlying dynamics is not in thermal equilibrium *i.e.* does not obey detailed balance, and the range of possibilities is hence wider [127, 128]. In the class of models considered in this work the distribution does not have to approach that of a stationary Gibbs-Boltzmann distribution with energy-like terms; dynamics can go on indefinitely, and the distribution of genotypes in a population can fluctuate without ever reaching a stationary state. Models of life, even with all the simplifying assumptions made here, hence allow for rich repertoires not easily captured by models too closely patterned after equilibrium statistical mechanics.

## Appendix A. Moments vs Cumulants

Here we briefly introduce moments and cumulants of a probability distribution and specify the discussion for the specific case of the Gaussian distribution. Let  $\mathbf{X} = (X_1, \dots, X_n)$  be a vector of random variables with pdf  $p(\mathbf{x})$ , then the *characteristic function* is

$$\phi(\mathbf{q}) = \int p(\mathbf{x}) e^{i\mathbf{q}\mathbf{x}} . \quad (\text{A.1})$$

with  $\phi(\mathbf{0}) = 1$ ,  $|\phi(\mathbf{q})| \leq 1$ . The function  $\phi(\mathbf{q})$  is a characterization of the probability distribution  $p(\mathbf{q})$  *i.e.* it completely determines its behaviour and properties. If the *raw moments*  $\langle \prod_i X_i^{m_i} \rangle$  exist, then

$$\langle \prod_i X_i^{m_i} \rangle = \left[ \prod_i \left( -i \frac{\partial}{\partial q_i} \right)^{m_i} \phi(\mathbf{q}) \right]_{\mathbf{q}=\mathbf{0}} . \quad (\text{A.2})$$

It is also possible to define the *cumulant generating function* as

$$\psi(\mathbf{q}) = \log \phi(\mathbf{q}) . \quad (\text{A.3})$$

Suppose that it is possible to expand  $\phi(\mathbf{q})$  and  $\psi(\mathbf{q})$  in power series about the origin (*i.e.* all derivatives exist); then we can formally write:

$$\phi(\mathbf{q}) = \sum_{r=1}^{\infty} i^r \sum_{\{\mathbf{m}\}} \langle X_1^{m_1} \dots X_n^{m_n} \rangle \frac{q_1^{m_1} \dots q_n^{m_n}}{m_1! \dots m_n!} \delta\left(r, \sum_{i=1}^n m_i\right) , \quad (\text{A.4})$$

$$\psi(\mathbf{q}) = \sum_{r=1}^{\infty} i^r \sum_{\{\mathbf{m}\}} \langle\langle X_1^{m_1} \dots X_n^{m_n} \rangle\rangle \frac{q_1^{m_1} \dots q_n^{m_n}}{m_1! \dots m_n!} \delta\left(r, \sum_{i=1}^n m_i\right) , \quad (\text{A.5})$$

where  $\langle X_1^{m_1} \dots X_n^{m_n} \rangle$  are defined in eq.(A.2) and  $\langle\langle X_1^{m_1} \dots X_n^{m_n} \rangle\rangle$  are the *cumulants* of the distribution  $p(\mathbf{x})$ . Both these two set of quantities stem from the same characteristic function  $\phi(\mathbf{q})$  and are alternative parametrizations of the probability distribution. Expanding and comparing eq.(A.4, A.5) one finds:

$$\begin{aligned} \langle\langle X_i \rangle\rangle &= \langle X_i \rangle , \\ \langle\langle X_i X_j \rangle\rangle &= \langle X_i X_j \rangle - \langle X_i \rangle \langle X_j \rangle , \\ \langle\langle X_i X_j X_k \rangle\rangle &= \langle X_i X_j X_k \rangle - \langle X_i X_j \rangle \langle X_k \rangle - \langle X_i X_k \rangle \langle X_j \rangle + \\ &\quad - \langle X_j X_k \rangle \langle X_i \rangle + 2 \langle X_i \rangle \langle X_j \rangle \langle X_k \rangle ; \end{aligned}$$

note that the first two cumulants are the means and covariances (second *central moments*). A diagrammatic method to compute cumulants was given in [122]; an extensive treatment from the probability-theory point of view can be found in [129].

As far as this work is concerned, an important difference is to be stressed. We have  $\langle X^{2n} \rangle \geq \langle X^n \rangle^2$  and thus all moments contain information about lower moments [122]. On the other hand, higher order cumulants contain information of decreasing significance and one can therefore consider the approximation that  $\langle\langle X^n \rangle\rangle = 0 \ \forall n > 2$ . In the language of quantum field theory, the moments  $\langle X_1 \dots X_n \rangle$  are *n-point correlation functions* while the  $\langle\langle X_1 \dots X_n \rangle\rangle$  are *n-point connected correlation functions* *i.e.* the sum over all *n*-points 1PI Feynman diagrams, a key ingredients of such theories [130].

Let us specify the above discussion to the case of a *multivariate Gaussian probability distribution*:

$$p(\mathbf{x}) = \frac{1}{\mathcal{Z}} e^{-\frac{1}{2}(\mathbf{x}-\boldsymbol{\mu})^T C^{-1}(\mathbf{x}-\boldsymbol{\mu})}, \quad (\text{A.6})$$

where  $\boldsymbol{\mu}$  is the mean and  $C$  is the covariance matrix,  $\mathcal{Z} = [(2\pi)^n \det(C)]^{-\frac{1}{2}}$  is the normalization. The characteristic function of such distribution is

$$\phi(\mathbf{q}) = e^{i\mathbf{q}^T \boldsymbol{\mu} - \frac{1}{2}\mathbf{q}^T C \mathbf{q}} \quad (\text{A.7})$$

and from this we see that *all cumulants of order  $\geq 2$  vanish*. Therefore, all moments can be expressed in terms only of first and second order cumulants. Since they are of interest for this work, let us evaluate the first four moments of this distribution using eq.(A.2) (different indices).

$$\begin{aligned} \langle X_i \rangle &= -i \frac{\partial}{\partial q_i} \phi(\mathbf{q}) \Big|_{\mathbf{q}=\mathbf{0}} \\ &= -i \left( i\mu_i - \sum_n C_{in} q_n \right) e^{i\mathbf{q}^T \boldsymbol{\mu} - \frac{1}{2}\mathbf{q}^T C \mathbf{q}} \Big|_{\mathbf{q}=\mathbf{0}} \\ &= \mu_i \\ \langle X_i X_j \rangle_{i \neq j} &= (-i)^2 \frac{\partial}{\partial q_j} \frac{\partial}{\partial q_i} \phi(\mathbf{q}) \Big|_{\mathbf{q}=\mathbf{0}} \\ &= - \left[ -C_{ij} + \left( i\mu_j - \sum_n C_{jn} q_n \right) \left( i\mu_i - \sum_n C_{in} q_n \right) \right] e^{i\mathbf{q}^T \boldsymbol{\mu} - \frac{1}{2}\mathbf{q}^T C \mathbf{q}} \Big|_{\mathbf{q}=\mathbf{0}} \\ &= C_{ij} + \mu_i \mu_j \\ \langle X_i X_j X_k \rangle_{i \neq j \neq k} &= (-i)^3 \frac{\partial}{\partial q_k} \frac{\partial}{\partial q_j} \frac{\partial}{\partial q_i} \phi(\mathbf{q}) \Big|_{\mathbf{q}=\mathbf{0}} \\ &= i \left[ -C_{jk} \left( i\mu_i - \sum_n C_{in} q_n \right) - C_{ik} \left( i\mu_j - \sum_n C_{jn} q_n \right) \right. \\ &\quad \left. - C_{ij} \left( i\mu_k - \sum_n C_{kn} q_n \right) + \left( i\mu_k - \sum_n C_{kn} q_n \right) \times \right. \\ &\quad \left. \times \left( i\mu_j - \sum_n C_{jn} q_n \right) \left( i\mu_i - \sum_n C_{in} q_n \right) \right] e^{i\mathbf{q}^T \boldsymbol{\mu} - \frac{1}{2}\mathbf{q}^T C \mathbf{q}} \Big|_{\mathbf{q}=\mathbf{0}} \\ &= \mu_i C_{jk} + \mu_j C_{ik} + \mu_k C_{ij} + \mu_i \mu_j \mu_k \end{aligned}$$

$$\begin{aligned}
\langle X_i X_j X_k X_l \rangle_{i \neq j \neq k \neq l} &= (-i)^4 \frac{\partial}{\partial q_l} \frac{\partial}{\partial q_k} \frac{\partial}{\partial q_j} \frac{\partial}{\partial q_i} \phi(\mathbf{q}) \Big|_{\mathbf{q}=\mathbf{0}} \\
&= \left\{ C_{ij} C_{kl} + C_{ik} C_{jl} + C_{jk} C_{il} + C_{kl} \left( i\mu_j - \sum_n C_{jn} q_n \right) \left( i\mu_i - \sum_n C_{in} q_n \right) + \right. \\
&\quad + C_{jl} \left( i\mu_k - \sum_n C_{kn} q_n \right) \left( i\mu_i - \sum_n C_{in} q_n \right) + C_{il} \left( i\mu_j - \sum_n C_{jn} q_n \right) \times \\
&\quad \times \left( i\mu_k - \sum_n C_{kn} q_n \right) + \left[ -C_{jk} \left( i\mu_i - \sum_n C_{in} q_n \right) - C_{ik} \left( i\mu_j - \sum_n C_{jn} q_n \right) \right. \\
&\quad - C_{ij} \left( i\mu_k - \sum_n C_{kn} q_n \right) + \left. \left( i\mu_k - \sum_n C_{kn} q_n \right) \left( i\mu_j - \sum_n C_{jn} q_n \right) \times \right. \\
&\quad \left. \left. \times \left( i\mu_i - \sum_n C_{in} q_n \right) \right] \left( i\mu_l - \sum_n C_{ln} q_n \right) \right\} e^{i\mathbf{q}^T \boldsymbol{\mu} - \frac{1}{2} \mathbf{q}^T C \mathbf{q}} \Big|_{\mathbf{q}=\mathbf{0}} \\
&= C_{ij} C_{kl} + C_{ik} C_{jl} + C_{jk} C_{il} + C_{ij} \mu_k \mu_l + C_{ik} \mu_j \mu_l + C_{il} \mu_j \mu_k + C_{jk} \mu_i \mu_l + \\
&\quad + C_{jl} \mu_i \mu_k + C_{kl} \mu_i \mu_j + \mu_i \mu_j \mu_k \mu_l .
\end{aligned}$$

## Appendix B. Random Genetic Drift

In this work we have considered the infinite population limit  $N \rightarrow \infty$  and neglected issues arising from taking into account the stochastic nature of the birth/death processes in a finite population [131]. In the case  $N < \infty$ , the element of chance introduced by the random sampling of the individuals that survive from one generation to another is alone capable of driving an allele to fixation or extinction.

Such an effect is well known in population genetics: it is the *genetic drift*, as discussed first by R.A. Fisher [17] and S. Wright [132] (Fisher-Wright or FW model). In their simplest model of genetic drift no recombination or mutations are included and selection is absent. Stochastic effects alone then drive the evolution: one says that these are *neutral* models. For the sake of simplicity, consider an haploid population of constant size  $N$ . Evolution is encoded in a series of discrete, non-overlapping generations. Each time step  $t \rightarrow t+1$  entails a replacement of the entire population, with a process akin to the sampling with replacement of coloured balls from an urn, this is the so called *beanbag population genetics*, see Fig.B1. The FW model employs a Markov-process formalism to predict that, sooner or later, the alleles either fixate or go extinct and the corresponding probabilities only depend on their initial frequency [6]. When trying to extend this approach to the case in which mutation, recombination and selection play a role in the evolutionary process, the calculations soon become cumbersome to work out and in order to deal with these difficulties a number of approximations have been proposed. M. Kimura [133, 134] showed that in large populations the discrete FW process can be approximated by a continuous time, continuous space diffusion process. Let  $x = i/N$  be the frequency of the allele +1,  $P(x, t)$  the probability of finding  $x$  at time  $t$ . Let us suppose that, together with genetic drift, there is also a selective advantage for the allele +1 *i.e.* the individuals with that allele have on average  $1+s$  offspring, those with  $-1$  only on average just 1; let also  $\sigma^2$  be the variance in the number of offspring. Finally, assume also that fluctuations are uncorrelated across individuals and generations (non-heritable). Then in a diffusion approximation the distribution of the variant frequency evolves according

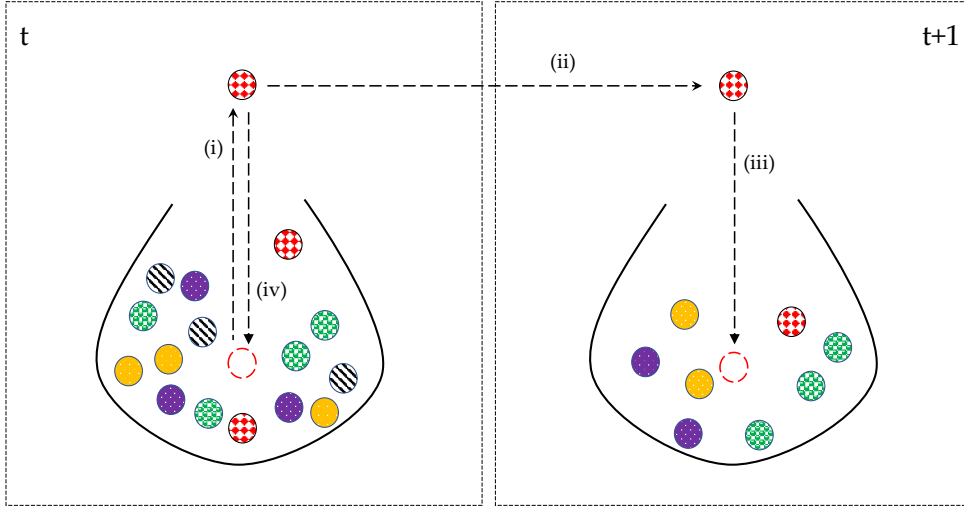


Figure B1: Beanbag population genetics. The population at  $t + 1$  is constructed from that at  $t$  (size  $N$ ) by (i) selecting a gene from  $t$  at random; (ii) copying this gene; (iii) placing the copy in the next generation; (iv) returning the original to the parent population. This algorithm is repeated until until the population at generation  $t + 1$  has size  $N$ .

to the following Fokker-Planck Equation (Kolmogorov forward equation) [122]:

$$\frac{\partial P(x, t)}{\partial t} = \left[ -s \frac{\partial}{\partial x} x(1-x) + \frac{\sigma^2}{2N} \frac{\partial^2}{\partial x^2} x(1-x) \right] P(x, t). \quad (\text{B.1})$$

The term with the first order derivative comes from the selection mechanism with strength  $s$ ; the second one is the drift term, which results from the variance  $\sigma^2$  in offspring number. As it should be, the latter is damped when increasing the population size and vanishes when  $N \rightarrow \infty$ . In a population of size  $N$ , the frequency  $x$  of a variant therefore has a diffusion constant  $\sigma^2/Nx(1-x)$ . Starting from eq.(B.1), it is possible to evaluate several relevant statistics *e.g.* the allele-frequency distributions, fixation probabilities, expected time for fixation/extinction (...) Nevertheless, such an approximation is not feasible when, for instance, fluctuations are correlated over generations and their effect is crucial for the fate of the population.

Including genetic drift in the KNS-model described in Sec.(2.3) is in principle straightforward. We will limit ourselves to describing the framework and the main results, details will be found in [39]. The crucial step is the translation of the ordinary differential equations eq.(68, 69) into discrete Langevin equations *i.e.* *stochastic differential equation* [122]:

$$\chi_i(t + \Delta t) = \chi_i(t) + \Delta t \sum_j \chi_{ij} \partial_{\chi_j} \langle F \rangle + \sqrt{\Delta t} \zeta_i(t) \quad (\text{B.2})$$

$$\chi_{ij}(t + \Delta t) = \chi_{ij}(t) + \Delta t [f_{ij}(1 - \chi_i^2)(1 - \chi_j^2) - rc_{ij}\chi_{ij}] + \sqrt{\Delta t} \zeta_{ij}(t) \quad (\text{B.3})$$



where  $\zeta_i(t), \zeta_{ij}(t)$  are white noise terms with zero mean and covariances determined by the multinomial sampling of the genotypes. Neglecting those of order  $\sigma/Nr$  and smaller, one finds the following expressions for the covariances:

$$\langle \zeta_i(t)\zeta_j(t') \rangle = \frac{\chi_{ij}}{N} \delta(t-t'), \quad \langle \zeta_{ij}(t)\zeta_{ij}(t') \rangle = \frac{(1-\chi_i^2)(1-\chi_j^2)}{N} \delta(t-t'). \quad (\text{B.4})$$

From these last expression the role of the population size for our observables can be understood: the first and second order cumulants will be subject to fluctuations whose magnitude scales as  $1/\sqrt{N}$  and vanish in the infinite population limit. As an example, let us consider the  $\{\chi_{ij}\}$ . In the QLE, these quantities relax much faster than the  $\{\chi_i\}$ , hence we can assume the latter constant when studying the dynamics of the former. In particular, it is possible to decompose the solution is a deterministic part, which is our eq.(66), and a stochastic contribution:

$$\chi_{ij}(t) = \frac{f_{ij}}{rc_{ij}} (1-\chi_i^2)(1-\chi_j^2) + \delta\chi_{ij}, \quad (\text{B.5})$$

where the autocorrelation of the of the last term is found to be

$$\langle \delta\chi_{ij}(t)\delta\chi_{ij}(t+\Delta t) \rangle = \frac{(1-\chi_i^2)(1-\chi_j^2)}{2Nrc_{ij}} e^{-rc_{ij}\Delta t}. \quad (\text{B.6})$$

Apart from the dependence on the system size we also observe the dependence on the recombination rate  $r$  which dampens not only the deterministic part but also the stochastic effects. Once the autocorrelations eq.(B.6) are known, the stochastic contribution to eq.(B.5) is determined; however, in order to use this result, one has to distinguish the case when the stochastic component dominates from the opposite one. With this *proviso*, it is possible to study the Langevin equations for  $\{\chi_i\}$  eq.(B.2) using eq.(B.5). This distinction between the two regimes is made by comparing the deterministic part of the  $\chi_{ij}(t)$  with the stochastic term upon averaging the latter over the timescale of the dynamics of the  $\{\chi_i\}$ , that given by the inverse of  $\partial_{\chi_i}\langle F \rangle$ , see eq.(69). It is also possible to take into account the mutational contribution  $\mu \neq 0$  into eq.(B.2), in which case one finds the deterministic component of  $\chi_{ij}(t)$  to dominate when  $N\mu \gg 1$  and  $f_{ij} \gg \mu$ ; otherwise the stochastic component dominates.

### Appendix C. KNS Theory for Categorical Data

A limitation of the discussion in Sec.(2.3) is the assumption of *biallelic* loci  $s_i = \pm 1$ . This is rarely true in real genetic data where one can find (at least) four different alleles, namely **A,C,G,T**. The framework we have set up and most importantly the results we have obtained can however be generalized to the case of multi-allelic loci (categorical data). Following [135], we here briefly revisit some aspects of the KNS theory and extend it to categorical data. Consider an infinite population, each individual is a genomic chain which consists in  $L$  loci  $g = \{z_1, \dots, z_L\}$ ; each locus can in turn take  $q_i$  values (alleles) *i.e.*  $z_i = 1, \dots, q_i$ .  $P(g, t)$  is the probability of finding the genotype  $g$  at time  $t$ . eq.(10) is generalized to

$$\nu_i(\alpha) = \langle \delta_{z_i, \alpha} \rangle, \quad (\text{C.1})$$

$$M_{ij}(\alpha, \beta) = \langle \delta_{z_i, \alpha} \delta_{z_j, \beta} \rangle - \nu_i(\alpha)\nu_j(\beta) : \quad (\text{C.2})$$

here the averages are over  $P(g)$ ,  $\delta$  indicates the  $\delta$ -Kronecker,  $\nu_i(\alpha)$  stands for the frequency of the allele  $\alpha$  at the  $i$ -th locus, while  $M_{ij}(\alpha, \beta)$  is the element of the covariance matrix between loci  $i$  and  $j$  relative to the alleles  $\alpha$  in  $i$  and  $\beta$  in  $j$ . The following normalizations hold:  $\sum_{\alpha=1}^{q_i} \nu_i(\alpha) = 1$ ,  $\sum_{\alpha=1}^{q_i} M_{ij}(\alpha, \beta) = \sum_{\beta=1}^{q_j} M_{ij}(\alpha, \beta) = 0 \forall i, j$ . One can still write formally eq.(1) but some more notational effort is required:

- **Fitness.** The formal expression for the fitness term is the same as in eq.(2)

$$\left. \frac{d}{dt} \right|_{fit} P(g) = (F(g) - \langle F \rangle) P(g) .$$

We only need to rewrite the fitness function in a form appropriate for the multi-allelic case:

$$F(g) = \bar{F} + \sum_i f_i(z_i) + \sum_{i,j} f_{ij}(z_i, z_j) , \quad (\text{C.3})$$

where  $f_i(z_i)$ ,  $f_{ij}(z_i, z_j)$  are functions of the alleles  $z_i, z_j$  and in general  $f_{ij}(z_i, z_j) \neq f_{ji}(z_i, z_j)$ . Unlike the biallelic case the matrix of epistatic fitness effects between loci  $i$  and  $j$  does not reduce to one real number.

- **Mutations.** Let  $\mu_{\alpha,\beta}^{(i)}$  be the mutation rate at which the allele  $\alpha$  mutates into  $\beta$  at locus  $i$ . In the most general framework,  $\mu_{\alpha,\beta}^{(i)} \neq \mu_{\beta,\alpha}^{(i)}$ . eq.(5) becomes

$$\left. \frac{d}{dt} \right|_{mut} P(g) = \sum_i \sum_{\alpha,\beta} \delta_{z_i,\alpha} \left( \mu_{\beta,\alpha}^{(i)} P(\mathcal{M}_{\alpha,\beta}^{(i)} g) - \mu_{\alpha,\beta}^{(i)} P(g) \right) . \quad (\text{C.4})$$

The operator  $\mathcal{M}_{\alpha,\beta}^{(i)}$  acts on the genomic sequence  $g$  as follows: if in the  $i$ -th locus of  $g$  there is the allele  $\alpha$  then it is changed to  $\beta$ , otherwise nothing happens.

- **Recombination.** No change is needed for the contribution due to recombination, that is, we can copy-paste from eq.(7)

$$\left. \frac{d}{dt} \right|_{rec} P(g) = r \sum_{\xi, g'} C(\xi) \left[ Q(g^{(1)}, g^{(2)}) P_2(g^{(1)}, g^{(2)}) - Q(g, g') P_2(g, g') \right] .$$

In eq.(6), we only need to formally substitute  $s_i \rightarrow z_i$ .

All other explanations, observations, limitations hold true as described in Sec.(2.3.2 - 2.3.4). As for the biallelic case, the two-genome distribution is assumed to factorize in a simple product of two one-genome Potts-like distributions:

$$P(g, t) = \frac{1}{\mathcal{Z}(t)} \exp \left( \sum_i h_i(z_i, t) + \sum_{i,j} J_{ij}(z_i, z_j, t) \right) , \quad (\text{C.5})$$

which is the generalization of eq.(53):  $\mathcal{Z}$  is the partition function,  $h_i(z_i, t)$ ,  $J_{ij}(z_i, z_j, t)$  are functions of the alleles  $z_i, z_j$  and of time  $t$ , we will drop the latter dependence in the next formulae. Due to the constraints eq.(C.1-C.2) it is clear that not all parameters  $\{h_i, J_{ij}\}$  are needed: there is an over parametrization issue in the previous Potts distribution as introduced here. One possible way to fix this *gauge invariance* is to impose the so called *Ising gauge*:  $\sum_{\alpha} h_i(\alpha) = \sum_{\alpha} J_{ij}(\alpha, \beta) = \sum_{\beta} J_{ij}(\alpha, \beta) = 0 \forall i, j$ . The stage is set at this point to introduce the QLE assumption: in the case when recombination is prominent and selection is weak we can assume the couplings  $J_{ij}$  to

be small. Neglecting the mutational contribution and following the same steps as in Sec.(4.1.1) we get to generalize eq.(61) to the following:

$$\begin{aligned}
 -\frac{\dot{Z}}{Z} + \sum_{i,\alpha} \dot{h}_i(\alpha) \delta_{z_i,\alpha} + \sum_{i,j,\alpha,\beta} \dot{J}_{ij}(\alpha,\beta) \delta_{z_i,\alpha} \delta_{z_j,\beta} = \\
 = r \sum_{i,j,\alpha,\beta} c_{ij} J_{ij}(\alpha,\beta) \left( \delta_{z_i,\alpha} E_Q[\delta_{z'_j,\beta}] + E_Q[\delta_{z'_i,\alpha}] \delta_{z_j,\beta} - \langle Q \rangle \delta_{z_i,\alpha} \delta_{z_j,\beta} - E_Q[\delta_{z'_i,\alpha} \delta_{z'_j,\beta}] \right) + \\
 + \sum_{i,\alpha} f_i(\alpha) \delta_{z_i,\alpha} + \sum_{i,j,\alpha,\beta} f_{ij}(\alpha,\beta) \delta_{z_i,\alpha} \delta_{z_j,\beta} .
 \end{aligned} \tag{C.6}$$

where  $c_{ij}$  has been introduced in eq.(14) and the following definitions have been employed:

$$\langle Q \rangle = \sum_{g'} Q(g,g') P(g') \tag{C.7}$$

$$E_Q[\delta_{z'_i,\alpha}] = \sum_{g'} \delta_{z'_i,\alpha} Q(g,g') P(g') \tag{C.8}$$

$$E_Q[\delta_{z'_i,\alpha} \delta_{z'_j,\beta}] = \sum_{g'} \delta_{z'_i,\alpha} \delta_{z'_j,\beta} Q(g,g') P(g') \tag{C.9}$$

We can compare terms in LHS and RHS of eq.(C.6) and extract a dynamical equation for the couplings of the Potts distribution:

$$\dot{J}_{ij}(\alpha,\beta) = f_{ij}(\alpha,\beta) - r \langle Q \rangle c_{ij} J_{ij}(\alpha,\beta) . \tag{C.10}$$

Finally, imposing the stationary condition and one can read off the steady state

$$J_{ij}(\alpha,\beta) = \frac{f_{ij}(\alpha,\beta)}{r \langle Q \rangle c_{ij}} , \tag{C.11}$$

In the case where the relative rate of recombination  $Q(g,g')$  is constant for all pairs  $g,g'$  or approximately so, it can be absorbed in  $r$ . We see that the analogy between the last formula and the one for the biallelic case is complete: eq.(64) generalizes to the multi-allelic case in the simplest possible way. Here too, we underline that even if recombination cannot influence the frequencies  $\{\nu_i(\alpha)\}$ , it couples the dynamics of each  $h_i(\alpha)$  to single locus statistics in every other site by means of the couplings  $J_{ij}(\alpha,\beta)$ , as it can easily read off from eq.(61). This framework has been used in [135] to reconstruct epistasis from a database of 3.000 genotypes (100.000 loci each) of the human pathogen *S. pneumoniae*.

#### Appendix D. Simulating Evolution with FFPopSim

For the purpose of simulating the evolutionary process, **FFPopSim** can be used, a software developed by F. Zanini and R.A. Neher. We here briefly describe its main features and refer to the documentation for an in-dept description of the algorithms [136].

**FFPopSim** is implemented in C++ with a Python2.7 wrapper. It allows population genetics simulations for a population of haploid individuals, identified by their genomes

$g = (s_1, \dots, s_L)$  with biallelic loci  $s_i = \pm 1$ . Considering the number of loci in our model is not small ( $L > 20$ ), for the sake of computational efficiency, we choose to run individual-based simulations, which in `FFPopSim` are implemented in the class `haploid_highd`. In such a case, a discrete generation scheme is employed, in which every individual at every generation undergoes each of the processes that drive evolution with tunable probabilities. `FFPopSim` keeps track of the distribution  $P(g)$  that changes under the effect of mutation, recombination, natural selection. Random drift is simulated by resampling each individual at each generation from a Poisson distribution with mean  $NP(g)$ , which results in a population of fluctuating size  $N \pm \mathcal{O}(\sqrt{N})$ . The algorithms for storing and handling genomic sequences are based on a *Fast Fourier Transform* (FFT) of the genotype space.

The class `haploid_highd` is instantiated by specifying the structure of the evolving population, the rates of the evolutionary mechanisms and initial conditions. In Tab.(D1) there is an example, we call this specific set QLE Simulation (QLES). In an individual-based model, the fundamental object undergoing evolution is not the genotype, but the *clone*  $c_i = (g_i, n_i)$  i.e. the pair of a genotype  $g_i$  and the number  $n_i(t)$  of individuals in the population that have that genotype at time  $t$ . In other words, the population  $\mathcal{P}$  is a set of clones. The initial conditions are specified by setting  $\{c_i\}$  i.e.  $N \times L$  Boolean values for the  $\{g_i\}$  and  $N$  integers for the  $\{n_i(0)\}$ . We will typically set random initial condition for the genotypes and  $n_i(0) = 1 \forall i$ .

At each generation, the size of each clone is updated and new clones that emerge because of mutations or recombinations are added. A discrete time step (generation)  $\Delta t = 1$  is implemented by enforcing mutations, recombination, selection, as follows:

	FFPopSim	QLES	Description
Structure	$N$	1.000	carrying capacity
	$L$	25	n. of loci
	$T$	5.000	n. of generations
	$r^*$	0.5	outcrossing rate
Drivers	$\omega$	0.5	crossover rate
	$\mu$	0.05	mutation rate
	$\{f_i\}$	0.0	additive fitness
	$\{f_{ij}\}$	$\mathcal{N}(0, \sigma_e)$	epistatic fitness

Table D1: Parameters of the QLE Simulation (QLES). The structure of the population is specified:  $N$  is the *carrying capacity*  $N$  i.e. the initial size of the population;  $L$  is the *number of loci*;  $T$  is the *number of generations*;  $r^*$  is the *outcrossing rate*;  $\omega$  is the *crossover rate* per site per generation;  $\mu$  is the *mutation rate* per site per generation;  $\{f_i, f_{ij}\}$  are the coefficients of the fitness function eq.(3). Random initial configuration. No additive fitness. Epistatic fitness coefficients are Gaussian distributed with zero mean and width  $\sigma_e = 0.004$ ,  $f_{ij} = f_{ji}$  and  $f_{ii} = 0 \forall i, j$ .

- **Mutations.** Mutations are bit-flip operations in a genotype. Each individual mutates with probability  $1 - e^{-L\mu}$ . Every individual that has been selected for mutations, suffers at least one of them, the number  $K$  being drawn from a Poisson distribution  $\mathcal{P}_{L\mu}(K)$  with mean  $L\mu$ .|| Target loci are chosen randomly.

||These probabilities are consequences of the discreteness of the computer simulation. The rate  $\mu$

- **Selection.** Let  $n_i(t)$  be the size of the clone  $i$  at time  $t$ . We enforce selection by updating  $n_i(t) \rightarrow n_i(t+1) \sim \mathcal{P}_\lambda$  where

$$\lambda = \frac{1}{\langle e^F \rangle} e^{F(g_i)+1-\frac{1}{N} \sum_j n_j(t)}. \quad (\text{D.1})$$

In words, we draw the size  $n_i(t+1)$  of the  $i$ -th clone at time  $t+1$  from a Poisson distribution with mean  $\lambda$  as in eq.(D.1), where  $F(g)$  is the fitness function eq.(3) and the average  $\langle e^F \rangle$  is over the entire population. We note that for  $F(g) \ll 1$ ,  $e^{F(g)}/\langle e^F \rangle - 1 \sim F(g) - \langle F \rangle$ , so that we retrieve eq.(2). The growth rate adjustment  $\exp(1 - \sum_j n_j(t)/N)$  is implemented to constrain the population close to the carrying capacity  $N$ .

- **Recombination.** A fraction  $r^*$  of the offspring at the previous fitness-step are designated for sexual reproduction.\*\* They are shuffled and randomly paired. For each pair a crossover pattern  $\{\xi_i\}$  as in Sec.(2.3.4) is created and the recombination is implemented by discarding parents and replacing them with two new individuals accordingly. Crossovers are assumed to happen independently between any two loci with rate  $\omega$ .

For the details of the technical implementation we refer to the documentation that accompanies the code in the GitHub repository [121]. As a demonstration, in Fig.D1-D6 we show the results for a simulation run with the parameters as in Tab.(D1), tuned so to set the system in a QLE regime *i.e.* weak selection effects, high recombination. Finally, for the details of our implementation, we refer to documentation attached to [121].

## Appendix E. Maximum Entropy and Information

In this last appendix we outline the link between the Boltzmann distribution, the principle of maximum entropy [137–139] and information theory; in [83, 114, 140] general treatments of the topic can be found, for a discussion related to the Inverse Ising Problem, see also [43].

The problem we want to tackle is that of guessing the shape of an unknown probability distribution, subject to one or more generic constraints. In particular, suppose we want to determine the discrete probability distribution  $p_r$  compatible with the constraints  $\sum_r p_r = 1$  and  $\sum_r p_r E_r = E$ . The argument is purely combinatorial: consider  $M$  independent casts of a fair die with  $R$  faces and let  $n_r \in 1, \dots, M$  be the number of times the outcome  $r \in 1, \dots, R$  is observed. The probability of a specific

as introduced in Sec.(2.3.3) is referred to a continuous-time formulation of the evolution. Let  $\mathcal{E}$  be the event that a mutation appears in an individual; suppose such events are independent and that the probability of two of them happening at the same time is negligible. If their average rate is  $\mu$  then the number  $k$  of events  $\mathcal{E}$  in the time interval  $\Delta t$  is  $\sim \mathcal{P}_{\mu\Delta t}$  where  $\mathcal{P}_\lambda(k) = \lambda^k e^{-\lambda}/k!$  is the Poisson distribution. The number of such mutations in a genome of length  $L$  in the interval  $\Delta t$  is the random variable  $K = \sum_{i=1}^L k_i$  that, being the sum of  $L$  i.i.d. Poisson random variables, is again Poisson distributed, with mean  $L\mu\Delta t$  *i.e.*  $K \sim \mathcal{P}_{L\mu\Delta t}$ . Finally, the probability that there is *at least* one mutation is  $1 - \mathcal{P}_{L\mu\Delta t}(0) = 1 - e^{-L\mu\Delta t}$ .

\*\*Note that  $r^* \neq r$ , the latter described in Sec.(2.3.4). The reason is that in general the outcrossing rate  $r^*$  is not the recombination rate  $r$ . In fact,  $r^*$  is treated as a probability while  $r$  is a rate that can take any positive value. Considering the discreteness of the computer simulation as done for mutations, we should have  $r^* = 1 - e^{-r}$ . However, as long as  $r \ll 1$  they approximately coincide  $r^* \sim 1 - (1 - r) = r$ .

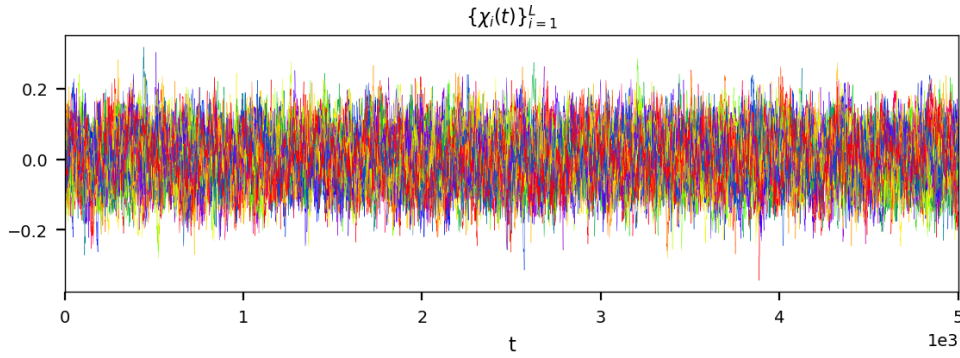


Figure D1: Simulation QLES, Tab.(D1). All-time evolution of the  $L$  first order cumulants  $\{\chi_i\}$ . In a QLE phase they fluctuate around the random-state values  $\chi_i \sim 0$ , since strong recombination rate to prevent any fixation of an allele in the population.

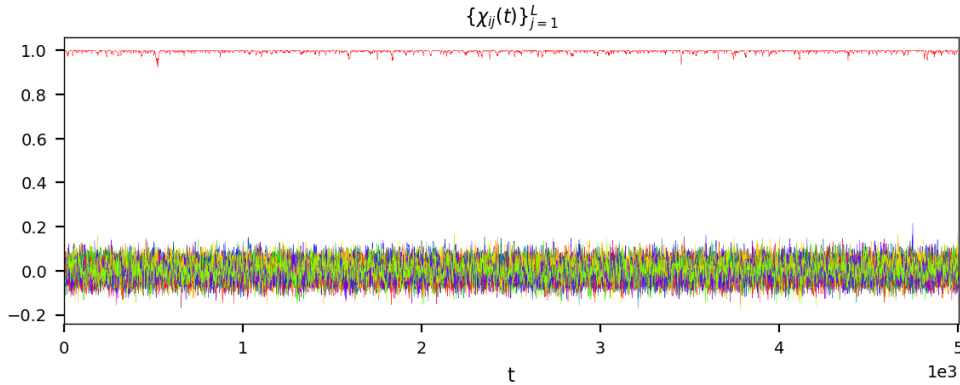


Figure D2: Simulation QLES, Tab.(D1). All-time evolution of the  $L$  second order cumulants  $\{\chi_{ij}\}_{i,j=1}^L$ . In a QLE phase they fluctuate around the random-state values  $\chi_{ij} \sim 0 \forall i \neq j$  and  $\chi_{ii} = 1 - \chi_i^2 \sim 1$ .

set of outcomes  $\{n_r\}$  is

$$\frac{M!}{\prod_{r=1}^R n_r!} \prod_{r=1}^R \left(\frac{1}{R}\right)^{n_r}, \quad (\text{E.1})$$

and using the Stirling approximation  $s! \sim s^s e^{-s}$ , its logarithm is  $-M \sum_r q_r \log q_r - M \log R$ , where  $q_r = n_r/M$ . Aside from the a constant, this quantity is  $\propto -\sum_r q_r \log q_r$ , which we recognize as the definition of the Shannon (information) entropy  $\mathcal{S}$ : if  $X$  is a discrete random variable with alphabet  $\mathcal{X}$  and probability distribution  $p(x) = Pr\{X = x\}, x \in \mathcal{X}$ , then

$$\mathcal{S}(X) = - \sum_{x \in \mathcal{X}} p(x) \log p(x). \quad (\text{E.2})$$

The idea now is that the best estimate for the probabilities  $p_r$  corresponds to the

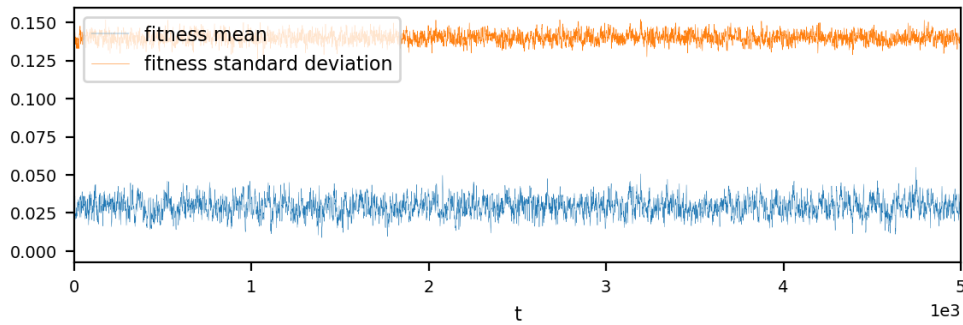


Figure D3: Simulation QLES, Tab.(D1). All-time evolution of the fitness mean and standard deviation in the population. In a QLE phase, fluctuations aside, they rapidly settle to their asymptotic values.

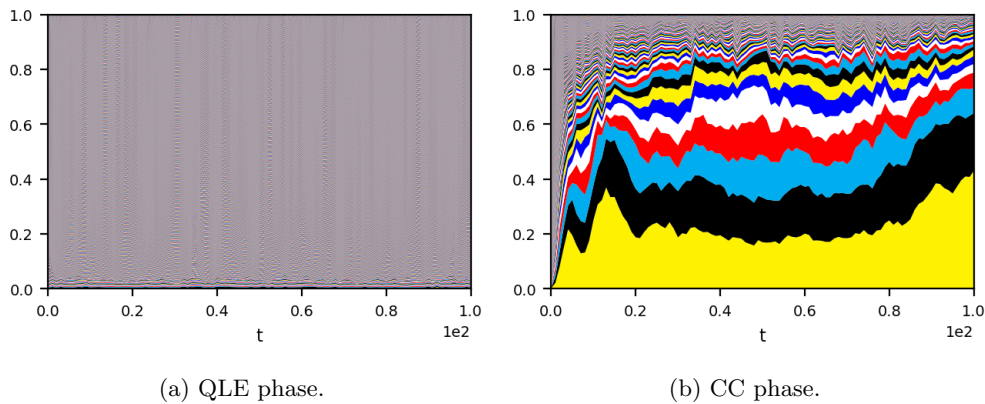


Figure D4: All-time evolution of the clonal structure of the population for the first 100 generations. On the x-axis, time. For each  $t$ , all the clones in the population are first ordered in descending order by size, then each one is assigned a different color (six colors repeated in the order: yellow - black - cyan - red - white - blue). Their relative size for each  $t$  is displayed as a vertical line, the largest at the bottom. *Left*: Simulation QLES, Tab.(D1). In a QLE phase, no significant clones emerge, most of the genotypes are present as single copies (dust-like plot). *Right*: In order to appreciate the difference with a population in a clonal competition, where few very fit genotypes compete against each other, we use the parameters :  $N = 1000, L = 25, T = 2000, \mu = 0.05, r = 0.05, \omega = 0.5, f_{ij} \sim \mathcal{N}(0, \sigma_e = 0.04)$ .

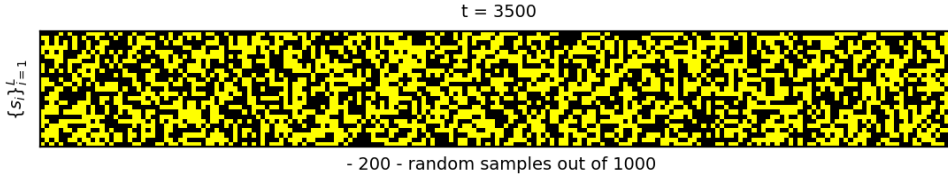


Figure D5: Simulation QLES, Tab.(D1). Instantaneous snapshot of a random sample (200 individuals) from the population at  $T = 3500$ . Each vertical strip is genotype, from a random sample of 200 individuals out of  $N$ ; each horizontal strip corresponds by consequence to one of the  $L$  loci. Y/B stand for  $\pm 1$ . In QLE phase, no patterns is obvious to the naked eye.

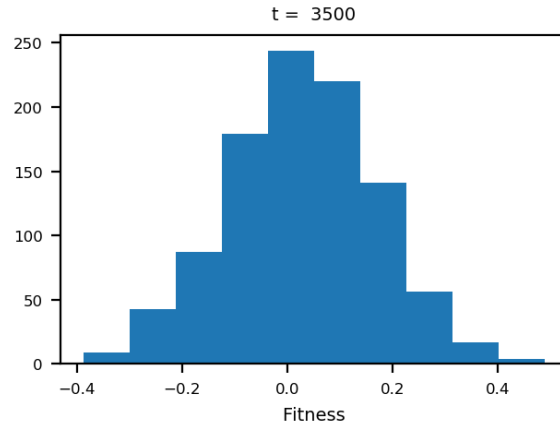


Figure D6: Simulation QLES, Tab.(D1). Instantaneous distribution of the fitness in the population at  $T = 3500$ . In QLE phase with gaussian epistatic fitness components  $f_{ij} \sim \mathcal{N}(0, \sigma_e)$  and weak epistasis, the resulting fitness function is approximately  $F(g) \sim \mathcal{N}(0, \sqrt{L(L-1)/2} \sigma_e)$ . Selection breaks the symmetry by promoting genotypes with fitness higher than the average.

set of  $\{n_r\}$  that are most likely and at the same time verify the desired constraint. Therefore, on a combinatorial basis, one may conclude that maximizing the Shannon entropy subject to the constraints  $\sum_r p_r = 1$  and  $\sum_r p_r E_r = E$  gives the optimal estimate  $p_r$ , because it is the one that is realized in the highest number of ways. If the total "energy"  $\sum_r = n_r E_r$  is fixed, this recipe leads to the Boltzmann distribution: following [138], we implement the constraints using Lagrange multipliers and setting to zero the derivative of

$$-\sum_{r=1}^R q_r \log q_r + \eta \left[ \sum_{r=1}^R q_r - 1 \right] + \lambda \left[ \sum_{r=1}^R q_r E_r - E \right] \quad (\text{E.3})$$

with respect to  $q_s$ , yielding

$$q_s = e^{-1+\eta} e^{\lambda E_s} = \frac{1}{\mathcal{Z}} e^{\lambda E_s} ; \quad (\text{E.4})$$



in the last expression we have determined  $\eta = 1 - \log \mathcal{Z}$  and  $\lambda$  is defined by the condition  $E = \frac{\partial}{\partial \lambda} \log \mathcal{Z}$ .

If the die is unfair, so that the outcome  $r$  has probability  $q_r^0$ , one maximises instead

$$\log \left( \frac{M!}{\prod_{r=1}^R n_r!} \prod_{r=1}^R (q_r^0)^{n_r} \right) \sim -M \sum_r q_r \log \frac{q_r}{q_r^0}. \quad (\text{E.5})$$

again by exploiting the Stirling approximation. This last quantity is proportional to (minus) the Kullback-Leibler distance  $D_{KL}$  between the distributions  $q_r, q_r^0$ . By definition, if  $p_1(x)$  and  $p_2(x)$  are two probability distributions for  $x \in \mathcal{X}$ , then

$$D_{KL}(p_1||p_2) = \sum_{x \in \mathcal{X}} p_1(x) \log \frac{p_1(x)}{p_2(x)}; \quad (\text{E.6})$$

The  $D_{KL}$  is a measure of the inefficiency of the distribution  $p_2$  when the true distribution is  $p_1$ , it is non-negative and it equals zero if and only if  $p_1 = p_2$ .

As an application of this discussion to the context of this work, let us consider the following problem. Suppose we have a system with  $N$  binary variables  $s_i$ , the distribution  $p(\mathbf{s})$  being unknown. Suppose also we have a set of observation from which we extract the first and second moments  $\chi_i = \langle s_i \rangle$ ,  $\phi_{ij} = \langle s_i s_j \rangle$ , which we consider as sufficient statistics of the system under investigation. According to the max-entropy receipt, the best guess for  $p(\mathbf{s})$  given  $\boldsymbol{\chi}, \boldsymbol{\phi}$  is computed by setting to zero the derivatives with respect to  $p$  of

$$-\sum_{\mathbf{s}} p(\mathbf{s}) \log p(\mathbf{s}) + \eta \left( \sum_{\mathbf{s}} p(\mathbf{s}) - 1 \right) + \sum_i h_i \left( \sum_{\mathbf{s}} p(\mathbf{s}) s_i - \chi_i \right) + \sum_{i < j} J_{ij} \left( \sum_{\mathbf{s}} p(\mathbf{s}) s_i s_j - \phi_{ij} \right), \quad (\text{E.7})$$

where we have used the Lagrange multipliers  $\eta, \mathbf{h}, \mathbf{J}$ . We get the distribution

$$p(\mathbf{s}) = e^{-1 + \eta} e^{\sum_i h_i s_i + \sum_{i < j} J_{ij} s_i s_j} = \frac{1}{\mathcal{Z}} e^{\sum_i h_i s_i + \sum_{i < j} J_{ij} s_i s_j}. \quad (\text{E.8})$$

where  $\mathcal{Z}$  is fixed by the normalization and  $\mathbf{h}, \mathbf{J}$  are chosen so to reproduce the observed moments  $\boldsymbol{\chi}, \boldsymbol{\phi}$ . We recognize in the previous equation the Boltzmann distribution eq.(18) with the Ising Hamiltonian eq.(17). The Shannon entropy of this distribution is readily computed to be

$$\mathcal{S} = - \sum_i h_i \chi_i - \sum_{i < j} J_{ij} \phi_{ij} + \log \mathcal{Z}. \quad (\text{E.9})$$

Despite its theoretical appeal and popularity in the domain of inference, the argument used above is different from that in the main body of this paper. Instead of emerging as a stationary state of a definite dynamic process, the Gibbs-Boltzmann distribution appears to be given a priori. The issue of the validity of a max-entropy approach to inference has been debated for a long time [141], for a critical appraisal by one of us, see [142]. We summarize some of the arguments that can be made in favor of a max-entropy distribution with pair-wise interactions with critical counter-points in italics:

- (i) it is justified when there is lack of data, in which case higher order statistics are poorly determined. *The choice of which statistics to consider is however*

up to the modeller. Suppose some investigator can determine the average speed ( $\langle |v| \rangle$ ) of molecules in a gas in a box; the max-entropy distribution based on that observation is  $\propto e^{-\beta|v|}$ . But the actual distribution is Maxwell-Boltzmann  $\propto e^{-\beta v^2}$ , even though mean square velocity ( $\langle v^2 \rangle$ ) is a higher order statistic which is more sensitive to outliers and noise.

- (ii) it is justified if data are generated by an equilibrium model with at most pairwise interactions. This is indeed correct, but the underlying reason is that the Gibbs-Boltzmann distribution is a stable equilibrium for a system evolving under dynamics that satisfy detailed balance.
- (iii) it is justified when models with higher order interactions  $J_{ijk\dots}$  can be reasonably approximated by simple Ising models; This is also correct, but is a statement of relative weakness of higher order effects, which may or may not hold.
- (iv) it is justified when the true distribution is so complicated that there is no other choice than trying to employ an "effective" Ising model which can be useful in deriving bounds e.g. for energy and entropy. A probability distribution can be visualized as a point in a space, which is  $2^N - 1$ -dimensional for a probability distribution on  $N$  Ising spins. It is indeed often the case that it is not meaningful to look for full representation, e.g. due to lack of data, and that one may instead look for representations in lower-dimensional model families. The Ising model has  $\frac{N(N+1)}{2}$  parameters which is much less. This  $\frac{N(N+1)}{2}$ -dimensional model family has many attractive properties, but for some data other families of equal dimensionality may be a better fit. This counter-argument, orthodox from the point of view of statistics, has been developed to great length in Information Geometry, see e.g. [143–145].

Internal to this work, the results reported in Section 6 in the main body of the paper are also arguments against max-entropy; a distribution which fluctuates indefinitely in time falls outside such a framework.

## References

- [1] Klug W, Cummings R, CA S and MA P 2012 *Concepts of Genetics* 3rd ed (Pearson Education) ISBN 9780321754356
- [2] Yoshiura K i, Kinoshita A, Ishida T, Ninokata A, Ishikawa T, Kaname T, Bannai M, Tokunaga K, Sonoda S, Komaki R, Ihara M, Saenko V A, Alipov G K, Sekine I, Komatsu K, Takahashi H, Nakashima M, Sosonkina N, Mapendano C K, Ghadami M, Nomura M, Liang D S, Miwa N, Kim D K, Garidkhuu A, Natsume N, Ohta T, Tomita H, Kaneko A, Kikuchi M, Russomando G, Hirayama K, Ishibashi M, Takahashi A, Saitou N, Murray J C, Saito S, Nakamura Y and Niikawa N 2006 *Nature Genetics* **38** 324–330
- [3] Yengo L, Sidorenko J, Kemper K E, Zheng Z, Wood A R, Weedon M N, Frayling T M, Hirschhorn J, Yang J, Visscher P M and the GIANT Consortium 2018 *Human Molecular Genetics* **27** 3641–3649 ISSN 0964-6906
- [4] Shu Y and McCauley J 2017 *Eurosurveillance* **22**
- [5] Peliti L 1997 *arXiv e-prints (Preprint cond-mat/9712027)*
- [6] Blythe R and McKane A 2007 *Journal of Statistical Mechanics: Theory and Experiment* **2007** P07018–P07018

- [7] Zeng H and Aurell E 2020 *Chinese Physics B*
- [8] Manrubia S, Cuesta J A, Aguirre J, Ahnert S E, Altenberg L, Cano A V, Catalán P, Diaz-Uriarte R, Elena S F, García-Martín J A *et al.* 2021 *Physics of Life Reviews*
- [9] Lässig M, Mustonen V and Walczak A M 2017 *Nature ecology & evolution* **1** 1–9
- [10] Wikipedia 2022 G. H. Hardy [Online; accessed 17-02-2022] URL [https://en.wikipedia.org/wiki/G.\\_H.\\_Hardy](https://en.wikipedia.org/wiki/G._H._Hardy)
- [11] Wikipedia 2022 Wilhelm Weinberg [Online; accessed 17-02-2022] URL [https://en.wikipedia.org/wiki/Wilhelm\\_Weinberg](https://en.wikipedia.org/wiki/Wilhelm_Weinberg)
- [12] Hardy G H 1908 *Science* **28** 49–50
- [13] Weinberg W 1908 *Jahreshefte des Vereins für vaterländische Naturkunde in Württemberg* **64** 368—382
- [14] Stern C 1943 *Science* **97**(2510) 137–138
- [15] Fisher R 1922 *Proceedings of the Royal Society of London. Series B, Biological sciences* **141**(905) 510–23
- [16] Fisher R 1922 *P. Roy. Soc. Edinb.* **42** 321–341
- [17] Fisher R 1930 *The Genetical Theory of Natural Selection* (Oxford: The Clarendon Press)
- [18] Kolmogorov A N 1935 *Dokl. Akad. Nauk SSSR* **3** 129
- [19] Wright S 1945 *Proc Natl Acad Sci U S A* **31**(12) 382–9 ISSN 00219002
- [20] Kimura M 1955 *Proc Natl Acad Sci U S A* **41**(3) 144–50 ISSN 00219002
- [21] Kimura M 1964 *Journal of Applied Probability* **1** 177–232
- [22] Shimakura N 1981 *Journal of Mathematics of Kyoto University* **21** 19–45
- [23] Hofbauer J 1985 *Journal of Mathematical Biology* **23**(1) 41–53
- [24] Huillet T E 2017 *Journal of Statistical Physics* **168**(1) 15–42
- [25] Svirezhev Y M and Passekov V P 2011 *Fundamentals of Mathematical Evolutionary Genetics (Mathematics and Its Applications no 22)* (Springer)
- [26] Shahshahani S 1979 *A new mathematical framework for the study of linkage and selection (Memoirs of the American Mathematical Society vol 17)* (Springer)
- [27] Aurell E, Ekeberg M and Koski T 2019 On a multilocus wright-fisher model with mutation and a svirezhev-shahshahani gradient-like selection dynamics arXiv:1906.00716
- [28] Manhart M, Haldane A and Morozov A V 2012 *Theoretical Population Biology* **82** 66–76 ISSN 0040-5809 URL <https://www.sciencedirect.com/science/article/pii/S0040580912000469>
- [29] Bochkov G and Kuzovlev Y E 1977 *Zh. Eksp. Teor. Fiz* **72** 238–243
- [30] Evans D J and Searles D J 2002 *Advances in Physics* **51** 1529–1585 (*Preprint* <https://doi.org/10.1080/00018730210155133>)
- [31] Jarzynski C 2011 *Annual Review of Condensed Matter Physics* **2** 329–351 (*Preprint* <https://doi.org/10.1146/annurev-conmatphys-062910-140506>)
- [32] Seifert U 2012 *Reports on Progress in Physics* **75** 126001
- [33] Maes C 1999 *Journal of Statistical Physics* **95** 367–392

- [34] Chetrite R and Gawedzki K 2008 *Communications in Mathematical Physics* **282** 469–518
- [35] Mustonen V and Lässig M 2009 *Trends in Genetics* **25** 111–119 ISSN 0168-9525
- [36] Kobayashi T J and Sughiyama Y 2015 *Phys. Rev. Lett.* **115**(23) 238102
- [37] Perunov N, Marsland R A and England J L 2016 *Phys. Rev. X* **6**(2) 021036
- [38] Kimura M 1965 *Genetics* **52** 875–90
- [39] Neher R A and Shraiman B I 2011 *Rev. Mod. Phys.* **83**(4) 1283–1300
- [40] Zeng H and Aurell E 2020 *Phys. Rev. E* **101**(5) 052409
- [41] Slatkin M 2008 *Nature Reviews Genetics* **9**(6) 477–485
- [42] Wainwright M J and Jordan M I 2008 *Foundations and Trends in Machine Learning* **1** 1–305
- [43] Nguyen H, Zecchina R and Berg J 2017 *Advances in Physics* **66** 197–261
- [44] Kappen H J and Rodríguez F B 1998 *Neural Comput.* **10** 1137–1156
- [45] Besag J 1975 *The Statistician* **24** 179–195
- [46] Ravikumar P, Wainwright M J and Lafferty J D 2010 *Ann. Stat.* **38** 1287–1319
- [47] Schneidman E, Berry M J, Segev R and Bialek W 2006 *Nature* **440** 1007–1012 ISSN 0028-0836
- [48] Lapedes A, Giraud B and Jarzynski C 2012 Using sequence alignments to predict protein structure and stability with high accuracy arXiv:1207.2484
- [49] Weigt M, White R A, Szurmant H, Hoch J A and Hwa T 2009 *Proc. Natl. Acad. Sci.* **106** 67–72
- [50] Mézard M and Mora T 2009 *Journal of Physiology-Paris* **103** 107–113 ISSN 0928-4257 neuromathematics of Vision
- [51] Burger L and van Nimwegen E 2010 *PLoS Comput. Biol.* **6** e1000633
- [52] Morcos F, Pagnani A, Lunt B, Bertolino A, Marks D S, Sander C, Zecchina R, Onuchic J N, Hwa T and Weigt M 2011 *Proc. Natl. Acad. Sci.* **108** E1293–E1301
- [53] Hopf T A, Colwell L J, Sheridan R, Rost B, Sander C and Marks D S 2012 *Cell* **149** 1607–1621
- [54] Jones D T, Buchan D W A, Cozzetto D and Pontil M 2012 *Bioinformatics* **28** 184–190
- [55] Andreatta M, Laplagne S, Li S C and Smale S 2014 *arXiv* **1311.1301v3**
- [56] Ekeberg M, Lökvist C, Lan Y, Weigt M and Aurell E 2013 *Phys. Rev. E* **87**(1) 012707
- [57] Ekeberg M, Hartonen T and Aurell E 2014 *J. Comput. Phys.* **276** 341–356
- [58] Feinauer C, Skwark M J, Pagnani A and Aurell E 2014 *PLoS Comput. Biol.* **10** e1003847
- [59] Vuffray M, Misra S, Lokhov A and Chertkov M 2016 Interaction screening: Efficient and sample-optimal learning of Ising models *Advances in Neural Information Processing Systems 29* ed Lee D D, Sugiyama M, Luxburg U V, Guyon I and Garnett R (Curran Associates, Inc.) pp 2595–2603
- [60] Berg J 2017 *J. Stat. Mech: Theory Exp.* **2017** 083402
- [61] Lokhov A Y, Vuffray M, Misra S and Chertkov M 2018 *Sci. Adv.* **4** e1700791

- [62] Jones D T, Singh T, Kosciolk T and Tetchner S 2015 *Bioinformatics* **31** 999–1006
- [63] Golkov V, Skwark M J, Golkov A, Dosovitskiy A, Brox T, Meiler J and Cremers D 2016 Protein contact prediction from amino acid co-evolution using convolutional networks for graph-valued images *Advances in Neural Information Processing Systems 29* ed Lee D D, Sugiyama M, Luxburg U V, Guyon I and Garnett R (Curran Associates, Inc.) pp 4222–4230
- [64] Michel M, Skwark M J, Menéndez Hurtado D, Ekeberg M and Elofsson A 2017 *Bioinformatics* **33** 2859–2866
- [65] Hopf T A, Ingraham J B, Poelwijk F J, Scharfe C P I, Springer M, Sander C and Marks D S 2017 *Nat. Biotechnol.* **35** 128–135
- [66] Ovchinnikov S, Park H, Varghese N, Huang P S, Pavlopoulos G A, Kim D E, Kamisetty H, Kyrpides N C and Baker D 2017 *Science* **355** 294–298 ISSN 0036-8075
- [67] Senior A W, Evans R, Jumper J, Kirkpatrick J, Sifre L, Green T, Qin C, Židek A, Nelson A W R, Bridgland A, Penedones H, Petersen S, Simonyan K, Crossan S, Kohli P, Jones D T, Silver D, Kavukcuoglu K and Hassabis D 2020 *Nature* **557** 706–710
- [68] Hiranuma N, Park H, Baek M, Anishchenko I, Dauparas J and Baker D 2021 *Nature Communications* **12**(1) 1340
- [69] Baldassi C, Zamparo M, Feinauer C, Procaccini A, Zecchina R, Weigt M and Pagnani A 2014 *PLoS One* **9** e92721
- [70] Figliuzzi M, Jacquier H, Schug A, Tenailon O and Weigt M 2016 *Mol. Biol. Evol.* **33** 268
- [71] Uguzzoni G, John Lovis S, Oteri F, Schug A, Szurmant H and Weigt M 2017 *Proc. Natl. Acad. Sci.* **114** E2662–E2671
- [72] De Leonardis E, Lutz B, Ratz S, Simona C, Monasson R, Weigt M and Schug A 2016 *Biophys. J.* **110** 364a
- [73] Skwark M J, Croucher N J, Puranen S, Chewapreecha C, Pesonen M, Xu Y Y, Turner P, Harris S R, Beres S B, Musser J M, Parkhill J, Bentley S D, Aurell E and Corander J 2017 *PLoS Genet.* **13** e1006508
- [74] Schubert B, Maddamsetti R, Nyman J, Farhat M R and Marks D S 2018 *bioRxiv* (Preprint <https://www.biorxiv.org/content/early/2018/06/05/325993.full.pdf>)
- [75] Zeng H L, Dichio V, Horta E R, Thorell K and Aurell E 2020 *Proceedings of the National Academy of Sciences* **117** 31519–31526
- [76] Roudi Y, Aurell E and Hertz J A 2009 *Front. Comput. Neurosci.* **3** 1–15 ISSN 1662-5188
- [77] Stein R R, Marks D S and Sander C 2015 *PLoS Comput. Biol.* **11** e1004182
- [78] Cocco S, Feinauer C, Figliuzzi M, Monasson R and Weigt M 2018 *Reports on Progress in Physics* **81** 032601
- [79] Sessak V and Monasson R 2009 *J. Phys. A: Math. Theor.* **42** 055001
- [80] Thouless D J, Anderson P W and Palmer R G 1977 *The Philosophical Magazine: A Journal of Theoretical Experimental and Applied Physics* **35** 593–601

- [81] Georges A and Yedidia J S 1991 *Journal of Physics A: Mathematical and General* **24** 2173–2192
- [82] Ricci-Tersenghi F 2012 *Journal of Statistical Mechanics: Theory and Experiment* **2012** P08015
- [83] Cover T M and Thomas J A 2006 *Elements of Information Theory* (USA: Wiley-Interscience) ISBN 0471241954
- [84] Mauri E, Cocco S and Monasson R 2021 *EPL (Europhysics Letters)* **132** 56001
- [85] Zeng H L, Mauri E, Dichio V, Cocco S, Monasson R and Aurell E 2020 *arXiv e-prints* arXiv:2006.16735 (*Preprint* 2006.16735)
- [86] Kingman J F C 1982 *Journal of Applied Probability* **19** 27–43
- [87] Kingman J 1982 *Stochastic Processes and their Applications* **13** 235–248 ISSN 0304-4149
- [88] Möhle M 1994 *Journal of Applied Probability* **31** 309–332
- [89] Chang J T 1999 *Advances in Applied Probability* **31** 1002–1026
- [90] Carinci G, Giardinà C, Giberti C and Redig F 2015 *Stochastic Processes and their Applications* **125** 941–969 ISSN 0304-4149
- [91] Park S C and Krug J 2007 *Proceedings of the National Academy of Sciences* **104** 18135–18140 ISSN 0027-8424
- [92] Fogle C A, Nagle J L and Desai M M 2008 *Genetics* **180** 2163–2173 ISSN 1943-2631
- [93] Brunet E, Rouzine I M and Wilke C O 2008 *Genetics* **179** 603–620 ISSN 1943-2631
- [94] Sella G and Hirsh A E 2005 *Proceedings of the National Academy of Sciences* **102** 9541–9546
- [95] Neher R A 2013 *Annual review of Ecology, evolution, and Systematics* **44** 195–215
- [96] Muller H 1964 *Mutation Research/Fundamental and Molecular Mechanisms of Mutagenesis* **1** 2 – 9 ISSN 0027-5107
- [97] Felsenstein J 1974 *Genetics* **78** 737–756
- [98] Charlesworth B and Charlesworth D 1997 *Genetics Research* **70** 63–73
- [99] Neher R and Shraiman B 2012 *Genetics* **191** 1283–1293
- [100] Loewe L 2006 *Genetics Research* **87** 133–159
- [101] Kondrashov A S 1994 *Genetics* **136** 1469–1473
- [102] Bell G 1988 *Journal of Evolutionary Biology* **1** 67–82
- [103] Schultz S T and Lynch M 1997 *Evolution* **51** 1363–1371
- [104] Desai M and Fisher D 2007 *Genetics* **176** 1759–1798
- [105] Charlesworth B 2012 *Genetics* **190** 5–22
- [106] Goyal S, Balick D J, Jerison E R, Neher R A, Shraiman B I and Desai M M 2012 *Genetics* **191** 1309–1319
- [107] Silander O K, Tenaillon O and Chao L 2007 *PLoS biology* **5** e94
- [108] Moya A, Elena S F, Bracho A, Miralles R and Barrio E 2000 *Proceedings of the National Academy of Sciences* **97** 6967–6973

- [109] Metzger J J and Eule S 2013 *PLoS computational biology* **9** e1003303
- [110] Rouzine I M, Brunet É and Wilke C O 2008 *Theoretical population biology* **73** 24–46
- [111] Neher R, Vucelja M, Mezard M and Shraiman B 2013 *Journal of Statistical Mechanics: Theory and Experiment* **2013**
- [112] Neher R A and Shraiman B I 2009 *Proceedings of the National Academy of Sciences* **106** 6866–6871 ISSN 0027-8424
- [113] Derrida B 1981 *Physical Review B* **24** 2613
- [114] Mezard M and Montanari A 2009 *Information, physics, and computation* (Oxford University Press) ISBN 9780198570837
- [115] Zeng H L, Liu Y, Dichio V and Aurell E 2021 Temporal epistasis inference from more than 3,500,000 SARS-CoV-2 Genomic Sequences arXiv:2112.12957
- [116] Krug J 2007 *Journal of Statistical Mechanics: Theory and Experiment* **2007** P07001–P07001
- [117] Castellani T and Cavagna A 2005 *Journal of Statistical Mechanics: Theory and Experiment* **2005** 05012
- [118] Neher R A, Kessinger T A and Shraiman B I 2013 *Proceedings of the National Academy of Sciences* **110** 15836–15841
- [119] Held T, Klemmer D and Lässig M 2019 *Nature communications* **10** 1–11
- [120] Desai M M, Fisher D S and Murray A W 2007 *Current biology* **17** 385–394
- [121] Dichio V 2021 dichio/studiodarwin Github URL <https://github.com/dichio/studiodarwin>
- [122] Gardiner C 2004 *Handbook of stochastic methods for physics, chemistry and the natural sciences* 3rd ed (*Springer Series in Synergetics* vol 13) (Berlin: Springer-Verlag) ISBN 3-540-20882-8
- [123] Good B, McDonald M, Barrick J, Lenski R and Desai M 2017 *Nature* **551** 45–50
- [124] Ao P, Kwon C and Qian H 2007 *Complexity* **12** 19–27 (Preprint <https://onlinelibrary.wiley.com/doi/pdf/10.1002/cplx.20171>)
- [125] Ao P 2008 *Communications in Theoretical Physics* **49** 1073–1090
- [126] Wang J 2015 *Advances in Physics* **64** 1–137 (Preprint <https://doi.org/10.1080/00018732.2015.1037068>)
- [127] Waddington C H 1957:2014 *The strategy of the genes: A discussion of some aspects of Theoretical Biology* (Routledge) ISBN 798-0-415-73519-3
- [128] Zhou J X, Aliyu M D S, Aurell E and Huang S 2012 *R. Soc. Interface* **9** 3539–3553
- [129] Gnedenko B 1998 *Theory of Probability* 6th ed (Taylor & Francis) ISBN 978-9-056-99585-0
- [130] Zinn-Justin J 2010 *Path integrals in quantum mechanics* (Oxford University Press) ISBN 978-0-19-856674-8
- [131] Messer P 2016 Neutral models of genetic drift and mutation *Encyclopedia of Evolutionary Biology* ed Kliman R M (Oxford: Academic Press) pp 119 – 123 ISBN 978-0-12-800426-5
- [132] Wright S 1931 *Genetics* **16** 97

- [133] Kimura M 1955 *Proceedings of the National Academy of Sciences of the United States of America* **41** 144
- [134] Neher R A and Walczak A M 2018 *arXiv e-prints (Preprint 1804.07720)*
- [135] Gao C, Cecconi F, Vulpiani A, Zhou H and Aurell E 2019 *Physical Biology* **16** 026002
- [136] Zanini F and Neher R 2012 *Bioinformatics* **28** 3332–3333
- [137] Jaynes E T 2003 *Probability Theory: The Logic of Science* (Cambridge University Press) ISBN 978-0-511-06589-7
- [138] Jaynes E T 1957 *Physical review* **106** 620
- [139] Jaynes E T 1982 *Proceedings of the IEEE* **70** 939–952
- [140] Pressé S, Ghosh K, Lee J and Dill K A 2013 *Rev. Mod. Phys.* **85**(3) 1115–1141
- [141] Auletta G, Rondoni L and Vulpiani A 2017 *The European Physical Journal Special Topics* **226** 2327–2343
- [142] Aurell E 2016 *PLoS computational biology* **12** e1004777
- [143] Amari S i 2012 *Differential-geometrical methods in statistics* vol 28 (Springer Science & Business Media)
- [144] Amari S 2000 *Neural Computation* **12** 2083–2107
- [145] Amari S 2021 *Japanese Journal of Mathematics* **16**(1) 1–48

## Acknowledgements

We thank Profs Simona Cocco and Rémi Monasson and Dott. Eugenio Mauri for numerous discussions and for a pleasant collaboration forming the background of the material presented in Section 5. We also thank Prof Joachim Krug for constructive remarks on the MS. The work of Vito Dichio was supported by Extra-Erasmus Scholarship (Department of Physics, University of Trieste) and Collegio Universitario 'Luciano Fonda' and has partially been presented in the form of a MSc thesis at University of Trieste (2020). He also warmly thanks Nordita (Stockholm, Sweden) and KTH (Stockholm, Sweden) for hospitality. The work of HLZ was sponsored by National Natural Science Foundation of China (11705097), Natural Science Foundation of Jiangsu Province (BK20170895), Jiangsu Government Scholarship for Overseas Studies of 2018. EA acknowledges support of the Swedish Research Council through grant 2020-04980. We finally thank Prof Johannes Berg for permission to re-use Fig.2, and Profs. B.H. Good and M.M. Desai for kindly allowing us to use previously unpublished Fig.21.